2013

Determination of Copper Speciation, Bioavailability and Toxicity in Saltwater Environments

Tara N. Tait
Wilfrid Laurier University, tait2990@mylaurier.ca

Determination of Copper Speciation, Bioavailability and Toxicity in Saltwater Environments

Tara N. Tait

Bachelor of Science, Honours Biomedical Toxicology Co-op, University of Guelph, 2011

THESIS

Submitted to the Department of Chemistry
in partial fulfillment of the requirements for
the degree of Master of Science

Wilfrid Laurier University
Waterloo, Ontario, Canada

Abstract

The speciation of copper plays a strong role in determining bioavailability and toxicity upon copper exposure in marine environments. Specifically, natural organic matter (NOM) can complex with copper, influencing speciation and decreasing bioavailability. The aim of this research was to determine accurate copper speciation values using literature and new techniques and applying the techniques that reflect the most accurate speciation values to investigate the influence of NOM quantity and quality on copper speciation and toxicity. The results from this study will have implications on the development of a marine Biotic Ligand Model (BLM). Free copper was measured using a flow-through ion selective electrode (ISE) system. A published external calibration Cu ISE method showed a wide variability in measured free copper values and so method improvements were investigated. This resulted in the development of an internal calibration flow-through ISE method. This new method showed an increase in sample reproducibility and agreed well with modeled free copper values for well defined systems. This method was then applied to measure free copper at the LC_{50} for toxicity assays performed for nine sample locations using the rotifer, *Brachionus plicatilis*. NOM was characterized for each site through dissolved organic carbon (DOC) concentrations, fluorescence excitation-emission matrices (FEEM) and fluorescence quenching, combined with spectral resolution techniques to quantify humic-, fulvic-, tryptophan- and tyrosine-like fractions. The toxicity results showed two trends with DOC. In the first case, DOC was protective against copper toxicity (r^2 = 0.72, *p*-value = 0.016), however a plateau in protective effect was observed above DOC concentrations above approximately 2 mg C L^{-1}. This suggests salt- induced colloid formation could be occurring resulting in a decrease of binding sites available to complex free copper. The second relationship between LC_{50} and DOC can be described by the equation LC_{50} (µg L^{-1}) = $25.15DOC^{0.47}$ (r^2 = 0.61, *p*-value = 0.008) including two outlier sites in statistical analysis or LC_{50} (µg L^{-1}) = $22.86DOC^{0.45}$ (r^2 = 0.71, *p*-value = 0.009) excluding the outlier sites. Humic- and fulvic-like fractions showed a linear correlation with toxicity however tryptophan and tyrosine showed no correlation. Overall, only fulvic-like fractions were significant. Free copper at the LC_{50} for each site remained constant (average pCu = 10.14), within the Biotic Ligand Model (BLM) prediction factor of two,

while the LC_{50} values ranged from 333 to 980 nM. This suggests that differences in water chemistries alter the total amount of copper that needs to be added to a system to reach a critical free copper concentration required to cause toxicity. This was supported by fluorescence quenching data that was used to determine binding capacities and stability constants for the different fluorescent fractions within DOC. Binding capacities at multiple fluorophores ranged from 4 to 1614 nmole mg C^{-1}. The sum of the binding capacities were linearly correlated with LC_{50} (r^2 = 0.67, *p*-value = 0.008) which supports the observed toxicity data that more total copper was required to reach the same free copper. Binding sites ranged from one to three ligands per sample. Binding was relatively strong for all sites, with log*K* values ranging from 9.33 to 11.22. In addition, free copper was calculated using this data and the results agreed with the ISE data within ± 0.3 pCu. This supports the theory that a critical free copper concentration is required to cause toxicity. As well these results confirm the applicability of fluorescence quenching techniques in marine water.

Acknowledgements

I would like to thank my supervisor Dr. Scott Smith for giving me the opportunity to complete my MSc. Degree as a member of his lab. The immense support and guidance he always provided was invaluable. I have learned so much under your supervision and am extremely grateful. I would also like to thank my co-supervisor, Dr. Jim McGeer. Your love of field work enabled me to have lots of samples to choose from for my research. Thank you to Dr. Ian Hamilton and Dr. Jim McGeer for graciously lending their time to be on my committee and giving me valuable input throughout my research. In addition to Dr. Jim McGeer, a huge thank you to Holly Gray, Jessie Cunningham, Dr. Martin Grosell and Teck Resources Inc. for providing me with samples for my research.

Thank you so much to the members of the Smith Lab. You made me feel welcome when I first started my research and I will not forget the many memories we've shared since then. A special thank you to Holly Gray and Rachael Diamond for your entire lab related help. As well, along with Petrease Patton, for keeping me sane when Science wanted nothing else but to make me crazy. Dr. Chris Cooper, thank you for showing me the way of the rotifers and for all your help and input over the last two years.

I also have to thank my family and friends for all their support they have given me in all my endeavours. A special thank you to Scott and my sister, Megan. Without the two of you I wouldn't have gotten through these past two years.

Finally, I would like to thank the funders who allowed this research to be possible: ICA (International Copper Association), CDA (Copper Development Association), ILZRO (International Lead and Zinc Research Organization), IZA (International Zinc Association), Teck Resources Inc., Vale Canada, Xstrata Zinc, NiPERA (Nickel Producers Environmental Research Association) and NSERC.

Table of Contents

Abstract i

Acknowledgements iii

Table of Contents iv

List of Abbreviations and Symbols vii

List of Figures viii

List of Tables x

Chapter 1 Introduction 1

1.1 Copper in Marine Systems 1

1.2 Natural Organic Matter 3

1.3 Effect of NOM on Copper Toxicity 6

1.4 Biotic Ligand Model 8

1.5 Toxicity Assays 10

1.6 Ion Selective Electrode 12

1.7 Anodic Stripping Voltammetry 14

1.8 Fluorescence 17

1.8.1 Fluorescence Excitation-Emission Matrix 19

1.8.2 Fluorescence Quenching 21

1.9 Research Goals and Objectives 22

1.10 Significance of Research 24

1.11 References 26

Chapter 2 Internal calibration flow-through ISE method for determining free Cu in salt water 33

2.0 Abstract 33

2.1 Introduction 34

2.2 Methods 35

2.2.1 Instrumentation 35

2.2.2 Sample Preparation 36

2.2.3 Internal Calibration Analysis Procedure 39

2.2.4 Literature Method Analysis Procedure 40
2.2.5 Internal Calibration Data Analysis 40
2.3 Results and Discussion 42
2.3.1 Literature Method Sample Variability 42
2.3.2 Internal Calibration Validation 44
2.3.3 Applicability in Marine Samples 47
2.4 Conclusions 49
2.5 References 50
Chapter 3 Influence of DOC source on free copper and toxicity to *Brachionus plicatilis* 52
3.0 Abstract 52
3.1 Introduction 53
3.2 Methods 57
3.2.1 Sampling, Storage and Selection 57
3.2.2 Dissolved Organic Carbon (DOC) Analysis 58
3.2.3 Fluorescence Measurement and Analysis 59
3.2.4 Toxicity Assay 62
3.2.5 Total Copper Analysis 65
3.2.6 Free Copper Analysis 66
3.3 Results and Discussion 68
3.3.1 DOC Analysis 68
3.3.2 Fluorescence Measurements 70
3.3.3 DOC Quantity on LC_{50} 76
3.3.4 DOC Quality on LC_{50} 82
3.3.5 Free Copper and LC_{50} 87
3.3.6 Effect of DOC on free copper 91
3.4 Conclusions 94
3.5 References 96

Chapter 4 Characterization of NOM interactions with copper in natural sea water using fluorescence quenching: Influence on toxicity 102
4.0 Abstract 102
4.1 Introduction 103
4.2 Methods 106
4.2.1 Experimental protocol 106
4.2.2 Data processing 108
4.3 Results and Discussion 113
4.4 Conclusions 118
4.5 References 120
Chapter 5 Conclusions and Future Work 123
5.1 Conclusions and Future Work 123
5.1.1 Objective 1 and 2 123
5.1.2 Objective 3 125
5.1.3 Implications of Research 128
5.2 References 131
APPENDIX A 132
A1. Solving for chemical equilibrium using MATLAB™ 132
A2. MATLAB script for modeling free Cu over a pH range 134
A3. MATLAB script for free copper at a constant pH 152
APPENDIX B 163
B1. DOC quality of water samples collected 163
B2. Effects of salinity adjustment on LC_{50} 165
B3. Contour plots for sampling sites used in toxicity assays 166
APPENDIX C 168
C1. MATLAB script for determining contribution of fluorophores to total fluorescence during fluorescence quenching titrations with copper 168
C2. MATLAB script for Ryan-Weber fitting combined with modeling free copper . 172
C3. Plots of contribution of fluorophores to total fluorescence 187
C4. Resolved fluorescence quenching curves with Ryan-Weber fitting 189
C5. Comparison of modeled free copper using fluorescence quenching data and measured free copper using the Cu ISE 194

List of Abbreviations and Symbols

ASW	Artificial Seawater
BLM	Biotic Ligand Model
CCC	Criterion Continuous Concentration
CCREM	Canadian Council of Resource and Environment Ministers
CMC	Criteria Maximum Concentration
DOC	Dissolved Organic Carbon
DOM	Dissolved Organic Matter
DPASV	Differential Pulse Anodic Stripping Voltammetry
EC_{50}	Median Effective Concentration (required to induce a 50% effect)
FEEM	Fluorescence Excitation Emission Matrix
ISE	Ion-Selective Electrode
LC_{50}	Median Lethal Concentration (required to induce 50% mortality)
logK	Equilibrium Constant
L_T	Binding Capacity
NIST	National Institute of Standards and Technology
NOM	Natural Organic Matter
OECD	Organization for the Economic Co-operation and Development
PARAFAC	PARAlell FACtor Analysis
Trp	Tryptophan
Tyr	Tyrosine

List of Figures

Figure 1.1 Molecular structure of humic acid. 4

Figure 1.2 Molecular structure of fulvic acid. 4

Figure 1.3 Molecular structure of tyrosine. 5

Figure 1.4 Molecular structure of tryptophan. 5

Figure 1.5 Schematic diagram of the Biotic Ligand Model. 10

Figure 1.6 Schematic drawing of the rotifer, *Brachionus plicatilis*. 11

Figure 1.7 Example of the excitation signal and resulting voltammogram using anodic stripping voltammetry for the analytes, cadmium and copper. 16

Figure 1.8 Visual representation of the standard addition technique. 17

Figure 1.9 Jablonski diagram 18

Figure 1.10 FEEM contour plot for the freshwater NOM isolate Luther Marsh.. 20

Figure 2.1 Schematic of the free copper ion selective electrode flow-through system. .. 36

Figure 2.2 Kinetic curve for ASW + 10 µM Trp + 786.8 nmol L^{-1} (50 ppb) Cu showing potential as a function of time. 42

Figure 2.3 Measured free copper concentrations using Eriksen et al. method compared to San Diego Bay Results from Chadwick et al. (2008).. 43

Figure 2.4 Measured and modeled free copper for ASW + 10 µM Trp with 78.7 nmol L^{-1} Cu, 157.4 nmol L^{-1} Cu, 392.7 nmol L^{-1} Cu, and 786.8 nmol L^{-1} Cu added over a pH range from 8.0 to 3.3. 45

Figure 2.5 Free copper measured over a concentration range of 78.7 to 786.8 nmol L^{-1} Cu at a constant pH calculated using the external and internal calibration methods. 46

Figure 2.6 Measured and modeled copper speciation of ASW + 10 µM Trp over concentration range of 78.7 to 786.8 nmol L^{-1} Cu at a constant pH (pH = 8). 47

Figure 2.7 Comparison of copper speciation measurements using the external calibration method and internal calibration method for Duxbury and PNNL.. 48

Figure 3.1 Comparison of DOC measurements before and after salinity adjustment and filtration. 69

Figure 3.2 Comparison of the percent change in DOC as a function of the percent change in salinity of water samples. 70

Figure 3.3 Fluorescence excitation-emission contour plots for Major Kollock Creek and Chesterman Beach. 71

Figure 3.4 Spectra of the four components used to describe fluorescent organic matter quality within the water samples. The spectra represent (a) humic-like, (b) tryptophan-like, (c) fulvic-like, and (d) tyrosine-like fractions. 72

Figure 3.5 Comparison of (a) humic-, (b) fulvic-, (c) tryptophan-, and (d) tyrosine-like components before and after salinity adjustment and filtration.. 74

Figure 3.6 Contributions of each component as a function of DOC to the observed fluorescence including (a) humic-like, (b) fulvic like, (c) tryptophan-like and (d) tyrosine-like..... 75

Figure 3.7 Total dissolved copper LC_{50} as a function of DOC representing a salt-induced colloid formation trend. 77

Figure 3.8 Total dissolved copper LC_{50} as a function of DOC. Trendline represents the relationship with LC_{50} (µg L^{-1}) = $25.15DOC^{0.47}$ (including outliers) or LC_{50} (µg L^{-1}) = $22.86DOC^{0.45}$(excluding outliers). 80

Figure 3.9 Comparison of predictive toxicity equations for *Brachionus plicatilis*, *Mytilus sp.*, *Crassostrea virginica*, *Dendraster excentricus*, and S*trongylocentrotis purpuratus*. 82

Figure 3.10 Copper LC_{50} as a function of (a) SAC_{340}, and (b) fluorescence index (FI).. 83

Figure 3.11 Copper LC_{50} as a function of fluorescent (a) humic-, (b) fulvic-, (c), tryptophan-, and (d) tyrosine-like components 85

Figure 3.12 Plots of DOC versus LC_{50} weighted by contribution of fluorescence for (a) humic-, (b) fulvic-, (c) tryptophan-, and (d) tyrosine-like components. 86

Figure 3.13 Free copper measurements at the LC_{50} for each site. 87

Figure 3.14 Free copper at the LC_{50} as a function of total copper at the LC_{50}. 89

Figure 3.15 Free copper at the LC_{50} as a function of DOC. 92

Figure 3.16 Free copper at the LC_{50} as a function of fluorescent (a) humic-, (b) fulvic-, (c), tryptophan-, and (d) tyrosine-like components.. 93

Figure 4.1 Contribution of humic-, fulvic-, tryptophan-, and tyrosine-like fractions to total fluorescence in Bouctouche. 110

Figure 4.2 Ryan Weber fitting of the resolved fluorophores for Bouctouche.. 113

Figure 4.3 Total binding capacity (L_T) as a function of LC_{50} for the binding sites found in each sample. 116

Figure 4.4 Comparison of free copper measured using the ion-selective electrode (pCu_{ISE}) and fluorescence quenching data (pCu_{FI}). 118

Figure 5.1 Summary schematic of the interaction of DOC on free copper and toxicity to the rotifer, Brachionus plicatilis. 130

List of Tables

Table 2.1 Chemical composition of artificial seawater. 37

Table 2.2 Location and basic water characteristics of marine samples. 39

Table 3.1 Description of sampling sites used for toxicity assays. 58

Table 3.2 Summary of test conditions for the rotifer species, *Branchionus plicatilus*. ... 63

Table 3.3 Measurements of DOC and salinity of the sea water samples used for the toxicity assays. Measurements are shown from both before and after salinity adjustment and filtration. 69

Table 3.4 Fluorescent measurements of humic- (HA), fulvic- (FA), tryptophan- (Trp) and tyrosine-like (Tyr) components of water used for toxicity assays. Measurements are from before and after salinity adjustments and filtration. 73

Table 3.5 SAC_{340} and Fluorescence Index (FI) of each water sample used for toxicity assay. 76

Table 4.1 Characteristics of water samples 107

Table 4.2 Binding characteristics (stability constant, Log*K* and binding capacity, L_T) of nine sea water samples with copper. 115

Table 4.3 Comparison of free Cu at the LC_{50} measured using the copper ion-selective electrode and calculated using the fluorescence data.. 117

Chapter 1 Introduction

1.1 Copper in Marine Systems

Copper is a trace element that is essential for proper functioning of plants, animals and microorgansims due to its requirement for many specific metabolic processes (ICA 1995). One key function is the dependence of copper for many oxygen defense systems such as Cu/Zn superoxide dismutase (SOD) which converts superoxide to hydrogen peroxide (ICA 1995, Ullrich & Duppel 1975). However, only low amounts are necessary for normal metabolic functioning and at increased concentrations can prove to be toxic (ICA 1995). Toxicity is usually due to copper interference with ion transport, most notably interference of sodium transport causing electrolyte imbalance and ionoregulatory failure (Grosell & Wood 2002; De Polo & Scrimshaw 2012). This can occur due to the affinity of copper for thiol (-SH) groups within enzymes such as Na^+/K^+ ATPase where copper binding causes a disruption in enzyme activity (Stauber and Florence 1985). In addition, the redox properties of copper can lead to the generation of reactive oxygen species when cellular copper levels are increased (Harris and Gitlin 1996).

Anthropogenic release of copper into marine systems has resulted in increasing trace levels of copper in the environment (Flemming & Trevors 1989). In marine systems, this is most often due to the use of copper as a biocide in antifouling paints and coatings used on the underside of ships (Chadwick et al. 2008). With over 53% of the United States population living along coastal regions (NOAA 2004) and Canada having the longest marine coastline of any country (Government of Canada 2003) there is an

increased concern of contamination of metals in the ocean due to anthropogenic inputs. Typical copper concentrations range from 0.12 – 0.38 µg L^{-1} in areas of open ocean (Mackey 1983) to levels over 6 µg L^{-1} in heavily impacted areas such as San Francisco Bay (Donat et al. 1994). Current U.S. EPA criteria for copper limits in seawater are a dissolved criterion continuous concentration (CCC) of 3.1 µg L^{-1} and a criteria maximum concentration (CMC) of 4.8 µg L^{-1} (U.S. EPA 2007). Currently there is no copper load limit into marine systems set by the Canadian government (CCREM 1987). However, British Columbia has set provincial limits with a total copper CCC of less than or equal to 2 µg L^{-1} and a CMC of 3 µg L^{-1} (BC MOE 1987).

The bioavailability of copper is influenced by the species of copper present in the system (ICA 1995, Chadwick et al. 2008; Eriksen et al. 2001; Eriksen et al. 2001a; Sunda & Hanson 1979). Determination of the true speciation of copper in marine systems is crucial in understanding and determining the bioavailability of copper for uptake into marine organisms. As such, true copper speciation and its relation to toxicity in salt waters will be the main focus of this project.

Copper can exist in many different forms in aquatic environments and factors within these environments can affect the speciation of copper to increase or decrease its toxicity to organisms. Most copper is found in the form of inorganic and organic complexes (Kogut & Voelker 2001; Paquin et al. 2000). Inorganic complexes include species such as copper hydroxides and copper carbonates. Organic ligands have been found to play a larger role on copper speciation and are generically classified as natural organic matter (NOM) (Sunda & Hanson 1979). NOM will be discussed in further detail in Section 1.2. The copper in both organic and inorganic complexes is unavailable or less

available to interact with organisms to cause toxicity. As such, free copper, Cu^{2+}, is often used as an indicator for toxicity since it is the species most available to be taken up by an organism (Chadwick et al. 2008; Eriksen et al. 2001, Sunda & Hanson 1979).

1.2 Natural Organic Matter

Natural organic matter (NOM) is a heterogenous mixture of organic compounds that contain potential binding sites for metals such as copper. Copper can form complexes with NOM at binding sites such as amino (Cu-NHR, $[Cu\text{-}NH_2R]^+$), carboxyl ($Cu\text{-}CO_2H$), phenolic (Cu-OAr) and sulfide or thiol groups (Cu-SH) (Smith et al. 2002). Although 90% of NOM in seawater remains to be properly characterized, within this fraction humic and fulvic acids are the most abundant, comprising anywhere from 5-25% of dissolved organic carbon (DOC) in marine surface waters (Benner 2002; Hunter & Liss 1981). Other components include carbohydrates, fatty acids and proteins/amino acids (Eikebrokk et al. 2006; Hunter & Liss 1981). These humic and fulvic acid fractions can be defined based on their solubility under different pH conditions. Humic acids are insoluble under acidic conditions (pH < 2), but solubility increases as pH increases, whereas fulvic acids are soluble under all pH conditions (Eikebrokk et al 2006; Thurman 1985). The concentration of NOM is usually measured as dissolved organic carbon (DOC). DOC is operationally defined as organic carbon that passes through a 0.45µm filter. Typical concentrations of dissolved organic carbon (DOC) in marine systems range from 0.5 – 10 mg C L^{-1} from open ocean to coastal waters (Benner 2002).

The origin of natural organic matter also plays a role in the composition of NOM. Allochthonous, or terrigenous, organic matter is terrestrially-derived from the

decomposition and leaching from soil and plant materials such as lignin, tannins and detritus and typically contains a higher humic and fulvic substance content (Birdwell & Engel 2009; McKnight et al. 2001). These humic and fulvic substances are heterogenous in structure, however Figure 1.1 and Figure 1.2 depicts the representative structures of humic and fulvic acids, respectively.

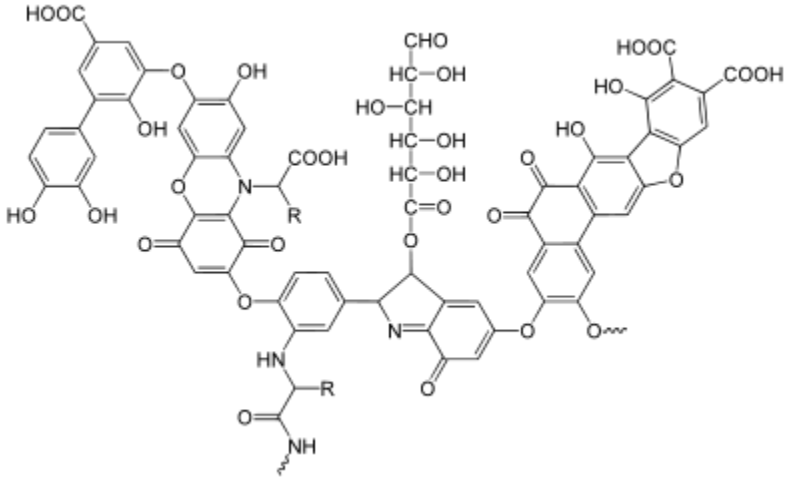

Figure 1.1 Molecular structure of humic acid.

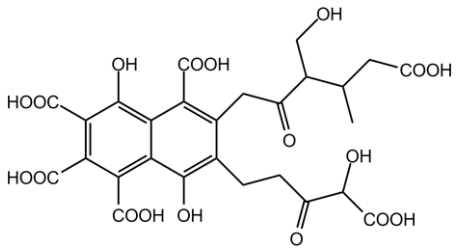

Figure 1.2 Molecular structure of fulvic acid.

Autochthonous organic matter is microbially-derived organic matter from bacterial and algal processes occurring in the water column. This type of organic matter usually contains a higher proteinaceous content containing amino acids such as tyrosine

and tryptophan (Birdwell & Engel 2009; McKnight et al. 2001). The structures of tyrosine and tryptophan can be found in Figure 1.3 and Figure 1.4, respectively.

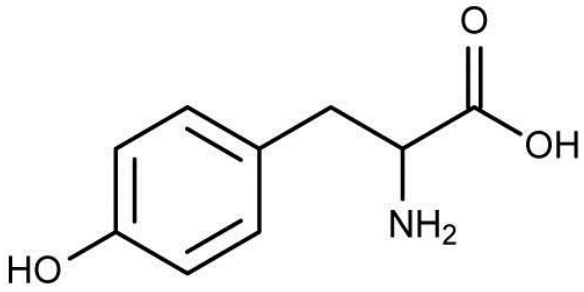

Figure 1.3 Molecular structure of tyrosine.

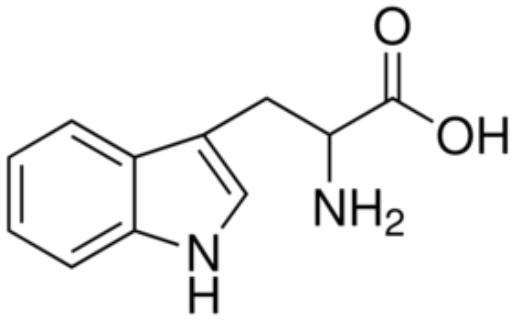

Figure 1.4 Molecular structure of tryptophan.

Typically, terrigenous organic matter is associated with a darker colour and relatively high amounts of aromatic and phenolic compounds, while autochthonous organic matter is lighter in colour and contains relatively low amounts of aromatic and phenolic groups (Eikebrokk et al. 2006). This colour can be described by the specific absorption coefficient of the DOC at 340 nm (SAC_{340}). A higher SAC_{340} (indicating terrigenous C) has been shown to decrease Cu bioavailability more than organic matter with a lower SAC_{340} (Schwartz et al. 2004). NOM origin can also be approximated using

fluorescence indices, as proposed by McKnight et al. (2001). A fluorescence index (FI) of approximately 1.4 and 1.9 indicates terrestrially-derived and microbially-derived NOM, respectively.

1.3 Effect of NOM on Copper Toxicity

The wide variety of binding sites in NOM decreases the toxicity of copper. Binding to NOM allows copper to form complexes that reduce the bioavailability of copper resulting in a protective effect (Arnold 2005; Santore et al. 2001). Increased NOM concentrations has been shown to be protective in marine organisms such as the blue mussel, *Mytilus sp.* (DePalma et al. 2011a; Nadella et al. 2009), the rotifer, *Branchionus plicatilus* (Arnold et al. 2010), and the sea urchin (*Parecentrotus lividus*) (Lorenzo et al. 2006). For instance, in the case of the blue mussel, *Mytilus trossolus*, the addition of 2.5 - 20 mg C L^{-1} DOC increased the reported EC_{50} value from 9.6 µg/L to 24 - 39 µg/L (Nadella et al. 2009).

The amount of DOC present in the system has been found to be predictive of toxicity to an organism. The relationship can be described using the equation $EC_{50} = 11.22\ DOC^{0.6}$ (Arnold et al. 2006). However this relationship does not take into account the source and molecular composition of the organic matter. The different sources and compositions of organic matter may influence the ability of NOM to protect against copper toxicity despite current toxicity models utilizing NOM in a homogeneous manner. Different NOM sources show variation in copper complexing capacities that could have an overall effect on NOM protection to copper toxicity (De Schamphelaere et al. 2004). Darker, terrigeneous organic matter has been found to provide a larger protective effect

against copper toxicity to organisms than ligher, microbially-derived organic matter (Luider et al. 2004; Pempkowiak et al. 1999; Schwartz et al. 2004). This is in agreement with Lorenzo et al. in which humic acids (2002) and fulvic acids (2006) (associated with terrigeneous NOM) proved protective to the sea urchin, *Paracentrotus lividus* against copper toxicity. Lorenzo and associates also suggest that fulvic substances are more relevant and protective than humic substances as it was found that the copper-humic substance complex may be partially available for uptake by an organism thereby reducing the protective effect (Lorenzo et al. 2005). These results were also observed in the blue mussel, *Mytilus trossolus*, when three different freshwater isolate NOM sources were studied (Nadella et al. 2009). The most protective NOM source was found to contain a 20% and 40% higher fulvic substance content than the two less protective NOM sources. This corresponded to 40% and 60% less protectivity, respectively, to the blue mussel (Nadella et al. 2009). In contrast, De Palma et al. (2011 & 2011a) found that the molecular composition of NOM from natural water samples did not significantly affect NOM protectivity to copper toxicity. Thus, the predictive EC_{50} equation determined by Arnold et al. (2006) remained consistent regardless of the NOM quality in this case. Due to the limited knowledge of how differences in NOM affects copper toxicity in marine systems, there is a need for further research in this area.

1.4 Biotic Ligand Model

In freshwater, a biotic ligand model (BLM) has been implemented as a predictive tool to estimate site-specific bioavailability and subsequent toxicity of metals, including copper. The BLM is a quantitative framework that can assess metal toxicity using bulk water quality measurements such as alkalinity, hardness, pH and DOC (measure of NOM). These qualities are used as input parameters to predict toxicity, thereby allowing site-specific water criteria guidelines to be determined (Paquin et al 2002). It predicts toxicity at the biotic ligand (ex. the gill of a fish) based on equilibration calculations of metal speciation. This model also takes into account the metal-biotic ligand interactions and the effect of competing cations in the system (Di Toro et al. 2001). The BLM for freshwater has been adopted as a regulatory tool by the U.S. EPA (2007) for copper however there is need for a BLM in saltwater environments. Investigations pertaining to salt water are currently underway for application of a marine BLM; however more information is needed before being accepted for regulatory use (Arnold 2005). This research supplements the development and implementation of a BLM for use in marine environments with focus on the free copper species.

A schematic of the BLM can be found in Figure 1.5. The BLM assumes that toxicity is proportional to the accumulation of metal at the biotic ligand. However, different factors in the water can affect this interaction. Cations such as calcium and sodium can compete with the bioavailable metal for binding to the biotic ligand. As well, organic and inorganic ligands in the water can form metal complexes decreasing the availability of the metal to interact with the biotic ligand. Some of the factors influencing

the bioavailability of copper are pH, alkalinity, salinity and NOM (Santore et al. 2001). At low pH, organic particle surface sites for binding become less available to bind metals, thus more free metal exists to cause toxicity (Millero et al. 2009). However, as pH increases the copper is able to form more copper complexes since fewer binding sites on NOM are protonated, thus decreasing the bioavailability of copper to cause toxicity (Santore et al. 2001). As well, there is an increase in copper hydroxide formation, reducing the amount of free copper (Paquin et al. 2000; Santore et al. 2001). Alkalinity with respect to copper toxicity has also shown to be protective. Increased cations such as Ca^{2+} and Mg^{2+} protect against copper toxicity by increasing the competition for copper binding at the biotic ligand (Santore et al. 2001). This is similar to salinity which also has been found to protect marine organisms against copper toxicity. Increased salinity increases the amount of inorganic ligand-copper complexation as well as increases the competition for uptake by the marine organisms with other cations such as Na^{+}, Mg^{2+} and Ca^{2+} (De Polo & Scrimshaw 2012).. As mentioned in Sections 1.2 and 1.3, the wide variety of binding sites in NOM also decreases the toxicity of copper. Binding to NOM allows copper to form complexes that reduce the bioavailability of copper resulting in a protective effect (Arnold 2005; Santore et al. 2001).

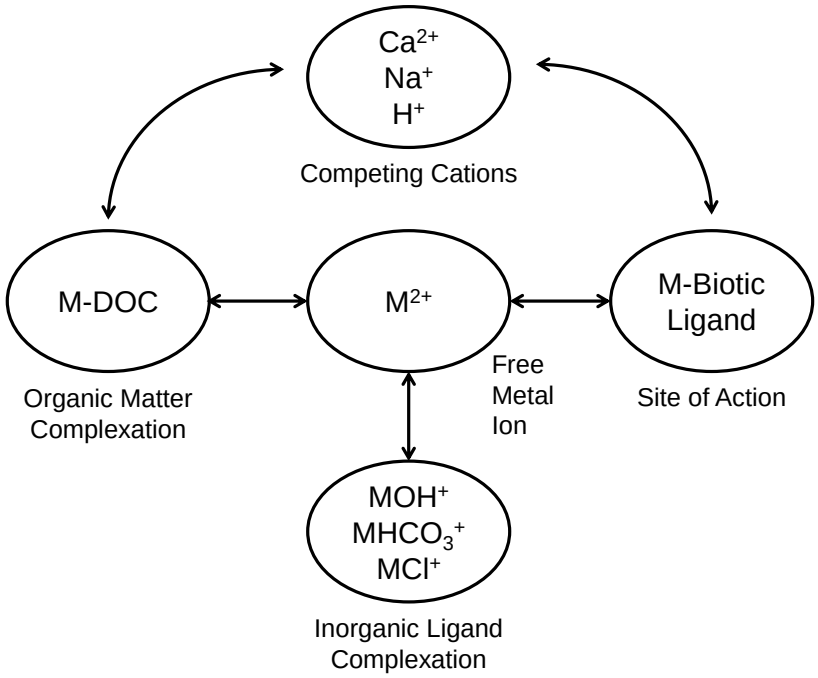

Figure 1.5 Schematic diagram of the Biotic Ligand Model (Adapted from Di Toro et al. 2001).

1.5 Toxicity Assays

Toxicity assays performed for this research used the rotifer species, *Branchionus plicatilus*. Assays were performed following the protocol recommended by the American Society for the Testing of Materials (ASTM 2004). Modifications described by Arnold et al. (2010) to increase the acute exposure time from 24 to 48 hours was also applied to the ASTM (2004) method. Further information regarding the toxicity assay parameters can be found in Chapter 3. *Brachionus plicatilis* is a euryhaline rotifer which are small zooplankton with a typical size of 0.1-1 mm in length (Biodiversity Institute of Ontario 2008). Rotifers are named for the corona at their head which resembles spinning wheels (rota (latin) = wheel and fera (latin) = to bear). The corona is used for movement and food acquisition. The mastax is the muscular pharynx of the rotifer containing a set of

hard jaws for grinding food. The posterior end of the rotifer is called the foot which can be used to anchor the rotifer (Biodiversity Institute of Ontario). A schematic of the rotifer, *Brachionus plicatilis* can be seen in Figure 1.6. *Brachionus plicatilis* have been previously reported as osmoconformers (Epp and Winston 1977) however recent literature suggests they are osmoregulators due to increased Na^+/K^+ ATPase activity in response to salinity consistent with other osmoregulating euryhaline invertebrates (Lowe et al. 2005). An increase in salinity results in an increase in Na^+/K^+ ATPase. This suggests that at increased salinities rotifers may be more sensitive due to an increase of stress on the rotifer from an increase in energetic cost to osmoregulate at higher salinities (Lowe et al. 2005).

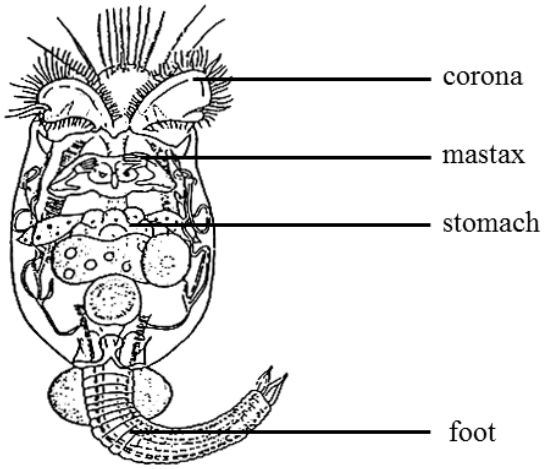

Figure 1.6 Schematic drawing of the rotifer, *Brachionus plicatilis* (Adapted from FAO 1996).

Rotifers are an ideal organism for aquatic toxicity testing due to their ecological impact in coastal marine environments. Rotifers exert grazing pressures due to feeding on phytoplankton and bacteria (Gilbert & Bogdan 1984), and are an important food

source for planktivorous fish, copepods and insect larvae (Biodiversity Institute of Ontario 2008; O'Brian 1979). In addition to the ecological significance of rotifers, there are many other reasons why they are an ideal organism to study copper toxicity in saltwater systems. *Brachionus plicatilis* have been found to be very sensitive to toxicants such as copper (Arnold et al. 2010). As well, these rotifers can survive 80 hours before the effect of food deprevation begins to cause toxicity allowing for acute studies without a feeding requirement (ASTM 2004). *Brachionus plicatilis* can be successfully cultured in a wide range of salinities from 0 to 40 ppt (Minkoff et al. 1983) and up to 97 ppt (Lubzens et al. 2001) allowing for the study of estuarine environments. In addition, rotifers are commercially available and toxicity assays are relatively easy and fast to perform due to their rapid reproduction rates and short generation times (ASTM 2004).

1.6 Ion Selective Electrode

An ion selective electrode (ISE) is a non-destructive tool that can be used to measure free copper (Cu^{2+}) by measuring the electrical potential developed across the sensing membrane of the electrode (Skoog et al. 2007). In the case of copper, this membrane is composed of a mixture of silver sulfide with copper sulfide (Ag_2S/CuS). The membrane contains a fixed activity of cupric ion, which is permeable to the membrane (Ross 1969). When the electrode is placed in a sample there is a flux of cupric ions across the membrane in the direction of lesser cupric ion activity. Since these ions carry a charge, a potential is developed across the membrane (Ross 1969). The developed potential is dependent on the concentration of free copper in the sample. This potential is

measured against a constant reference potential using a reference electrode and can be described by the Nernst equation (Ross 1969; Skoog et al. 2007) where,

$$E = E^o - \frac{RT}{nF}\ln(\mathrm{Q}) \qquad \text{Equation 1.1}$$

Where, E and E° are the measured electrode potential and the reference potential (constant), respectively. R is the gas constant (8.315 J mol^{-1} K^{-1}), T is the temperature in Kelvin, n is the ionic charge, and F is the Faraday constant (96487 C mol^{-1}). Q is the reaction quotient in terms of activity of the reactant (α_{cu2+}) and product species. For copper, this becomes

$$E = E^o - \frac{RT}{nF}\ln\frac{1}{a_{\mathrm{Cu2+}}} \qquad \text{Equation 1.2}$$

Accounting for the constants, assuming room temperature (298 K) and converting from the natural logarithm to the base ten logarithm by multiplying by 2.303, the equation can now be written as

$$E = E^o - \frac{0.0592}{2}\log\frac{1}{a_{\mathrm{Cu2+}}} \qquad \text{Equation 1.3}$$

The resulting electrode slope should therefore be approximately 29.6 mV per decade in a correctly working copper electrode. For copper, pCu is the negative logarithm of the cupric ion activity, thus the copper electrode provides a direct measure of the pCu in solution (Skoog et al. 2007). Thus the equation can now become,

$$E = E^o - 0.0296\ \mathrm{pCu} \qquad \text{Equation 1.4}$$

Since free copper is thought to be the most bioavailable species to cause toxicity, accurate values of free copper are needed and it is believed that ISE techniques may reflect the true speciation of copper in aquatic systems. However, the observance of chloride interference of the Cu ISE in high chloride media has limited the use of Cu ISEs in sea water (Jasinski, Trachtenberg & Andrychuk 1974; Westall, Morel & Hume 1979). Belli and Zirino (1993) examined the performance of the Cu ISE across a range of chloride concentrations (0 to 1.0 M NaCl) and found that the Cu ISE responded well in all cases. The Cu ISE has since been used to measure free copper at at a variety of sites including San Diego Bay (Rivera-Duarte & Zirino 2004) and Pearl Harbour (Chadwick et al. 2008). Recent literature has also found that free Cu^{2+} better correlated to observed toxicity than anodic stripping voltammetry (Eriksen et al. 2001, 2001a). Thus, Cu ISE will be used to measure free copper in this project.

1.7 Anodic Stripping Voltammetry

Anodic stripping voltammetry (ASV) techniques were utilized to determine total copper throughout the course of this project. ASV is a non-destructive technique that involves the deposition of the analyte onto the working electrode which behaves as a cathode during this first step. The working electrode is a mercury drop (Skoog et al. 2007). For copper, this deposition step concentrates the copper in the solution by plating it onto the electrode to form a copper amalgam by reducing the free copper in solution from Cu^{2+} to Cu^{0}. After the deposition stage, the electrode carries out an anodic sweep in which the potential of the electrode is increased to more positive potential values. This redissolves (or strips) the copper from the electrode back into solution. During this

stripping step, the copper is being oxidized back to its original form (from Cu^0 to Cu^{2+}) (Skoog et al. 2007). The analyte will be stripped from the working electrode based on its oxidation potential, which is unique to each metal (Wang 2006). For copper, the peak potential can be found at -0.1 V versus an Ag/AgCl reference electrode. This method is advantageous in trace metal analysis since the preconcentration step allows for very low detection limits (Skoog et al. 2007). A longer deposition time results in lower detection limits. Figure 1.7 shows an example of the excitation signal as voltage versus time as well as the resulting voltammogram for cadmium and copper. The peak height of each analyte is proportional to the concentration of the analyte in the bulk solution. This is due to the flow of electrons during the stripping step. Electrons are generated during oxidation of the analyte and these electrons create a current which is measured. With increasing analyte concentrations, more electrons are released during the oxidation process, thus the generated current (and therefore peak height) will also be increased.

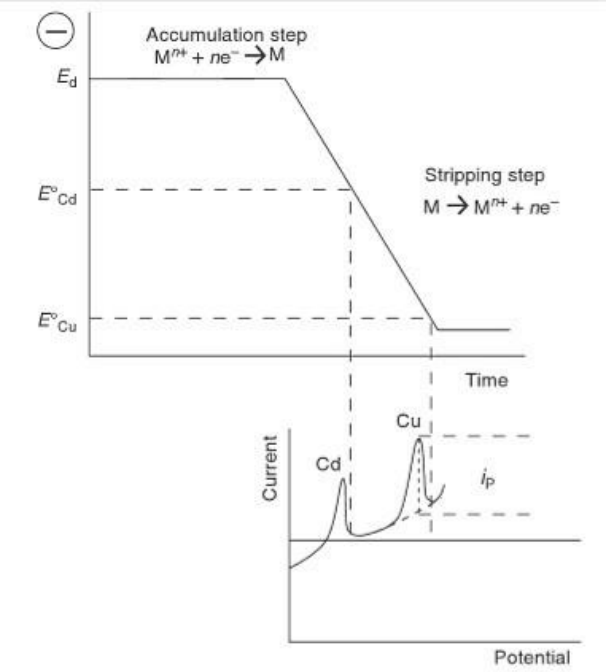

Figure 1.7 Example of the excitation signal (top) and resulting voltammogram (bottom) using anodic stripping voltammetry for the analytes, cadmium and copper (Wang 2006). Note: The peak height, i_p, of each analyte from the voltammogram is proportional to the concentration of the analyte in the bulk sample solution.

To determine the total metal concentration, standard addition techniques are typically performed after oxidation (H_2O_2) and UV digestion. Voltammetry only measures labile copper (free copper and copper complexed to inorganic ligands). Copper complexed by organic matter are not detected by ASV. Thus, digestion of the NOM in each sample is performed prior to analysis to ensure all the copper in the sample exists in the form of free or inorganic copper complexes.

Standard addition is a technique which involves the successive addition of a standard solution containing the analyte being measured in one or more increments to the sample solution (Skoog et al. 2007). The original sample and the sample after each addition are measured. The original concentration of the sample can then be determined

by extrapolating a line through the data back through the x-intercept (Skoog et al. 2007). An example of the standard addition method can be seen in Figure 1.8. The standard addition technique is advantageous because it ensures that the instrument response is due only to changes in analyte concentration, rather than from components within the sample matrix that could interfere with the analyte signal (Skoog et al. 2007).

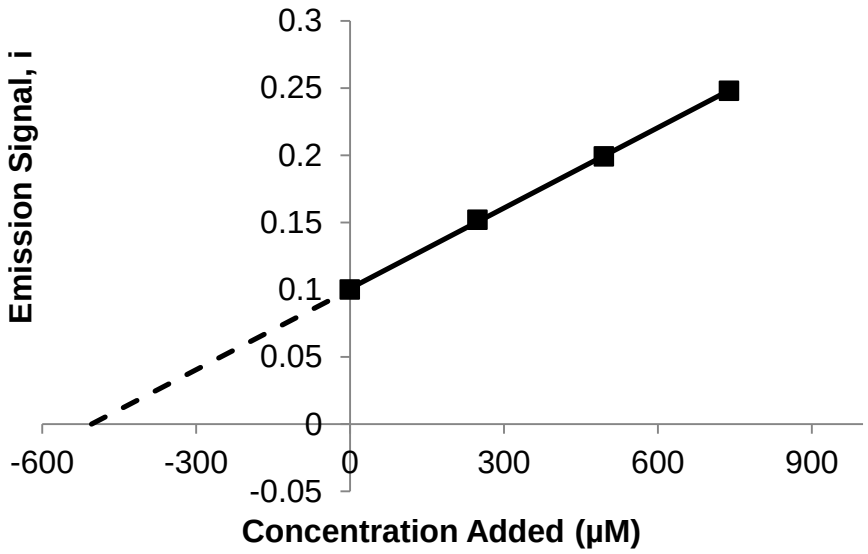

Figure 1.8 Visual representation of the standard addition technique showing experimental data points and extrapolation back through the x-intercept to determine original sample concentration (Recreated from Skoog et al. 2007).

1.8 Fluorescence

Fluorescence techniques can be used to characterize NOM and metal speciation (Chen et al. 2003; da Silva et al. 1998; Mackey 1983; Smith & Kramer 2000). NOM can be used for fluorescence techniques due to the presence of aromatic structural groups with electron-donating functional groups (Chen et al. 2003). A Jablonski diagram (Figure 1.9) illustrates the electron transfers which can occur. The first step is the transition of an electron from a lower energy level to a higher energy level. When light

from an external source interacts with a fluorescent molecule (fluorophore) the molecule can absorb the light energy and be promoted to a higher energy (excited) state. Once excited, a molecule can return to ground state through a variety of non-radiative transitions (vibrational relaxation and internal conversion) or through radiative processes (fluorescence and phosphorescence) (Skoog et al. 2007). Relaxation of the electron within vibrational levels results in vibrational relaxation. Internal conversion occurs in cases where a vibrational energy level is coupled to a vibrational level in a lower electronic energy level. Phosphorescence occurs due to intersystem crossing of an electron from an excited singlet state to an excited triplet state then deactivation back to ground state. The probability of this occurring is enhanced if the vibrational levels of two states overlap (like internal conversion). Both phosphorescence and fluorescence occurs when a photon is emitted.

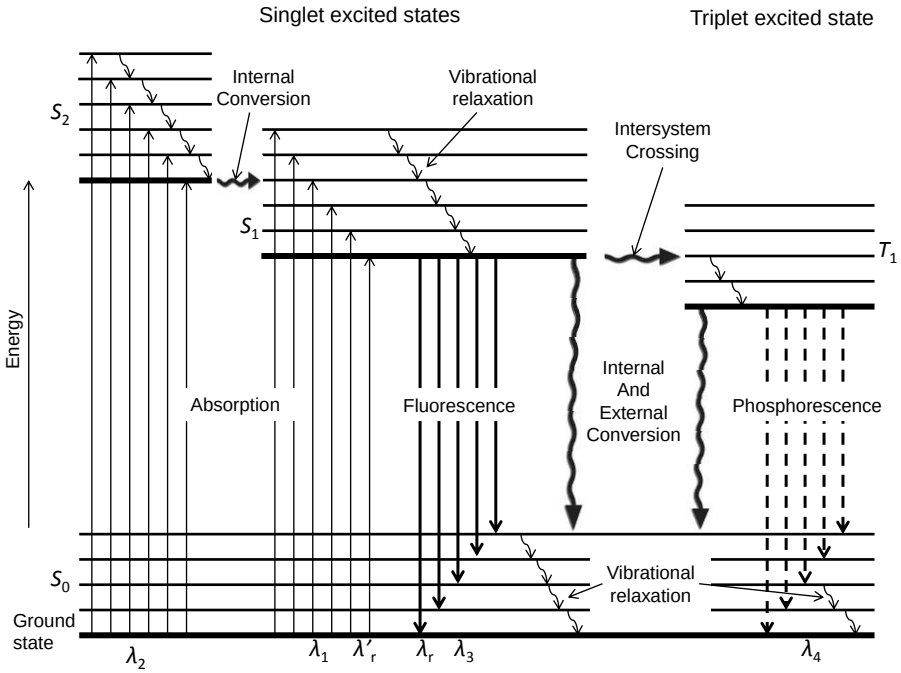

Figure 1.9 Jablonski diagram (Recreated from Skoog et al. 2007)

1.8.1 Fluorescence Excitation-Emission Matrix

The different fluorophores within a heterogenous system can be distinguished based on different fluorescent properties. The compilation of data from simultaneously measuring excitation and emission wavelengths result in a fluorescence excitation-emission matrix (FEEM). An FEEM provides qualitative information on the chemical composition of NOM based on the intensities and positions of the fluorophores in the matrix. Terrigenous components (humic and fulvic acids) fluoresce at longer wavelengths than proteinaceous components (Baker 2001). Fulvic and humic-like components can be detected in the Ex/Em ranges of 300-350 nm/400-450 nm and 250-390 nm/460-520 nm, respectively (McKnight et al. 2001; Smith & Kramer 1999; Stedmon & Markager 2005; Wu et al 2003). Microbially-derived carbon can be detected in the Ex/Em ranges of 225-275 nm/350 nm and 225-270 nm/300 nm representing tryptophan and tyrosine-like components, respectively (Baker 2001; Stedmon and Markager 2005). NOM characterization using this method has been used to identify components in aquatic systems ranging from freshwater (Cory & McKnight 2005; Winter et al. 2007) to seawater (Coble 1996; Cory & McKnight 2005). An example of an FEEM contour plot can be seen in Figure 1.10.

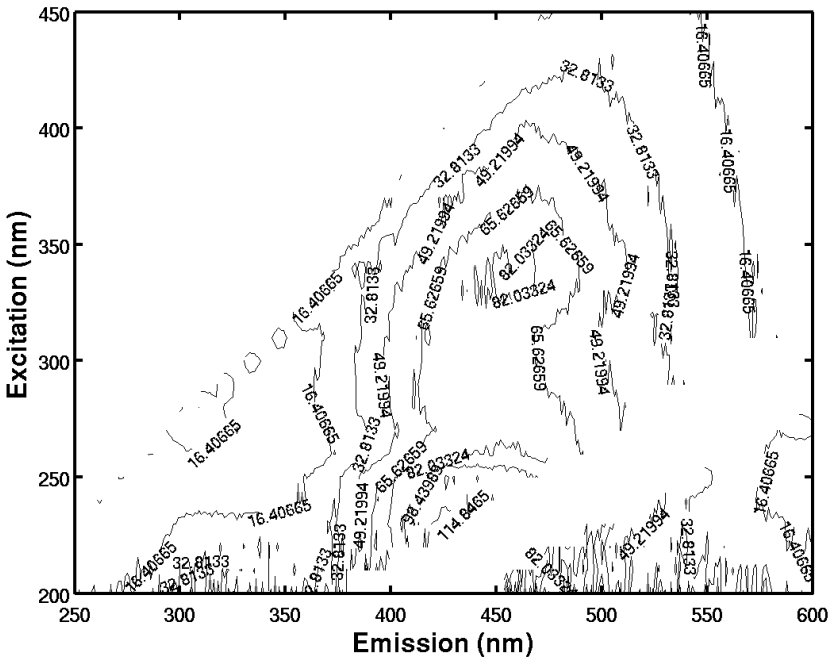

Figure 1.10 FEEM contour plot for the freshwater NOM isolate Luther Marsh. Between approximately 400 – 500 nm there are emission maxima corresponding to two excitation maxima at approximately 270 nm and 325 nm representing humic and fulvic fractions.

Parallel factor analysis (PARAFAC) can be used to determine the relative quantities of the humic, fulvic, tryptophan and tyrosine-like components observed by fluorescence. Through spectral deconvolution of a stack of FEEMs, PARAFAC is able to quantify the minimum number of components to describe each FEEM (Stedmon & Bro 2008). PARAFAC models 3-way data sets of excitation, emission and fluorescence intensity using the following equation (Stedmon & Bro 2008),

$$x_{ijk} = \sum_{f=1}^{F} a_{if} b_{if} c_{kf} + \varepsilon_{ijk} \ , i = 1,.,I; j = 1,.,J; k = 1,.,K; \qquad \text{Equation 1.5}$$

Where x_{ijk} is the FEEM with of the i^{th} sample with j emission wavelength and k excitation wavelength with dimensions I, J and K. $\mathcal{E}_{ijk}$ is the residual mathematical noise

(unexplained signal) not accounted for in PARAFAC. *a*, *b* and *c* represent the abundance (concentration), emission spectra, and excitation spectra of the resolved fluorophores, respectively. For *F* number of resolved fluorophores, the measured signal is the sum of the contribution from each and can be calculated using the above equation (Stedmon & Bro 2008).

1.8.2 Fluorescence Quenching

The fluorescence of NOM is known to be quenched in the presence of metals such as copper (da Silva et al. 1998). Since there is a relationship between fluorescence intensity and metal concentration, fluorescence quenching techniques can be used for copper speciation analysis and will be used in this study (Chen et al. in press; da Silva et al. 1998; Smith & Kramer 2000). Fluorescence quenching of NOM due to increasing concentrations of copper is primarily due to static quenching (da Silva et al. 1998), in which the quencher interacts with the ground state fluorophore to form the 'dark' complex, thereby decreasing the fluorescence (Skoog et al. 2007).

The fluorescence quenching curve can be fitted with a Ryan Weber equilibrium model (See Equation 1.6) where *I* is the overall fluorescence intensity, C_M and C_L are the total metal and ligand concentrations, respectively, *K* is the conditional stability constant and I_{ML} is a limiting value below which fluorescence will no longer decrease with metal addition (Ryan & Weber 1982). Using this model, the stability constants (log*K*) and binding capacities (L_T) of the NOM can be determined.

$$I = \left(\frac{(I_{ML}-100)}{2KC_L}\right)\left[(KC_L + KC_M + 1) - \sqrt{(KC_L + KC_M + 1)^2 - 4K^2C_LC_M}\right] \quad \text{Equation 1.6}$$

The amount of free NOM and copper-NOM complexes can be calculated as a function of the log*K* and binding capacities of the NOM (da Silva et al. 1998; Smith & Kramer 2000). From these values, the total metal concentration can be calculated and the amount of free and bound copper can then be determined (Smith & Kramer 2000). Fluorescence quenching in freshwater has been validated for aluminum with salicyclic acid and 2-hydroxy-3-napthoic acid by Smith et al. (1998). Hernández et al. (2006) were able to solve for log*K* and binding capacity of copper with humic acids in pig slurries and amended soils. Suwannee River fulvic acid (SRFA) titrations with copper validated copper fluorescence quenching by its ability to predict free copper (Smith & Kramer 2000). In addition, preliminary work using fluorescence quenching techniques has validated fluorescence quenching methods for copper in marine environments using Luther Marsh organic matter in artificial seawater (Diamond 2012).

1.9 Research Goals and Objectives

The objectives of this research are summarized as follow:

1. To determine true copper speciation in seawater using literature methods and new techniques to determine which techniques offer the most accurate measurement of copper speciation.

2. To validate a new method for determining free copper using a Cu ISE in seawater.

3. To apply an integrated approach to investigate the effect of DOC source on copper speciation and toxicity in aquatic organisms.

The first and second objectives will be addressed in Chapter 2: Internal calibration flow-through ISE method for determining Free Cu in salt water. A published literature Cu ISE method was used to measure free copper of natural marine waters. A new method for measuring free copper using ISE was developed, validated and compared to the data from the published literature to establish a more reliable method to measure free copper.

Objective three will be fulfilled by Chapter 3: Influence of DOC source on free copper and toxicity to *Brachionus plicatilis*. Toxicity studies while simultaneously measuring copper speciation will be performed using the rotifer, *Brachionus plicatilis*. Copper speciation during these toxicity studies will be measured using ISE, ASV and fluorescence quenching techniques. DOC quality will be characterized using fluorescence techniques.

Chapter 4: Characterization of NOM interactions with copper in natural sea water using fluorescence quenching will also tie into objective one and three. In this chapter, DOC characteristics such as stability constants and binding capacities of the DOC will be determined using fluorescence quenching techniques. The relation of these parameters to the toxicity observed in Chapter 3 will be discussed. In addition, free copper will be calculated using the fluorescence data and compared to free copper measurements made in Chapter 3. These comparisons will help validate both the Cu ISE and fluorescence spectroscopy methods for measuring free copper in marine systems, thereby helping to accomplish objective one.

The findings of these three chapters and future work in these areas will be summarized in Chapter 5: Conclusions and Future Work. Supplementary information

can be found in the attached Appendices. Appendix A includes an example for solving simultaneous chemical equilibria and the resulting MATLAB scripts used to determine free copper in Chapter 2. Appendix B provides supplementary information related to Chapter 3 including the DOC characteristics of all water samples, the effects of salting up of samples on toxicity and fluorescence excitation-emission contour plots. Appendix C provides the matlab scripts for determining contribution of fluorophores within NOM to total fluorescence and the resulting multiresponse fitting to determine binding characteristics and copper speciation. Plots of the resulting fitting and comparison of modelled and measured free copper are also provided.

1.10 Significance of Research

It has been suggested that in some cases there is an overestimation of copper toxicity when determining copper load limits into the environment due to different water chemistries and what metal species are present in the system (Paquin et al. 2002). Understanding the speciation of copper and the species that are bioavailable to cause toxicity can help determine more accurate site-specific guidelines for copper water quality criteria in saltwater environments. Obtaining reliable and true copper speciation measurements in saltwater environments is crucial if bioavailability models are to be accurate and provide a robust method for determining and predicting toxicity. Information resulting from this study can be used to expand the use of the BLM for application in salt water and strengthen the validity of a saltwater BLM to be used for regulatory purposes.

The measurement of true copper speciation is also crucial for determining copper toxicity over different NOM concentrations and compositions. Currently only the concentration of DOC is used as an input parameter for the BLM (U.S. EPA 2007). If DOC composition relationships are found to have an effect on toxicity then this information can be incorporated into a saltwater BLM to provide a better estimate of toxicity. The information obtained from this project will aid in the development and implementation of a saltwater BLM to determine site-specific regulations and guidelines for copper load limits into marine systems.

1.11 References

American Society for the Testing of Materials International (ASTM). 2004. Standard guide for acute toxicity test with the rotifer Brachionus. E 1440-91. Annual book of ASTM standards. Vol 11.05. West Conshohocken, PA, 830-837.

Arnold, W.R., 2005. Effects of dissolved organic carbon on copper toxicity: implications for saltwater copper criteria. *Integrated Environmental Assessment and Management*. **1**, 34-39.

Arnold, W.R., Cotsifas, J., Corneillie, K.M. 2006. Validation and update of a model used to predict copper toxicity to the marine bivalve *Mytilus sp*. *Environmental Toxicology*. **21**, 65-70.

Arnold, W.R., Diamond, R.L., Smith, D.S. 2010. The effects of salinity, pH, and dissolved organic matter on acute copper toxicity to the rotifer, *Brachionus plicatilis* ("L" strain). *Archives of Environmental Contamination and Toxicology*. **59**, 225-234.

Baker, A., 2001. Fluorescence excitation–emission matrix characterization of some sewage-impacted rivers. *Environmental Science and Technology.* **35**, 948–953.

Belli, S.L., Zirino, A. 1993. Behaviour and calibration of the copper(II) ion-selective electrode in high chloride media and marine waters. *Analytical Chemistry*. **65**, 2583-2589.

Benner, R. Chemical composition and reactivity. In: Hansell, D.A., Carlson, C.A. (Eds.), Biogeochemistry of Marine Dissolved Organic Matter. Elsevier, USA, 59–90. 2002.

Biodiversity Institute of Ontario, Paul D. N. Hebert (Lead Author);Mark McGinley (Topic Editor) "Rotifera". In: Encyclopedia of Earth. Eds. Cutler J. Cleveland (Washington, D.C.: Environmental Information Coalition, National Council for Science and the Environment). [First published in the Encyclopedia of Earth November 18, 2008; Last revised Date November 18, 2008; Retrieved June 11, 2012 <http://www.eoearth.org/article/Rotifera>

Birdwell, J.E., Engel, A.S. 2009. Variability in terrestrial and microbial contributions to dissolved organic matter fluorescence in the Edwards Aquifer, central Texas. *Journal of Cave and Karst Studies*. **71**(2), 144-156.

BC MOE (British Columbia Ministry of the Environment). Water Quality Criteria for Copper. Available at http://www.env.gov.bc.ca/wat/wq/BCguidelines/copper/copper.html#toc.

CCREM (Canadian Council of Resource and Environment Ministers). 1987. Canadian Water Quality Guidelines. Prepared by the Task Force on Water Quality Guidelines of the Canadian Council of Resource and Environment Ministers.

Chadwick, D.B., Rivera-Duarte, I., Rosen, G., Wang, P.F., Santore, R.C., Ryan, A.C., Paquin, P.R., Hafner, S.D., Choi, W. 2008. Demonstration of an integrated model for predicting copper fate and effects in DoD harbors. SPAWAR Technical Report 1972. Project ER-0523.

Chen, J., LeBoeuf, E.J., Dai, S., Gu, B. 2003. Fluorescence spectroscopic studies of natural organic matter fractions. *Chemosphere*. **50**, 639-647.

Chen, W., Smith, D.S., Guéguen, C. 2013. Influence of water chemistry and dissolved organic matter (DOM) molecular size on copper and mercury binding determined by multiresponse fluorescence quenching. *Chemosphere*. In press.

Coble, P.G. 1996. Characterization of marine and terrestrial DOM in seawater using excitation-emission matrix spectroscopy. *Marine Chemistry*. **51**(4), 325-346.

Cory, R.M., McKnight, D.M. 2005. Fluorescence spectroscopy reveals ubiquitous presence of oxidized and reduced quinones in dissolved organic matter. *Environmental Science and Technology*. **39**, 8142–8149.

da Silva, J.C.G.E, Machado, A.A.S.C., Oliveira, C.J.S., Pinto, M.S.S.D.S. 1998. Fluorescence quenching of anthropogenic fulvic acids by Cu(II), Fe(III) and UO^{2+}_2. *Talanta*. **45**, 1155-1165.

DePalma, S.G.S., Arnold, W.R., McGeer, J.C., Dixon, D.G., Smith, D.S., 2011. Variability in dissolved organic matter fluorescence and reduced sulfur concentration in coastal marine and estuarine environments. *Applied Geochemistry*. **26**, 394-404.

DePalma, S.G.S., Arnold, W.R., McGeer, J.C., Dixon, D.G., Smith, D.S., 2011a. Effects of dissolved organic matter and reduced sulphur on copper bioavailability in coastal marine environments. *Ecotoxicology and Environmental Safety*. **74**, 230-237.

De Polo, A., Scrimshaw, M. 2012. Challenges for the development of a biotic ligand model predicting copper toxicity in estuaries and seas. *Environmental Toxicology and Chemistry*. **31** (2), 230-238.

De Schamphelaere, K.A.C., Vasconcelos, F.M., Tack, F.M.G., Allen, H.E., Janssen, C.R. 2004. Effect of dissolved organic matter source on acute copper toxicity to *Daphnia magna*. *Environmental Toxicology and Chemistry*. **23**(5), 1248-1255.

Diamond, R.L. 2012. Characterizing dissolved organic matter and Cu^{2+}, Zn^{2+}, Ni^{2+}, and Pb^{2+} binding in salt water and implications for toxicity. MSc. Thesis. Wilfrid Laurier University. Waterloo, Ontario.

Di Toro, D.M. Allen, H.E., Bergman, H.L., Meyer, J.S., Paquin, P.R., Santore, R.C. 2001. Biotic ligand model of the acute toxicity of metals 1. Technical basis. *Environmental Toxicology and Chemistry*. **20**, 2383-2396.

Donat, J.R., Lao, K.A., Bruland, K.W. 1994. Speciation of dissolved copper and nickel in South San Francisco Bay: a multi-method approach. *Analytica Chimica Acta*, **284**, 547–571.

Eikebrokk B., Juhna, T., Østerhus, S.W. 2006. Water treatment by enhanced coagulation – Operational status and optimization issues. Techneau Report D 5.3.1a.

Epp, R.W., Winston, P.W. 1977. Osmotic regulation in the brackish-water rotifer *Brachionus plicatilis*. *The Journal of Experimental Biology*. **68**, 151-156.

Eriksen, R.S., Nowak, B., van Dam, R.A. 2001. Copper speciation and toxicity in a contaminated estuary. Supervising Scientist Report 163. Department of Sustainability, Environment, Water, Population and Communities, Canberra, Australia.

Eriksen, R.S., Mackey, D.J., van Dam, R., Nowak, B. 2001a. Copper speciation and toxicity in Macquarie Harbour, Tasmania: an investigation using a copper ion selective electrode. *Marine Chemistry*. **74**, 99-113.

FAO (Food and Agriculture Organization of the United Nations). 1996. Manual on the production and use of live food for aquaculture. FAO Fisheries Technical Paper 361.

Flemming, C.A., Trevors, J.T. 1989. Copper toxicity and chemistry in the environment: A review. *Water, Air, and Soil Pollution*. **44**, 143-158.

Gilbert, J.J., Bogdan, K.G. Rotifer Grazing: In Situ Studies on Selectivity and Rates. In: Meyers, D.G., Strickler, J.R. (Editors). Trophic Interactions Within Aquatic Ecosystems, AAAS Selected Symposium, vol. 85, Westview Press, Inc. 1984. p.97-133.

Government of Canada. 2003. Water and Canada: Preserving a Legacy for People in the Environment.

Grosell, M., Wood, C.M. 2002. Copper uptake across rainbow trout gills: Mechanisms of apical entry. *The Journal of Experimental Biology*. **205**, 1179-1188.

Harris, Z.L., Gitlin, J.D. 1996. Genetic and molecular basis for copper toxicity. *The American Journal of Clinical Nutrition*. **63**, 836S-841S.

Hernández, D., Plaza, C., Senesi, N., Polo, A. 2006. Detection of copper (II) and zinc (II) binding to humic acids from pig slurry and amended soils by fluorescence spectroscopy. *Environmental Pollution*. **143**, 212-220.

Hunter, K.A., Liss, P.S. Organic sea surface films. In: Duursma, E.K., Dawson, R. (Editors). Marine Organic Chemistry: Evolution, composition, interactions and chemistry of organic matter in seawater. New York (NY): Elsevier/North-Holland Inc; 1981. p. 259-297.

International Copper Association (ICA). 1995. The biological importance of copper: A literature review. ICA Project No. 223.

Jasinski, R., Trachtenberg, I., Andrychuk, D. 1974. Potentiometric measurement of copper in seawater with ion selective electrodes. *Analytical Chemistry*. **46** (3), 364-369.

Kogut, M.M., Voelker, B.M. 2001. Strong copper-binding behavior of terrestrial humic substances in seawater. *Environmental Science and Technology*. **35**, 1149-1156.

Lorenzo, J.I., Nieto, O., Beiras, R., 2002. Effect of humic acids on speciation and toxicity of copper to Paracentrotus lividus larvae in seawater. *Aquatic Toxicology*. **58**, 27-41.

Lorenzo, J.I., Beiras, R., Mubiana, V.K., Blust, R. 2005. Copper utake by mytilus edulis in the presence of humic acids. *Environmental Toxicology and Chemistry*. **24**(4), 973-980.

Lorenzo, J.I., Nieto, O., Beiras, R., 2006. Anodic stripping voltammetry measures copper bioavailability for sea urchin larvae in the presence of fulvic acids. *Environmental Toxicology and Chemistry*. **25**, 36-44.

Lowe, C.D., Kemp, S.J., Bates, A.D., Montagnes, D.J.S. 2005. Evidence that the rotifer Brachionus plicatilis is not an osmoconformer. *Marine Biology*. **146**, 923-929.

Lubzens, E. Zmora, O., Barr, Y. 2001. Biotecnology and aquaculture of rotifers. *Hydrobiologia*. **446/447**, 337-353.

Luider, C.D., Crusius, J., Playle, R.C., Curtis, P.J. 2004. Influence of natural organic matter source on copper speciation by Cu binding to fish gills, by ion selective electrode and by DGT gel samles. *Environmental Science and Technology*. **38**, 2865-2872.

Mackey, D.J. 1983. Metal-organic complexes in seawater – An investigation of naturally occurring complexes of Cu, Zn, Fe, Mg, Ni, Cr, Mn and Cd using high-performance liquid chromatography with atomic fluorescence detection. *Marine Chemistry*. **13**, 169-180.

McKnight, D.M., Boyer, E.W., Westerhoff, P.K., Doran, P.T., Kulbe, T., Andersen, D.T. 2001. Spectrofluorometric characterization of dissolved organic matter for indication of precursor organic material and aromaticity. *Limnology and Oceanography*. **46** (1), 38-48.

Millero, F.J., Woosley, R. Ditrolio, B., Waters, J. 2009. Effect of ocean acidification on the speciation of metals in seawater. *Oceanography*. **22**, 72-85.

Minkoff, G., Lubzens, E., Kahan, D. 1983. Environmental factors affecting hatching of rotifer (*Brachionus plicatilis*) resting eggs. *Hydrobiologia*. **104**, 61-69.

Nadella, S.R., Fitzpatrick, J.L., Franklin, N., Bucking, C., Smith, D.S., Wood, C.M., 2009. Toxicity of Cu, Zn, Ni and Cd to developing embryos of the blue mussel (Mytilis trossolus) and the protective effect of dissolved organic carbon. *Comparative Biochemistry and Physiology Part C.* **149**, 340-348.

NOAA. 2004. Population trends along the coastal united states: 1980–2008. Technical report, National Oceanic and Atmospheric Administration, National Ocean Service.

O'Brian,W.J. 1979. The predator-prey interaction of planktivorous fish and zooplankton. *American Scientist*. **67**, 572–581.

Paquin, P.R., Santore, R.C., We, K.B., Kavvadas, C.D., Di Toro, D.M. 2000. The biotic ligand model: a model of the acute toxicity of metals to aquatic life. *Environmental Science and Policy*. **3**, 175-182.

Paquin, P.R., Gorsuch, J.W., Apte, S., Batley, G.E., Bowles, K.C., Campbell, P.G.C., Delos, C, G., Di toro, D.M., Dwyer, R.L., Galvez, F., Gensemer, R.W., Goss, G.G., Hogstrand, C., Janseen, C.R., McGeer, J.C., Naddy, R.B, Playle, R.C., Santore, R.C., Schneider, U., Stubblefield, W.A., Wood, C.M., Wu, J.B. 2002. The biotic ligand model: a historical overview. *Comparative Biochemistry and Physiology Part C*. **133**, 3-35.

Pempkowiak, J., Kozuch, J., Grzegowska, H., Gjessing, E.T. 1999. Biological vs. chemical properties of natural organic matter isolated from selected Norwegian lakes. *Environment International*. **25**(2/3), 357-366.

Rivera-Duarte, I., Zirino, A. 2004. Response of the Cu(II) ion selective electrode to Cu titration in artificial and natural shore seawater and in the measurement of the Cu complexation capacity. *Environmental Science and Technology*. **38**, 3139-3147.

Ross, J.W. Solid-state and liquid membrane ion-selective electrodes. In: Durst, R.A. (Ed.). Ion-Selective Electrodes. Washington D.C. (WA): Department of Commerce National Bureau of Standards; 1969. p. 57-88.

Ryan, D.K., Weber, J.H. 1982. Fluorescence quenching titration for determination of complexing capacities and stability constants of fulvic acids. *Analytical Chemistry*. **54**, 986-990.

Sanchez-Marin, P., Santos-Echeandia, J., Nieto-Cid, M., Alvarez-Salgado, X.A., 2010. Effect of dissolved organic matter (DOM) of contrasting origins on Cu and Pb speciation and toxicity to *Paracentrotus lividus* larvae. *Aquatic Toxicology*. **96**, 90-102.

Santore, R.C., Di Toro, D.M., Paquin, P.R., Allen, H.E., Meyer, J.S. 2001. Biotic ligand model of the acute toxicity of metals 2. Application to acute copper toxicity in freshwater fish and *daphnia*. *Environmental Toxicology and Chemistry*. **20**, 2397-2402.

Schwartz, M.L., Curtis, P.J., Playle, R.C. 2004. Influence of natural organic matter source on acute copper, lead, and cadmium toxicity to rainbow trout oncorhynchus mykiss. *Environmental Toxicology and Chemistry*. **23**, 2889-2899.

Skoog, D.A., Holler, F.J., Crouch, S.R. 2007. Principles of Instrumental Analysis. 6th ed. Brooks & Cole: Thomson Corp. United States.

Smith, D.S., Kramer, J.R. 1999. Fluorescence analysis for multi-site aluminum binding to natural organic matter. *Environment International.* **25**. 295–306.

Smith, D.S., Kramer, J.R. 2000. Multisite metal binding to fulvic acid determined using multiresponse fluorescence. *Analytica Chimica Acta*. **416**, 211-220.

Smith, D.S., Bell, R.A., Kramer, J.R. 2002. Metal speciation in natural waters with emphasis on reduced sulfur groups as strong metal binding sites. 2002. *Comparative Biochemistry and Physiology Part C.* **133**, 65-74.

Stauber, J.L., Florence, T.M. 1985. Interactions of copper and manganese: A mechanism by which manganese alleviates copper toxicity to the marine diatom, Nitzschia closterium (Ehrenberg) W. Smith. *Aquatic Toxicology*. **7**(4), 241-254.

Stedmon, C.A., Bro, R. 2008. Characterizing dissolved organic matter fluorescence with parallel factor analysis: a tutorial. *Limnology and Oceanography: Methods.* **6**. 572–579.

Stedmon, C.A., Markager, S. 2005. Resolving the variability in dissolved organic matter fluorescence in a temperate estuary and its catchment using PARAFAC analysis. *Limnology and Oceanography.* **50**. 686–697.

Sunda, W.G., Hanson, P.J. 1979. Chemical speciation of copper in river water. In Jenne, E. Editor. Chemical modeling in aqueous systems. ACS Symposium Series; American Chemical Society: Washington, DC, 147-180.

Thurman E.M. Organic geochemistry of natural waters. Dordrecht: Martinus Nijhof/Dr. W. Junk Publishers; 1985.

U.S. EPA. 2007. National recommended water quality criteria. Available at http://water.epa.gov/scitech/swguidance/standards/current/index.cfm.

Wang, J. 2006. Controlled-potential techniques. In Analytical Electrochemistry. 3rd ed. John Wiley & Sons, Hoboken, NJ.

Westall, J.C., Morel, F.M.M., Hume, D.N. 1979. Chloride interference in cupric ion selective electrode measurements. *Analytical Chemistry*. **51**(11) 1792-1798.

Winter, A., Fish, T., Playle, R., Smith, D.S., Curtis, P. 2007. Photodegradation of natural organic matter from diverse freshwater sources. *Aquat. Toxicol.* **84**, 215–222.

Wu, F.C., Evans, R.D., Dillon, P.J. 2003. Separation and characterization of NOM by high-performance liquid chromatography and on-line three-dimensional excitation emission matrix fluorescence detection. *Environmental Science and Technology*. **37**, 3687–3693.

Chapter 2 Internal calibration flow-through ISE method for determining free Cu in salt water

2.0 Abstract

Copper can exist in many different forms in aquatic environments and factors within these environments can affect the speciation and bioavailability of copper. Copper bound to organic and inorganic ligands is unavailable to interact with organisms to cause toxicity. As such, free copper is often used as an indicator for copper toxicity since it is the species most available to be taken up by an organism. Thus, the determination of copper speciation is important in understanding the bioavailability of copper and its potential to cause toxicity to marine organisms. Free ionic copper was measured using a flow-through ion selective electrode (ISE). Four different marine samples were collected from various locations and analyzed during a fixed pH copper titration using a published external standard calibration ISE method. Free cupric determinations in the range 10^{-12} to 10^{-7} mol L^{-1} were consistent with published literature but replicate measures showed up to two orders of magnitude variability. To improve reproducibility an internal calibration method was developed. The new method was validated using artificial seawater with added tryptophan as the model ligand. The free Cu was modelled using NIST binding constants and compared well to measured values. The free copper measured using the improved method showed the same trends as the external calibration data but reproducibility increased to an order of magnitude or better. For example, in one natural sea water sample the external calibration yielded a concentration range from $10^{-10.5}$ to$10^{-7.5}$ mol L^{-1} and this was reduced to $10^{-9.9}$ to $10^{-9.5}$ mol L^{-1} using the internal calibration method. This ability to more reliably measure free copper is significant for predicting and measuring toxicity upon copper exposure.

2.1 Introduction

Copper is an important trace element required for proper functioning of aquatic organisms however can be toxic at increased concentrations due to interference with ion transport (Grosell & Wood 2002; De Polo & Scrimshaw 2012). The ability for copper to cause toxicity is based on its speciation. Copper is mostly found as inorganic and organic complexes which renders copper unavailable to interact with an organism to cause toxicity (Paquin et al. 2000). As such, free copper, Cu^{2+}, is often used as an indicator for toxicity since it is the species most available to be taken up by an organism (Chadwick et al. 2008; Eriksen et al. 2001, Sunda & Hanson 1979). Therefore, it is important that the measurement of free copper be accurate and reliable for assessing copper toxicity in aquatic environments.

Previous use of Cu ion-selective electrodes (ISEs) in sea water has been limited due to the observance of chloride interference (Jasinski, Trachtenberg & Andrychuk 1974; Westall, Morel & Hume 1979). However, this phenomemon was examined in Belli & Zirino (1993) and it was found that the Cu ISE was suitable for use in high chloride media such as seawater. The Cu ISE has since been used to measure free copper at metal impacted sites such San Diego Bay (Rivera-Duarte & Zirino 2004) as well as for use in comparing free Cu to observed toxicity (Erikson et al. 2001 & 2001a). Nonetheless, in some cases up to two orders of magnitude variability between measurments have been seen in copper titration data (Chadwick et al. 2008). This variability has two potential sources. The first is differences in sample characteristics, like time of collection between samples from the same location, causing the resulting

variability in the data. The second is due to method reproducibility issues. This work will attempt to examine the source of variability seen in the literature.

A flow-through Cu ISE system was previously developed by Eriksen et al. (1999). A flow through system is advantageous because membrane fouling by membrane dissolution or silver chloride precipitation is negligible or non-existent since the solution is always being flushed through the system and not static (Eriksen et al. 1999). Copper released from the ISE itself is also flushed through the system instead of accumulating at the electrode surface, allowing for a more accurate measurement of copper in the sample (Eriksen et al. 1999). This published method and a new internal calibration flow-through method will be utilized to determine free copper concentrations in natural and artificial sea water samples. Validation of the internal calibration method will also be presented. The reproducibility of the new method will also be compared to the published method from Eriksen et al. (1999).

2.2 Methods

2.2.1 Instrumentation

All studies were conducted in a flow-through system using an Orion copper electrode (Model 94-29, Boston, MA, USA) contained within an ISE micro-Flowcell (FIAlab, Bellevue, WA). The flow cell was contained within a faraday cage made from wire wrapped to electrical ground (a water tap). An Orion double junction Ag/AgCl reference electrode (Model 900200, Boston, MA, USA) using ASW prepared using OECD Annex 10 (OECD 2001; Annex 10 2007) (Refer to Section *2.2.2 Sample Preparation*) as the outer filling solution was located in a separate compartment at the end of the system

(waste stream) to avoid interference of the CuISE by silver. Each electrode was connected to a potentiometer (Tanager, Model 9501, Ancaster, ON). A valveless metering pump, the Cerampump FMI "Q" Pump (GQ6, Fluid Metering Inc., Syosset, NY) was used to deliver the test solution through the system. For measurements of free copper following the literature method, a KD Scientific syringe pump (Model KDS100; Massachusetts, USA) was used for sample delivery. A schematic of the flow-through system can be seen in Figure 2.1.

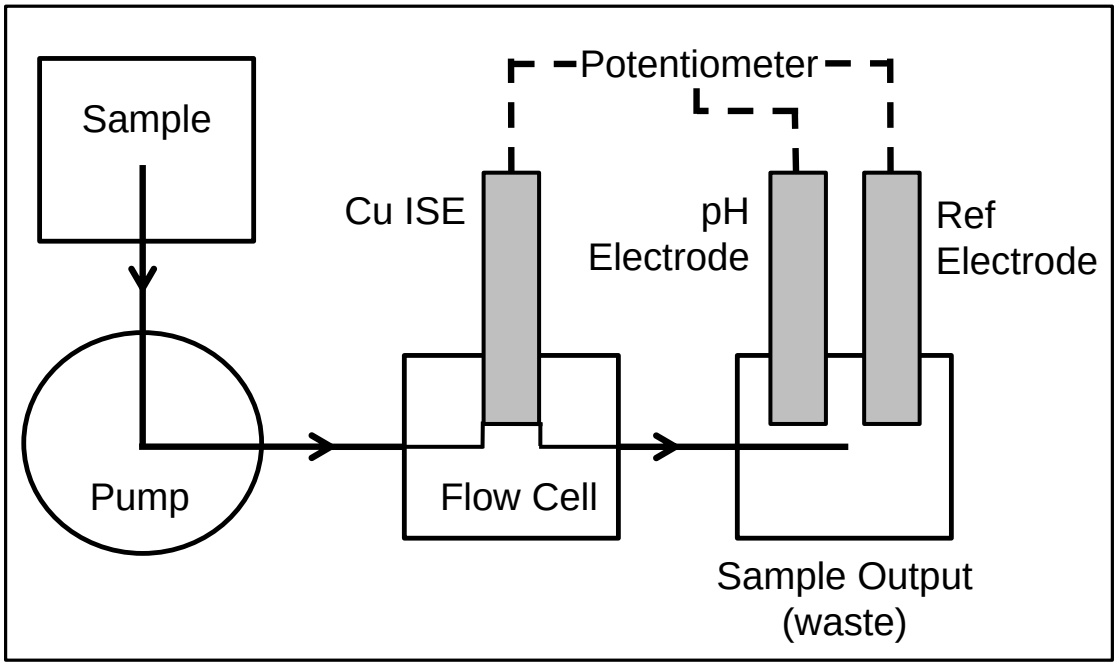

Figure 2.1 Schematic of the free copper ion selective electrode flow-through system.

2.2.2 Sample Preparation

A copper ion buffer containing 15 mM ethylenediamine (ReagentPlus ≥ 99%, Sigma Aldrich, St. Louis, MO), 1 mM $CuSO_4 \cdot 5H_2O$ (BioShop Canada Inc., Burlington, ON) and 0.6 M NaCl (Fisher Scientific, New Jersey, NY) was prepared as in Eriksen et al. (1999). The pCu (pCu = -log[Cu^{2+}]) of this buffer solution could be varied by

adjusting the pH of the sample with the pCu calculated as a function of pH (Eriksen et al. 1999):

$$pCu = 125.39 - 86.958\ x\ pH + 22.788\ x\ pH^2 - 2.7572\ x\ pH^3 + 0.16079\ x\ pH^4 - 3.6683\ x\ 10^{-3}\ x\ pH^5 \quad \text{Equation 2.1}$$

At higher pH values pCu is higher, corresponding to a lower amount of free Cu. The buffer was pH adjusted to around pH 8 for a pCu of 14.86. For the literature method, a low pCu buffer was also made by adjusting the pH to 6 for a pCu of 8.31.

An artificial seawater solution was prepared following the marine medium chemical composition from the Organization for the Economic Co-operation and Development (OECD) Annex 10 (OECD 2001; Annex 10 2007). The chemical composition can be found in Table 2.1. All test solutions were prepared using this synthetic seawater.

Table 2.1 Chemical composition of artificial seawater (OECD 2001; Annex 10 2007).

Chemical	**Amount**
Sodium fluoride (NaF)[a]	3 mg L^{-1}
Strontium chloride hexahydrate ($SrCl_2 \cdot 6H_2O$)[a]	20 mg L^{-1}
Boric acid (H_3BO_3)[b]	30 mg L^{-1}
Potassium bromide (KBr)[c]	100 mg L^{-1}
Potassium chloride (KCl)[b]	700 mg L^{-1}
Calcium chloride dihydrate ($CaCl_2 \cdot 2H_2O$)[a]	1.47 g L^{-1}
Sodium sulfate (Na_2SO_4)[a]	4.0 g L^{-1}
Magnesium chloride ($MgCl_2 \cdot 6H_2O$)[c]	10.78 g L^{-1}
Sodium chloride (NaCl)[a]	23.5 g L^{-1}
Sodium metasilicate nonahydrate ($Na_2SiO_3 \cdot 9H_2O$)[a]	20 mg L^{-1}
Sodium bicarbonate ($NaHCO_3$)[d]	200 mg L^{-1}

[a] Fisher Scientific (New Jersey, NY), [b] Sigma Aldrich (St. Louis, MO), [c] BDH (West Chester PA), [d] EMD Chemicals (Gibstown, NJ).

A 1.0 x 10^{-2} M stock solution of reagent-grade L-tryptophan (Trp) (> 98% pure, Sigma Aldrich, St. Louis, MO) and a 1.0 M stock solution of cupric sulfate pentahydrate ($CuSO_4 \cdot 5H_2O$) (BioShop Canada Inc., Burlington, ON) were prepared using ultrapure water (18.2 MΩ, MilliQ). Discrete copper titrations were prepared by adding 10 µM Trp to the ASW to act as a model ligand. Tryptophan was added as the model ligand since it is known that it will bind copper and the stability constant for binding to copper is known. Thus, speciation could be modeled using National Institute of Standards and Technology (NIST) values (Martell & Smith 2001) and compared to experimental findings. An example of solving for simultaneous chemical equilibria required to model speciation can be found in Appendix A1. Copper additions of 78.4, 157.4, 392.7 and 786.8 nmol L^{-1} Cu (5, 10, 25 and 50 ppb Cu, respectively) was added to the ASW + Trp solutions and allowed to equilibrate overnight before free copper was measured using the flow-through system.

Marine water samples from Duxbury (Massachusetts), PNNL (Washington), Jimbo (Florida) and Bearcut (Florida) were collected in polypropylene bottles and stored at 4°C (Table 2.2). These samples were filtered using a 0.45µm pore size cellulose nitrate membrane filter (Whatman, Germany). Copper additions of 0, 78.4, 157.4, 392.7 and 786.8 nmol L^{-1} Cu (0, 5, 10, 25 and 50 ppb Cu, respectively) were added to 50 mL aliquots of the filtered sample and allowed to equilibrate overnight before free copper was measured. Each sample was pH adjusted to pH 8.0 ± 0.1 before analysis.

Table 2.2 Location and basic water characteristics of marine samples.

Sample	Location (lat/long)	Salinity (ppt)	DOC (mg C L^{-1})
Bearcut (FL)	25.7307 / -80.1611	35	2.06
Jimbo (FL)	25.7747 / -80.1454	36	3.47
Duxbury (MA)	42.0364 / -70.6710	36	1.77
PNNL (WA)	46.3481 / -119.280	35	1.80

2.2.3 Internal Calibration Analysis Procedure

The CuISE was polished weekly using aluminum oxide (< 10 micron, 99.7%, Sigma Aldrich, St. Louis, MO) followed by silver electrode polish (Corning Inc, Tewksbury, MA). Following polishing and for overnight storage the CuISE was left in the flow cell in the pH 8 copper ion buffer with the sample delivery pump turned off after running buffer at a fast flow rate (~160 ml h^{-1}) for two minutes.

A fast flow rate (~160 ml h^{-1}) was used initially to ensure the sample was through the system and that a complete electric circuit was maintained. The flow rate was then reduced to the measuring flow rate of 10 ml h^{-1} and measured until stabilization of the potential signal was achieved. Typically, stabilization of the sample required 2 to 5 hours to satisfy the stability criteria of a less than 0.1 mV min^{-1} change. After stabilization the final pH was measured. For ASW samples, the process was repeated at various pH points from pH 8.0 down to pH 3.3. For determination of pCu in a sample the whole range of pH adjustments need not be performed. Instead, the samples were measured at a pH of 8 and at two lower pH points ranging from pH 3.3 to pH 5 for a total of three measurements per sample per copper concentration. After the lowest pH

measurement, the system was flushed with ASW for 2 min at the fast flow rate, followed by the copper ion buffer for 2 min before the next sample was measured.

It should be noted that at higher concentrations of free copper (lower pH) there was some slight noise associated with the potential reading. In these cases, the average potential of the noise was used as the measured potential once the stability criterion was met and did not seem to impact the final results. This is consistent with the observations noted in Belli & Zirino (1993) in which the noise increased with increasing concentrations of copper.

2.2.4 Literature Method Analysis Procedure

For the full procedure of the literature method for determining free copper using flow-through analysis please refer to Eriksen et al. (1999). This method was applied to all four marine samples. The Cu ISE was calibrated each day before any samples were run using the low and high pCu copper ion buffers after which a calibration curve was generated and used to determine free Cu of each sample. Like above, a fast flow rate (129 ml h^{-1}) was used to ensure the sample was distributed through the system. The flow rate was then reduced to a measuring flow rate of 1.0 ml h^{-1}. The same stability criterion as the internal calibration method was applied for these measurements.

2.2.5 Internal Calibration Data Analysis

All data analysis was performed in MATLAB™ (MathWorks Inc., MA, USA). For the one-point internal calibration, the stable potential readings for the lowest pH points allow for a one-point internal calibration to be performed to determine free Cu. At the lowest pH points it was assumed that total copper is equal to the free copper,

corrected for chloride complexation using NIST values (Martell & Smith 2001). The potential for the two lowest pH measurements for each sample were averaged to determine the measured electrode potential (E). The reference potential (E°) is calculated using E, and assuming a Nernstian slope (m) of 29.6 mV per decade along with the adjusted total copper ($Cu_{Tadjust}$) as seen in Equation 2.2. Once E° has been calculated then $logCu^{2+}$ can be calculated for the pH 8 measurement using Equation 2.3.

$$E^0 = E - mlogCu_{Tadjust} \qquad \text{Equation 2.2}$$

$$logCu^{2+} = \frac{(E-E^0)}{m} \qquad \text{Equation 2.3}$$

A copy of the MATLAB script used to determine free copper in the model system over varying pH and at a constant pH of 8 can be found in Appendix A2 and A3, respectively.

2.3 Results and Discussion

A typical sample kinetic curve can be observed in Figure 2.2. The shape of the kinetic curve was similar for all samples using both the internal and external calibration methods.

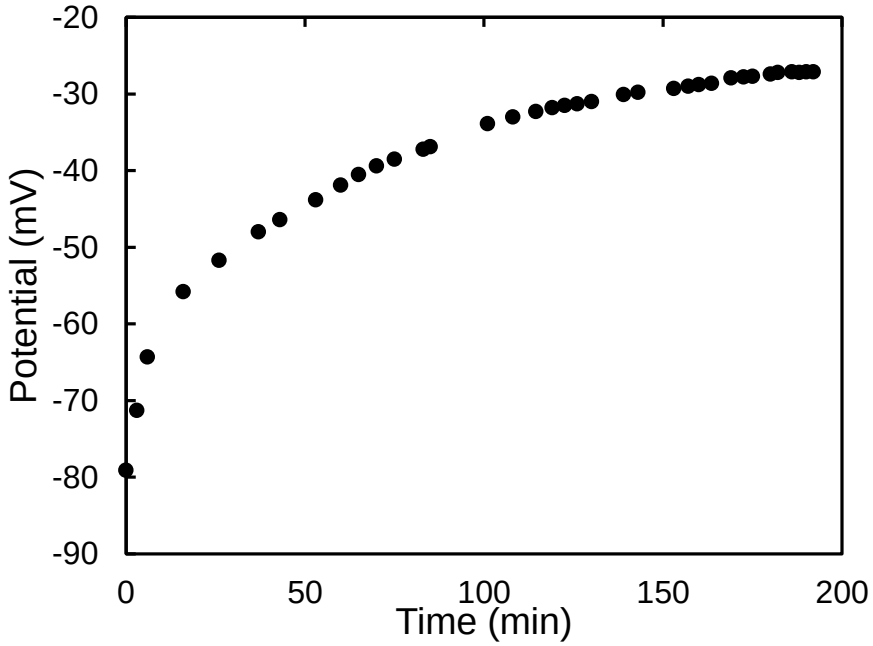

Figure 2.2 Kinetic curve for ASW + 10 µM Trp + 786.8 nmol L^{-1} (50 ppb) Cu showing potential as a function of time. The stability criteria of less than 0.1 mV min^{-1} change was achieved at 192 minutes.

2.3.1 Literature Method Sample Variability

The free copper measurement results from the titration of the four marine samples with copper can be seen in Figure 2.3. This figure also shows free copper data from Chadwick et al. (2008) for comparison. The titration data of the seawater samples measured using the Eriksen et al. (1999) method compared well to the literature data from San Diego Bay. Free copper concentrations ranged from approximately 10^{-12} mol L^{-1} to 10^{-7} mol L^{-1} which is consistent with the concentration range seen in the literature.

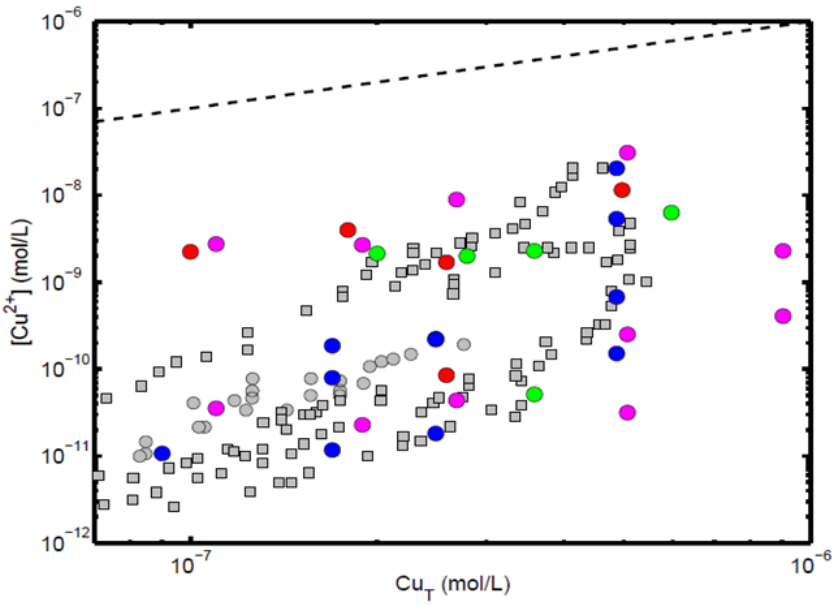

Figure 2.3 Measured free copper concentrations using Eriksen et al. method compared to San Diego Bay Results from Chadwick et al. (2008). Grey = Chadwick et al. (2008) data, Red = Bearcut (FL), Green = Jimbo (FL), Blue = PNNL (WA), Magenta = Duxbury (MA).

Also comparable to the literature data, the titration data from sample replicates showed up to two orders of magnitude difference in free copper concentrations. Figure 2.3 illustrates the wide variability between titrations. The variability seen in the Chadwick et al. (2008) data could have been due to sample variation such as location and time of year the samples were collected. However, the free copper titrations measured in our lab were replicates from the same sample from one collection period and one location. This suggests that measurement reproducibility was an issue, rather than being due to sample differences. This confirms the need for improvements to the literature method to increase reproducibility of results. These improvements resulted in the development of the internal calibration method with the results discussed below.

2.3.2 Internal Calibration Validation

An internal calibration is advantageous over an external calibration method since it takes into account any electrode fouling that may have occurred. In this method solutions with copper additions are pH adjusted from a range of pH 8 to pH 3.3 and a one-point calibration is performed to determine free copper. Validation was performed using ASW with added tryptophan as a model ligand so that free copper could be modeled in this system. Figure 2.4 shows the strong agreement of modeled versus measured free copper concentrations over varying pH. At low pH, organic particle surface sites for binding become less available to bind copper, thus more free metal exists (Millero et al. 2009). However, as pH increases the copper is able to form more copper complexes since fewer binding sites on NOM are protonated, thus decreasing the amount of free copper present (Santore et al. 2001). As well, there is an increase in copper hydroxide formation, also reducing the amount of free copper (Paquin et al. 2001; Santore et al. 2001). There is a slight discrepancy between the measured and expected values at 78.7 nmol L^{-1} Cu (5 ppb Cu) at pH 8. However the detection limit of the CuISE is around 31.5 nmol L^{-1} Cu (2 ppb) total copper. Thus, at the 78.7 nmol L^{-1} total Cu concentration the limit of detection is being approached with respect to free copper.

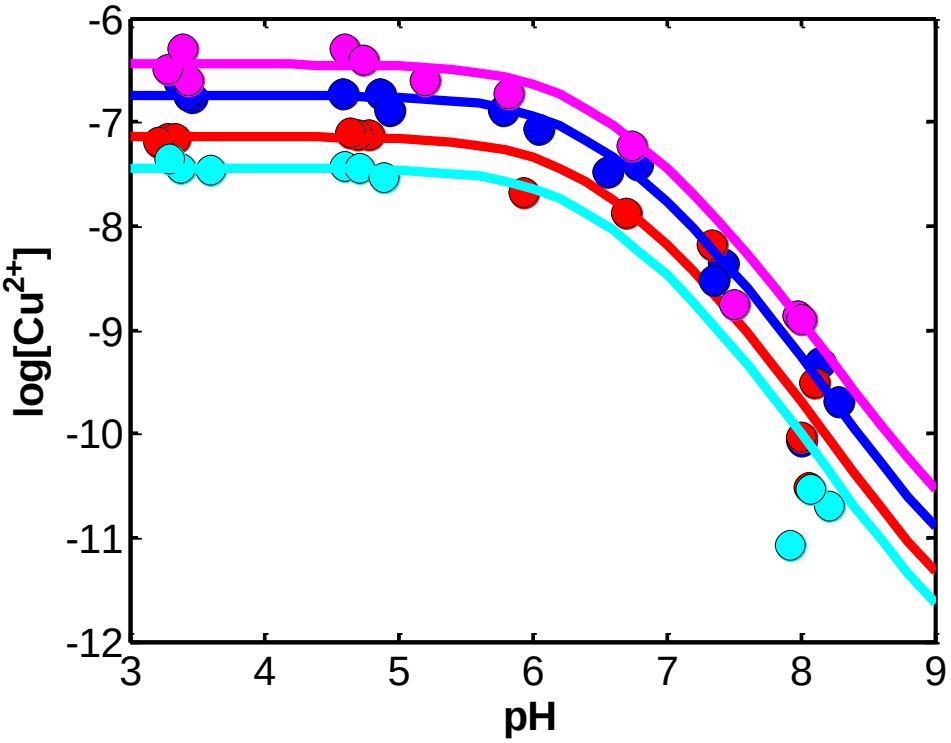

Figure 2.4 Measured (circles) and modeled (lines) free copper for ASW + 10 µM Trp with 78.7 nmol L^{-1} Cu (5 ppb Cu; light blue), 157.4 nmol L^{-1} Cu (10 ppb Cu; red), 392.7 nmol L^{-1} Cu (25 ppb Cu; blue), and 786.8 nmol L^{-1} Cu (50 ppb Cu; magenta) added over a pH range from 8.0 to 3.3.

To understand the quantitative effects of the internal versus external calibration methods at a constant pH of 8, the free copper at each total copper concentration was calculated using the internal (●) and external calibration method (◊) and can be seen in Figure 2.5. The external calibration values were calculated using the average calibration curve (mV = -28.549pCu + 255.7) from all calibration performed previously using the literature method. This figure shows the free copper values calculated using the external calibration method are relatively constant, regardless of the total copper added. However, as expected, when the one-point internal calibration is performed the amount of free copper increases with increased total copper.

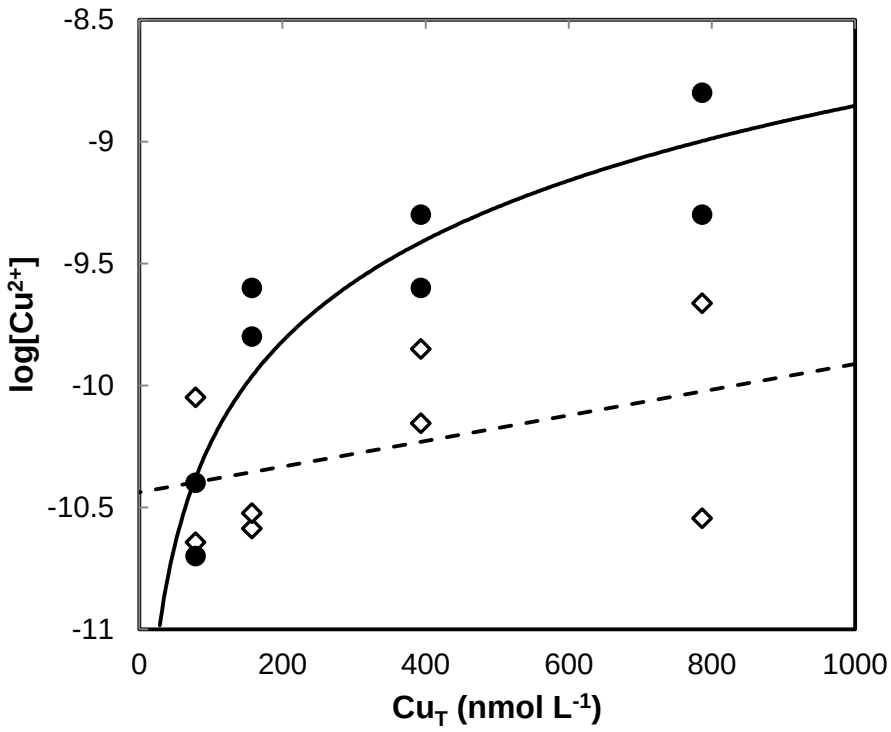

Figure 2.5 Free copper measured over a concentration range of 78.7 to 786.8 nmol L^{-1} (5-50 ppb) Cu at a constant pH (pH = 8) calculated using the external (◊) and internal (●) calibration methods. Dashed line represents the trend in the external calibration data while the solid line represents the trend of the internal calibration data.

The internal calibration data can be compared to the expected free copper at each concentration in Figure 2.6. Figure 2.6 shows good agreement with the model, adding strength to the validity of the method.

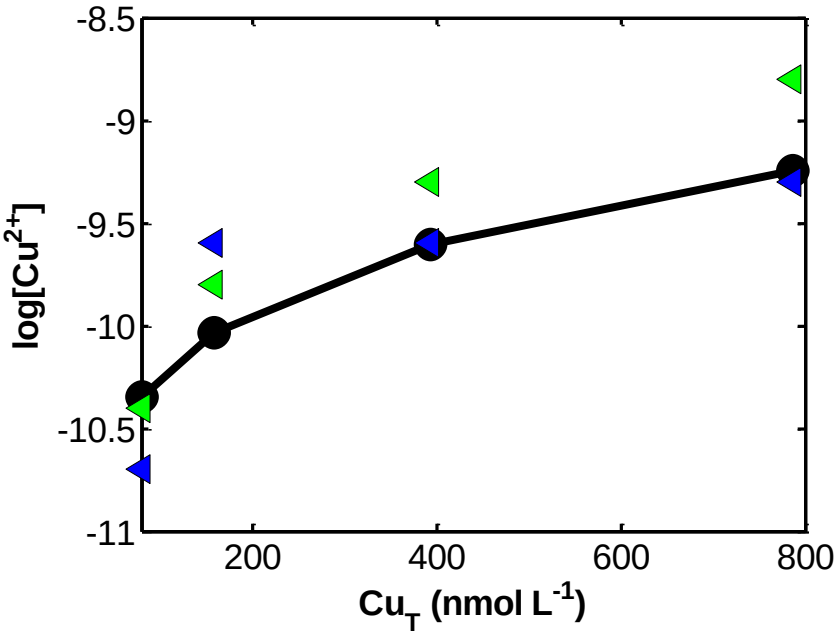

Figure 2.6 Measured (triangles) and modeled (circles with lines) copper speciation of ASW + 10 µM Trp over concentration range of 78.7 to 786.8 nmol L^{-1} (5-50 ppb) Cu at a constant pH (pH = 8).

2.3.3 Applicability in Marine Samples

Discrete copper titrations of ASW using the new internal calibration flow-through ISE method were found to yield successful results. As such, discrete copper titrations of natural marine samples were performed to determine whether the new method would be successful in these waters. Copper titrations of Duxbury (MA) and PNNL (WA) samples using the new internal calibration method were performed and the results compared to the literature method in Figure 2.7. As can be seen in Figure 2.7, the free copper concentrations are similar between methods. The variability between replicates was also considerably reduced using the internal calibration method as compared to the external calibration method. For example, Duxbury spiked with 392.7 nmol L^{-1} (25 ppb) Cu showed a free copper concentration ranging from $10^{-10.5}$ to $10^{-7.5}$ mol L^{-1} using the

external calibration method. However, this variability was reduced to between $10^{-9.9}$ – $10^{-9.5}$ mol L^{-1} using the new internal calibration method. These results show that the internal calibration method is applicable and increases the reproducibility of measurements in natural marine waters.

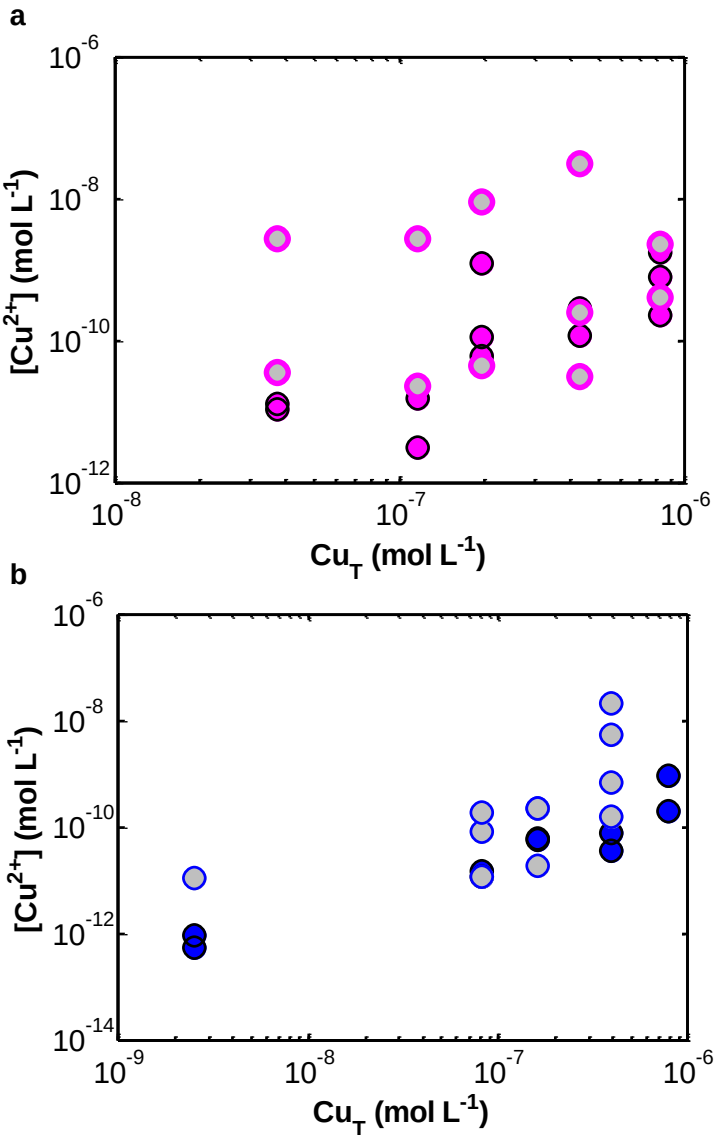

Figure 2.7 Comparison of copper speciation measurements using the external calibration method and internal calibration method. a. Duxbury; magenta – Internal Calibration method, grey – External calibration method. b. PNNL; blue – Internal Calibration method, grey – External calibration method.

2.4 Conclusions

Replicate measurements of sea water samples using a published method showed up to two orders of magnitude variability between free copper measurements. This suggests that method reproducibility issues cause the variability seen in free copper measurements rather than sample differences. This resulted in the development of a new method for determining free copper in sea water. The work presented here describes a new method for the determination of free copper in sea water using an internal calibration flow-through ISE method. The new method was successfully validated using a model system and comparison of methods in natural water samples showed the ability of the new method to accurately measure free copper in the environment. The increased reproducibility from two orders of magnitude to within an order of magnitude using the new method ensures more reliable results are obtained. This is important as accurate measurement of free copper is significant for predicting and measuring bioavailability and toxicity of copper to aquatic organisms.

2.5 References

Belli, S.L., Zirino, A. 1993. Behaviour and calibration of the copper(II) ion-selective electrode in high chloride media and marine waters. *Analytical Chemistry*. **65**, 2583-2589.

Chadwick, D.B., Rivera-Duarte, I., Rosen, G., Wang, P.F., Santore, R.C., Ryan, A.C., Paquin, P.R., Hafner, S.D., Choi, W. 2008. Demonstration of an integrated model for predicting copper fate and effects in DoD harbors. *SPAWAR Technical Report 1972*. Project ER-0523.

De Polo, A., Scrimshaw, M. 2012. Challenges for the development of a biotic ligand model predicting copper toxicity in estuaries and seas. *Environmental Toxicology and Chemistry*. **31** (2), 230-238.

Eriksen R.S., Mackey, D.J., Alexander, P., De Marco, R., Wang, X.D. 1999. Continuous flow methods for evaluating the response of a copper ion selective electrode to total free copper in seawater. *Journal of Environmental Monitoring*. **1**, 483-487.

Eriksen, R.S., Nowak, B., van Dam, R.A. 2001. Copper speciation and toxicity in a contaminated estuary. *Supervising Scientist Report 163*. Department of Sustainability, Environment, Water, Population and Communities, Canberra, Australia.

Eriksen, R.S., Mackey, D.J., van Dam, R., Nowak, B. 2001a. Copper speciation and toxicity in Macquarie Harbour, Tasmania: an investigation using a copper ion selective electrode. *Marine Chemistry*. **74**, 99-113.

Grosell, M., Wood, C.M. 2002. Copper uptake across rainbow trout gills: Mechanisms of apical entry. *The Journal of Experimental Biology*. **205**, 1179-1188.

Jasinski, R., Trachtenberg, I., Andrychuk, D. 1974. Potentiometric measurement of copper in seawater with ion selective electrodes. *Analytical Chemistry*. **46** (3), 364-369.

Martell, A., Smith, R. NIST database 46 version 6. NIST, Gaithersburg, MD 20899 (2001)

Millero, F.J., Woosley, R. Ditrolio, B., Waters, J. 2009. Effect of ocean acidification on the speciation of metals in seawater. *Oceanography*. **22**, 72-85.

OECD Environment, Health and Safety Publications Series on Testing and Assessment. No. 29 Guidance Document on Transformation/Dissolution of Metals and Metal Compounds in Aqueous Media. ENV/JM/MONO(2001)9. April (2001).

Paquin, P.R., Santore, R.C., We, K.B., Kavvadas, C.D., Di Toro, D.M. 2000. The biotic ligand model: a model of the acute toxicity of metals to aquatic life. *Environmental Science & Policy*. **3**, 175-182.

Rivera-Duarte, I., Zirino, A. 2004. Response of the Cu(II) ion selective electrode to Cu titration in artificial and natural shore seawater and in the measurement of the Cu complexation capacity. *Environmental Science and Technology*. **38**, 3139-3147.

Santore, R.C., Di Toro, D.M., Paquin, P.R., Allen, H.E., Meyer, J.S. 2001. Biotic ligand model of the acute toxicity of metals 2. Application to acute copper toxicity in freshwater fish and *daphnia*. *Environmental Toxicology and Chemistry*. **20**, 2397-2402.

Sunda, W.G., Hanson, P.J. 1979. Chemical speciation of copper in river water. In Jenne, E. Editor. Chemical modeling in aqueous systems. *ACS Symposium Series; American Chemical Society*: Washington, DC, 147-180.

Westall, J.C., Morel, F.M.M., Hume, D.N. 1979. Chloride interference in cupric ion selective electrode measurements. *Analytical Chemistry*. **51**(11) 1792-1798.

Chapter 3 Influence of DOC source on free copper and toxicity to *Brachionus plicatilis*

3.0 Abstract

The toxicity of copper in marine systems is dependent on its speciation and bioavailability. Natural organic matter (NOM) can complex copper resulting in decreased bioavailability of copper to cause toxicity. At a molecular level, NOM quality can vary which may alter copper binding and the resulting speciation and toxicity. The purpose of this study was to measure acute copper LC_{50} values in natural marine waters and identify the relationships between NOM quality on toxicity and copper speciation. This has implications on the development and application of a marine biotic ligand model (BLM) for copper in salt water. NOM was characterized using dissolved organic carbon (DOC) concentration, absorbance and fluorescence measurements to determine NOM source and quantify humic-, fulvic-, tryptophan- and tyrosine-like fractions within NOM. Static acute copper toxicity tests (48-h LC_{50}) were performed using the euryhaline rotifer, *Brachionus plicatilis*. Ion selective electrode (ISE) measurements of free copper were performed at the LC_{50} concentrations to determine the influence of DOC source on copper speciation. LC_{50} values ranged from 333 nM to 980 nM with DOC concentrations ranging from 0.55 mg C L^{-1} to 7.57 mg C L^{-1}. DOC was found to be protective, however the degree of protectivity decreased as DOC increased (r^2 = 0.72, p-value = 0.016). This suggests salt induced colloid formation could be occurring resulting in a decrease of binding sites available to complex free copper. Free copper remained relatively constant (within the BLM prediction factor of two) between each sample site with an average pCu of 10.14. Overall, this study is consistent with other studies that suggest free copper is the best species for predicting toxicity. As well, no significant correlation between NOM source and copper toxicity were observed as compared to total DOC concentration and copper toxicity, suggesting that NOM quality does not need to be taken into account for copper toxicity modeling in salt water.

3.1 Introduction

Copper is a trace element that is essential for proper functioning of plants, animals and microorgansims due to its requirement for many specific metabolic processes (ICA 1995). However, only low amounts are necessary for normal metabolic functioning and at increased concentrations copper can be toxic. Toxicity is usually due to copper interference with ion transport, most notably interference of sodium transport causing electrolyte imbalance and ionoregulatory failure (Grosell & Wood 2002; De Polo & Scrimshaw 2012).

With over 53% of the United States population living along coastal regions (NOAA 2004) and Canada having the longest marine coastline of any country (Government of Canada 2003) there is an increased concern of contamination of metals in the ocean due to anthropogenic input. Typical copper concentrations range from 0.12 – 0.38 µg L^{-1} in areas of open ocean (Mackey 1983) to levels over 6 µg L^{-1} in heavily impacted areas such as San Francisco Bay (Donat et al. 1994). Current U.S. EPA criteria for copper limits in seawater are a dissolved copper criterion continuous concentration (CCC) of 3.1 µg L^{-1} and a criteria maximum concentration (CMC) of 4.8 µg L^{-1} (U.S. EPA 2007). Currently there is no copper load limit into marine systems set by the Canadian government (CCREM 1987) but provinces, like British Columbia, have their own provincial limits with a total copper CCC of less than or equal to 2 µg L^{-1} and a CMC of 3 µg L^{-1} (BC MOE 1987).

The Biotic Ligand Model (BLM) is a predictive tool used to estimate site-specific bioavailability and subsequent toxicity of metals (Di Toro et al. 2001; Santore et al. 2001;

Paquin et al. 2002). Modeling is based on bulk water chemistries and the interaction between the metal and the site of toxic action, which is called the biotic ligand (eg. The gills of a fish). The freshwater BLM has been adopted as a regulatory tool by the U.S. EPA (2007) for copper however there is need for a BLM in saltwater environments. Investigations pertaining to salt water are currently underway for application of a marine BLM; however more information is needed on copper speciation and natural organic matter (NOM) source before the BLM is accepted for regulatory use (Arnold 2005). The focus of this study was to characterize each of these parameters for further development of the marine BLM.

The bioavailability of copper is influenced by the species of copper present in the system (Chadwick et al. 2008; Eriksen et al. 2001; Eriksen et al. 2001a; Sunda & Hanson 1979). Copper can exist in many different forms in aquatic environments and factors within these environments can affect its toxicity to organisms. Most copper is found in the form of inorganic and organic complexes (Kogut & Voelker 2001; Paquin et al. 2000). Organic ligands have been found to play a larger role on copper speciation and are generically classified as natural organic matter (NOM) (Sunda & Hanson 1979). The copper in both organic and inorganic complexes is unavailable to interact with organisms to cause toxicity. As such, free copper, Cu^{2+}, is often used as an indicator for toxicity since it is the species most available to be taken up by an organism (Chadwick et al. 2008; Eriksen et al. 2001, Sunda & Hanson 1979).

The concentration of NOM is usually measured as dissolved organic carbon (DOC). DOC is operationally defined as organic carbon that passes through a 0.45µm filter. Typical concentrations of dissolved organic carbon (DOC) in marine systems range

from 0.5 – 10 mg C L^{-1} from open ocean to coastal waters (Benner 2002). Increased DOC concentrations have been shown to be protective in marine organisms such as the blue mussel, *Mytilus sp.* (DePalma et al. 2011), the rotifer, *Branchionus plicatilus* (Arnold et al. 2010), and the sea urchin (*Parecentrotus lividus*) (Lorenzo et al. 2006). However, variation in NOM source may influence copper toxicity. Different NOM sources show variation in copper complexing capacities that could have an overall effect on NOM protection (De Schamphelaere et al. 2004). This was seen by Nadella et al. (2009) in which marine water spiked with three different sources of exogenous NOM resulted in different levels of protection to copper toxicity in *Mytilus trossolus*. The most protective NOM source was found to contain 20% and 40% higher fulvic substance content than the two less protective NOM sources. This corresponded to 40% and 60% less protectivity, respectively, to the blue mussel (Nadella et al. 2009).

NOM can be broadly classified into two groups, allochthonous and autochthonous (McKnight et al. 2001). Allochthonous, or terrigenous, organic matter is terrestrially-derived from the decomposition and leaching from soil and plant materials such as lignin, tannins and detritus and typically contains a higher humic and fulvic substance content. Autochthonous organic matter is microbially-derived organic matter from bacterial and algal processes occurring in the water column and usually contains a higher proteinaceous content (Birdwell & Engel 2009; McKnight et al. 2001). Typically, terrigenous organic matter is associated with a darker colour and relatively high amounts of aromatic and phenolic compounds, while autochthonous organic matter is lighter in colour and contains relatively low amounts of aromatic and phenolic groups (Eikebrokk et al. 2006). This colour can be described by the specific absorption coefficient of the

DOC at 340 nm (SAC_{340}). Darker, terrigeneous organic matter (higher SAC_{340}) has been found to be more protective to copper toxicity than ligher, microbially-derived organic matter (lower SAC_{340}) (Luider et al. 2004; Pempkowiak et al. 1999; Schwartz et al. 2004). NOM origin can also be approximated using fluorescence indices, as proposed by McKnight et al. (2001). A fluorescence index (FI) of approximately 1.4 and 1.9 indicates terrestrially-derived and microbially-derived NOM, respectively.

Fluorescence spectroscopy can be used to distinguish different fluorescent molecules (fluorophores) within a heterogenous system. The compilation of data from simultaneously measuring excitation and emission wavelengths result in a fluorescence excitation-emission matrix (FEEM). The intensity and position of the fluorophores within the matrix provides information on the chemical composition of NOM. Terrigenous components (humic and fulvic acids) fluoresce at longer wavelengths than proteinaceous components (Baker 2001). Fulvic- and humic-like components can be detected in the Ex/Em ranges of 300-350 nm/400-450 nm and 250-390 nm/460-520 nm, respectively (McKnight et al. 2001; Smith & Kramer 1999; Stedmon & Markager 2005; Wu et al 2003). Tyrosine and Tryptophan can be detected in the Ex/Em ranges of 225-275 nm/350 nm and 225-270 nm/300 nm, respectively, representing microbially-derived carbon sources (Baker 2001; Stedmon and Markager 2005). NOM characterization using this method has been used to identify components in aquatic systems ranging from freshwater (Cory & McKnight 2005; Winter et al. 2007) to seawater (Coble 1996; Cory & McKnight 2005).

Parallel factor analysis (PARAFAC) can be used to determine the relative quantities of the humic-, fulvic-, tryptophan- and tyrosine-like components observed by

fluorescence. Through spectral deconvolution of a stack of FEEMs, PARAFAC is able to quantify the minimum number of components to describe each FEEM (Stedmon & Bro 2008). Here, four components, humic-, fulvic-, tyrosine- and tryptophan-like fractions will be analysed for correlations with copper toxicity. De Palma et al. (2011) looked at the same components for correlations with copper toxicity to *Mytilus sp.*, however no significant correlations were found suggesting DOC was predictive of toxicity independent of dissolved organic matter (DOM) quality.

The objectives of this study were to (1) Measure acute toxicity of copper in the rotifer, *Brachionus plicatilis* in natural marine waters, (2) Identify relationships between LC_{50} in rotifers and the free Cu, concentrations of humic-, fulvic-, tyrosine- and tryptophan-like components of DOC, SAC_{340} and FI, (3) Identify the relationship between DOC source and free copper, and (4) Evaluate whether NOM quality should be included as an input parameter into a marine BLM for copper.

3.2 Methods

3.2.1 Sampling, Storage and Selection

Ambient water samples were collected from marine and estuarine sites along the coasts of Canada and the USA. Samples were collected in high density polyethylene bottles while submerged to ensure no airspace in the bottle. Samples were transported to Wilfrid Laurier University, Waterloo, ON, Canada in coolers. The bottles were stored at 4°C. After sub-sampling, Ar was used to fill the headspace. In total, 28 samples were collected. DOC quality was used to determine a subset of samples to measure copper toxicity (refer to *Section 3.2.3*). Samples were chosen to encompass low and high

concentrations (and combinations within) of each of the four parameters (humic, fulvic, tryptophan and tyrosine content). The DOC quality of all 28 sample sites can be found in Appendix B1. The locations of the 9 sites that were selected for toxicity assays are described in Table 3.1

Table 3.1 Description of sampling sites used for toxicity assays.

Sample	Location	Coordinates	Collection
Bouctouche (BT)	NB	46.471532 / -64.717283	Nov 2011
Petit Rocher (PR)	NB	47.783534 / -65.708606	May 2012
Major Kollock Creek (MKC)	NB	46.813469 / -64.912441	May 2012
Naufrage Harbour (NH)	PEI	46.46763 / -62.417343	May 2012
Rathtrevor Beach (RB)	BC	49.321793 / -124.264684	Aug 2012
Hawke's Bay (HB)	NFLD	50.616142 / -57.182465	Aug 2012
Blackberry Bay (BB)	BC	49.151791 / -125.89802	Nov 2012
Chesterman Beach (CB)	BC	49.11336 / -125.88692	Nov 2012
Jimbo	Miami, FL	25.77471 / -80.1454	Jan 2013

3.2.2 Dissolved Organic Carbon (DOC) Analysis

DOC concentrations of all ambient and salinity adjusted grab samples were measured using a Shimadzu TOC-$L_{CPH/CPN}$ (Shimadzu Corporation). Filtered (0.45µm cellulose nitrate membrane filter; Whatman, Germany) samples (20 mL) were acidified with 2-3 drops of concentrated OmniTrace HCl (EMD Chemicals, Gibstown, NJ). Standard total carbon solutions of 5, 10 and 20 mg C L^{-1} prepared from potassium hydrogen phthalate (BDH, West Chester, PA) and dissolved in ASW were measured with samples to allow for an external calibration. Refer to Section *3.2.4* for the chemical

composition of ASW. MilliQ water rinses were performed after every sample to ensure removal of any salt deposits from the analyzer syringe.

3.2.3 Fluorescence Measurement and Analysis

Daily standards of 2.4 µM tyrosine, 1.0 µM tryptophan and 5 mg C L^{-1} (Nordic Reservoir) or 10 mg C L^{-1} (Southhampton) were prepared. These solutions were prepared from stock solutions of reagent grade L-tyrosine (1.0 $x10^{-3}$M) (>98% pure, Sigma-Aldrich, St. Louis, MO) and L-tryptophan (1.0$x10^{-2}$M) (>98% pure, Sigma-Aldrich, St. Louis, MO) prepared using ultrapure water (18.2MΩ, MilliQ). Organic matter was commercially available terrestrial reverse osmosis organic matter isolate, Nordic Reservoir NOM (IHSS, MA, USA) or Southhampton DOC, a reverse osmosis and cation exchange resin (Amberlite IR-118H, Sigma) organic matter isolate from a wetland near Southampton, PEI, Canada. Details on sample location, preparation, storage and characterization for Southampton DOC can be found in Cooper et al. (2013). This daily standard was used to determine relative fluorophore component concentrations using a one point calibration and PARAFAC (see below).

An aliquot of each water sample was passed through a 0.45 µm cellulose nitrate membrane filter (Whatman, Germany) and the filtrate measured in a 1 cm quartz cuvette using a Varian Cary Eclipse Fluorescence Spectrophotometer (Varian, Mississauga, ON). Fluorescence emission wavelengths were measured from 250 nm to 600 nm in 1 nm increments for every 10 nm excitation wavelengths between 200 nm and 450 nm. Both the excitation and emission monochromator slit widths were set to 5 nm for all measurements. The photomultiplier tube was set to high sensitivity (800 V). When

sample fluorescence intensity was very low the photomultiplier tube was set to 1000 V and the daily standard was diluted by a factor of 10 in these cases. The use of daily standards at the same operating conditions as the samples allowed for relative concentrations of each component to be determined, corrected for instrument settings, thereby allowing a comparison between samples measured at different instrument settings.

A Varian Cary 50 UV/VIS Spectrophotometer (Varian, Mississauga, ON) was used to measure absorbance on each sample following fluorescence measurements. Absorbance was measured from 250 nm to 600 nm in order to correct for inner filter effects (if needed) as well as to determine SAC_{340} for each sample. SAC_{340} was calculated based on the following equation (Schwartz et al. 2004),

$$SAC_{340} = 2303\ x\ \frac{Abs_{340}}{DOC} \qquad \text{Equation 3.1}$$

Fluorescence indices to estimate NOM source were calculated for each water sample as in McKnight et al. (2001) using the following equation:

$$FI_{ex370} = \frac{em_{450}}{em_{500}} \qquad \text{Equation 3.2}$$

where FI_{ex370} is the fluorescent index at 370 nm excitation, and em_{450} and em_{500} are the emission intensities at 450 nm and 500 nm, respectively.

MATLAB™ (MathWorks Inc., MA, USA) was used to generate a three-dimensional fluorescence excitation-emission matrix (FEEM) for each sample. Rayleigh

scattering was removed from the spectra during preprocessing to prevent mathematical interferences in later spectral analysis. For sample measurements in which the absorbance at 254 nm was less than 0.3 units, inner filter effect corrections were not necessary (Ohno 2002). Data that required inner filter corrections were performed using Equation 3.3 (Larsson et al. 2007) where F is the corrected fluorescence intensity, F_o is the observed fluorescence, b is the path length, A_{ex} is the absorbance at the excitation wavelength and A_{em} is the absorbance at the emission wavelength.

$$F = F_o(10^{-b(A_{ex}+A_{em})}) \qquad \text{Equation 3.3}$$

Fluorescence intensities were expressed in arbitrary fluorescence units (counts) to avoid propagation of errors and additional assumptions in data analysis. The same instrument was used for all fluorescence measurements. The FEEMs were resolved using PARAFAC and constrained to four fluorescent components. Pure spectras of tyrosine and tryptophan were processed and weighted to recover pure tyrosine and tryptophan as components during analysis (DePalma et al. 2011). These made up the proteinaceous component of the resolved components. The spectra of the terrigenous material was labelled as humic-like and fulvic-like components. These spectra were based on the observation that higher molecular weight material fluoresces at longer wavelengths (DePalma et al. 2011; Wu et al. 2003). Therefore, after processing tyrosine-like, tryptophan-like, humic-like and fulvic-like components were defined. The concentrations of these components within each sample were determined using the resolved component concentrations from the daily standards.

3.2.4 Toxicity Assay

All toxicity tests on the nine selected samples were conducted using the euryhaline rotifer, *Brachionus plicatilis* purchased from Florida Aqua Farms Inc. (Dade City, Florida). Static acute toxicity tests (48-h) were performed following ASTM (2004) guidelines with modifications from Arnold et al. (2010). A summary of these recommendations can be seen in Table 3.2. *B. plicatilis* resting cysts were hatched in 6-well tissue culture plates (Falcon, Becton Dickinson) in artificial seawater (ASW) (ASTM 2004) at 30 ppt and a pH of 8.0 ± 0.1. Hatching took place under continuous light (2500 lux) at 25°C. Newly hatched rotifers (<6 hr old) were transferred to the exposure chamber, a 24-well tissue culture plate (Falcon, Becton Dickinson) containing 2 mL of the test solution. 6 replicates of 10 rotifers per exposure concentration (ctrl + 5 concentrations) were performed for each sea water sample. The test chamber was in continuous darkness and maintained at 25 ± 1 °C. The rotifers were observed at the end of the 48-h exposure under a microscope. Individual rotifers were considered dead if there was no movement of body or body parts within 5 s of observation (ASTM, 2004). Test acceptability was less than 10% mortality in the control (ASTM 2004).

Table 3.2 Summary of test conditions for the rotifer species, *Branchionus plicatilus*, as recommended by the American Society for the Testing of Materials (ASTM 2004) and actual experimental conditions applied (Adapted from Arnold et al. 2010).

Parameter	**ASTM (2004) Recommendations**	**Experimental**
Hatching salinity	15 g L^{-1}	30 g L^{-1}
Light during hatching	1000-3000 lux	2500 lux
Test type	Static acute	Static acute
Test container	Multiwell tissue culture plate	24 well high-grade polystyrene
Duration	24 h	48 h
End point	LC_{50}	LC_{50}
Temperature	25 ± 1°C	25 ± 1°C
pH	8.00	7.90 – 8.06
Dilution water	Reconstituted seawater	ASW
Test salinity	15 g L^{-1}	30 g L^{-1}
Photoperiod	Continuous darkness	Continuous darkness
Test chamber size	2.5 mL	3.25 mL
Test solution volume	1.0 mL	2.0 mL
Test concentration	5 plus a control	5 plus a control
Age of test animals	0-2 h	0-6 h
No. of reps per [Cu]	3	6
No. of neonates per [Cu]	30	60
Feeding	None	None
Aeration	None	None
End point	Mortality	Mortality
Test acceptability	≤ 10% control mortality	≤ 10% control mortality

The ASW was made using the following concentrations of salts: 11.31 g NaCl, 0.36 g KCl, 0.54 g $CaCl_2$, 1.97 g $MgCl_2 \cdot 6H_2O$, 2.39 g $MgSO_4 \cdot 7H_2O$, and 0.17 g $NaHCO_3$ dissolved in 1 L ultrapure water (18.2MΩ, MilliQ) (Guillard, 1983; ASTM, 2004). Salinity was adjusted to 30 ± 0.1 ppt using ultrapure water.

The nine samples used for the toxicity assays were adjusted to a salinity of 30 ± 0.1 ppt using a mixture of the ASW salts or ultrapure water. The sample was then filtered through a 0.45 µm cellulose nitrate filter (Whatman, Germany). The filtrate was pH adjusted to 8.0 ± 0.1 using 0.1 M NaOH (Orion 91-57BN pH electrode and Orion 420A+ meter, Thermo Electron Corp.). The effects of salinity adjustment of the samples on the resulting toxicity can be found in Appendix B2. Sub-aliquots of the filtrate were distributed into 6 separate teflon (Nalgene) containers. A 1.0 mM solution of $CuSO_4 \cdot 5H_2O$ (BioShop Canada Inc., Burlington, ON) was prepared in ultrapure water and was used to spike the test concentrations into the appropriate containers. Concentrations ranged from zero added copper (control) up to 300 µg L^{-1} Cu depending on the sample water tested. These solutions were allowed to equilibrate for 24 h in darkness before rotifer transfer to the test solutions was initiated.

The LC_{50} values for the toxicity data were determined using Probit analysis. For statistical analysis of relationships to toxicity, both linear and non-linear regression was applied depending on the observed trend.

3.2.5 Total Copper Analysis

Total copper measurements were made on sub-aliquots of the control sample and samples spiked with copper for the toxicity assay as well as solutions containing copper concentrations equivalent to the 48-h LC_{50}. UV digestion of each sample to remove organic components was required prior to total copper analysis using differential pulse anodic stripping voltammetry (DPASV). UV digestion was performed using a 705 UV Digester (Metrohm). 100 µL of 30% H_2O_2 was added to 10 mL of sample within the sample vessel. Irradiation time was 60 min at a temperature of 89 ± 2°C.

DPASV analyses were carried out with a Static Mercury Drop electrode (SMDE) and a Pt rod counter electrode (Metrohm) held in a Metrohm 663 VA stand (Metrohm) coupled to a computer controlled AutoLab PGSTAT128N potentiostat/galvanostat (Eco Chemie, Metrohm). Nova 1.7 software (Eco Chemie, Metrohm) was used for analysis of peaks. The experimental conditions followed manufacturer recommendations (Metrohm Application Bulletin No. 231/2e). These conditions were: 1mL of KCl-sodium acetate buffer (1.5 mol L^{-1} KCl, 0.5 mol L^{-1} CH_3COONa and 50 mL 30% w/v NaOH L^{-1}) was added to 10 mL of sample. The pH was then adjusted to 6.400 (±0.005). Problems with metal contamination of the KCl resulted in some samples being run using a KNO_3-sodium acetate buffer (1.5 mol L^{-1} KNO_3, 0.5 mol L^{-1} CH_3COONa and 50 mL 30% w/v NaOH L^{-1}). The sample was purged for 5 min with Ar after which copper was accumulated on a mercury drop for 90 s with stirring. The equilibration time was 10 s and the differential pulse ranged from -1.250 to 0.000 V. The original sample along with successive additions of copper to the sample solution was measured. The standard

addition solution was prepared daily at a concentration of 157 µM from a 1000 mg L^{-1} copper standard solution (Assurance grade, SPEXCertiPrep, New Jersey). Standard addition analysis by linear regression (Refer to Chapter 1, Section 1.7) was then used to determine the original concentration of copper in the sample.

3.2.6 Free Copper Analysis

Solutions containing total copper concentrations equivalent to the 48-h LC_{50} for all marine samples were prepared and allowed to equilibrate for 24 h before analysis. Free copper was measured using the internal calibration flow-through method described in Chapter 1. All measurements were conducted in a flow-through system using an Orion copper electrode (Model 94-29, Boston, MA, USA) contained within an ISE micro-Flowcell (FIAlab, Bellevue, WA). The flow cell was contained within a faraday cage made from wire wrapped to electrical ground (a water tap). An Orion double junction Ag/AgCl reference electrode (Model 900200, Boston, MA, USA) using ASW prepared using OECD Annex 10 (OECD 2001; Annex 10 2007) as the outer filling solution was located in a separate beaker at the end of the system to avoid interference of the Cu ISE by silver. Each electrode was connected to a potentiometer (Tanager, model 9501, Ancaster, ON). A valveless metering pump, the Cerampump FMI "Q" Pump (GQ6, Fluid Metering Inc., Syosset, NY) was used to deliver the test solution through the system at a flow rate of 10 ml h^{-1}. The CuISE was polished weekly using aluminum oxide (< 10 micron, 99.7%, Sigma Aldrich, St. Louis, MO) followed by silver electrode polish (Corning Inc, Tewksbury, MA). Following polishing and for overnight storage the CuISE was left in the flow cell in the copper ion buffer (15 mM ethylenediamine

(ReagentPlus ≥ 99%, Sigma Aldrich, St. Louis, MO), 1 mM $CuSO_4 \cdot 5H_2O$ (BioShop Canada Inc., Burlington, ON) and 0.6 M NaCl (Fisher Scientific, New Jersey, NY)) at pH 8.0 with the sample delivery pump turned off after running buffer at a fast flow rate (~160 ml h^{-1}) for two minutes.

Before analysis, the sample was pH adjusted to 8.0 ± 0.1. A fast flow rate (~160 ml h^{-1}) was used to ensure the sample was through the system and that a complete electric circuit was maintained after which the flow rate was reduced to the measuring flow rate of 10 ml h^{-1}. The sample was delivered through the system until stabilization of the potential signal was achieved, which generally took 2 to 5 hours. The measurement was satisfied when the acceptable criterion of a less than 0.1 mV min^{-1} change was achieved. After stabilization the final pH was measured. The process was repeated at a pH of 3.3 ± 0.1. After the lowest pH measurement, the system was flushed with ASW for 2 min at the fast flow rate, followed by the copper ion buffer for 2 min before the next sample was measured.

A one-point internal calibration was performed using the lower pH measurement to determine free Cu. The electrode is assumed to have a linear Nerstian response with a slope of 29.6 mV per decade. For the low pH sample it is assumed that the total copper equals the free copper, corrected for chloride complexation using the NIST $\log K_{CuCl}$ of 0.3 (NIST, 2001). This allows the free copper to be determined at pH 8.0. Statistical comparisons of the free copper measurements were determined using a two-way ANOVA followed by the Student-Newman-Keuls post-hoc test. A limit of $p < 0.05$ was used to indicate significance.

3.3 Results and Discussion

3.3.1 DOC Analysis

DOC concentrations were measured as an approximation of NOM in each of the nine grab samples before and after salinity adjustment and filtration and are shown in Table 3.3. DOC concentrations of the nine samples ranged from 0.55 mg C L^{-1} to 7.57 mg C L^{-1} after salinity adjustment and filtration. It was expected that there may have been some loss of DOC when increasing the salinity of the samples due to the salting-out effect. This effect refers to the decrease in solubility of non-electrolytes with an increase in ionic strength (Xie et al. 1997; Millero 2001). This effect has been observed for DOC in marine coastal waters (Mantoura & Woodward 1983). This was not always the case in this data set. A comparison of the DOC measurements before and after salinity adjustment and filtration can be seen in Figure 3.1. Most samples showed a slight decrease in DOC after adjustment, however there was no apparent trend between the percent change in DOC and the direction and percent change of salinity suggesting that variability may have been due to instrumental error (Figure 3.2).

Table 3.3 Measurements of DOC and salinity of the sea water samples used for the toxicity assays. Measurements are shown from both before and after salinity adjustment and filtration.

Sample	**DOC (mg C L^{-1})**		**Salinity**	
	Before	After	Before	After
Bouctouche	4.36	4.83	19.1	30.1
Petit Rocher	2.13	2.10	23.2	30.2
Major Kollock Creek	7.86	7.57	12.8	29.9
Naufrage Harbour	5.50	5.20	4.3	29.9
Rathtrevor Beach	1.52	1.37	24.4	30.1
Hawke's Bay	1.54	1.28	25.0	30.0
Blackberry Bay	1.45	2.03	8.3	29.9
Chesterman Beach	0.82	0.55	30.3	30.1
Jimbo	1.34	1.13	34.8	30.1

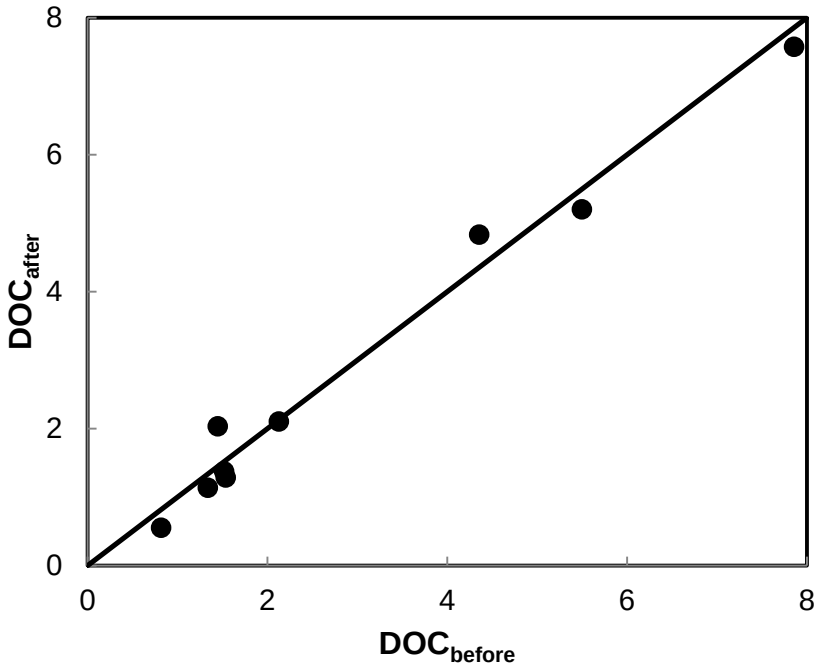

Figure 3.1 Comparison of DOC measurements before and after salinity adjustment and filtration. A 1:1 line is represented by the solid black line.

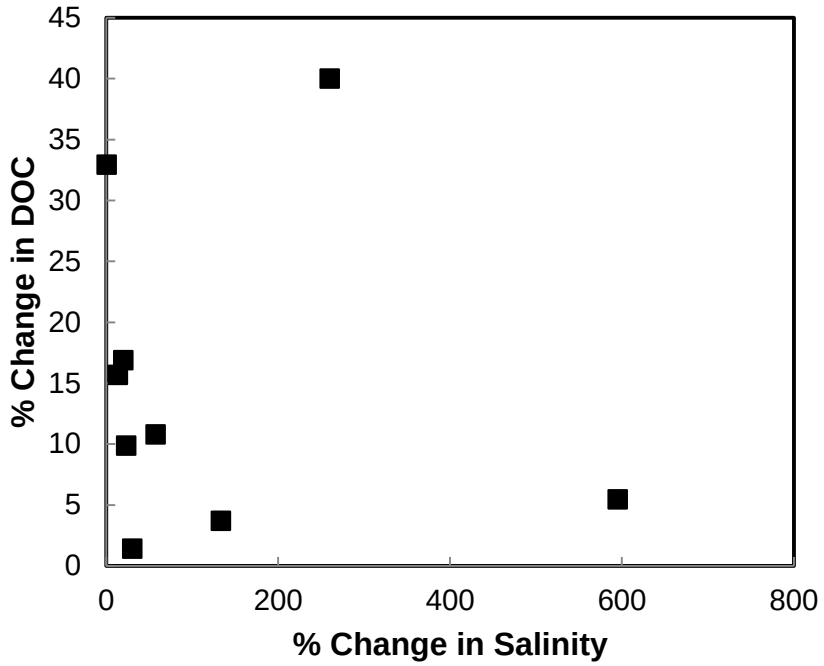

Figure 3.2 Comparison of the percent change in DOC as a function of the percent change in salinity of water samples.

3.3.2 Fluorescence Measurements

The fluorophores within NOM can be distinguished based on different fluorescent properties. Fluorescence spectroscopy can be used to produce FEEMs. These FEEMs were visualized as contour plots using MATLAB™ to show the fluorescence intensity trends with Ex/Em wavelengths. These plots showed a clear qualitative indication of the presence of humic-, fulvic-, tyrosine- and tryptophan-like fractions for each of the samples based on their unique Ex/Em intensity signals. Two examples of contour plots can be found in Figure 3.3. Higher intensities at Ex/Em ranges of 340 nm/425 nm and 260 nm/460 nm identify fulvic- and humic-like components. Tryptophan and tyrosine components show higher intensities at 275 nm/350 nm and 225 nm/300 nm, respectively.

Figure 3.3a represent Major Kollock Creek (MKC) and Figure 3.3b corresponds to Chesterman Beach (CB). These two FEEMs illustrate the differences in optical properties between samples. MKC shows a large intensity peak at emissions at 420 nm and 460 nm, corresponding to fulvic- and humic-like components. In contrast, CB showed large intensity peaks at emissions of 300 nm and 350 nm, corresponding to tyrosine- and tryptophan-like components. Contour plots for all samples can be found in Appendix B3.

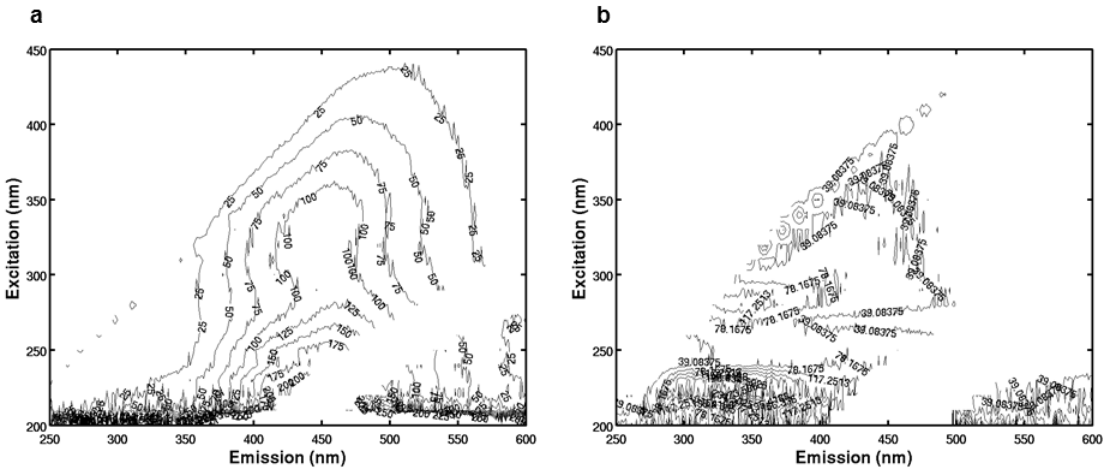

Figure 3.3 Fluorescence excitation-emission contour plots for two water samples. Major Kollock Creek (a) has higher fulvic- and humic-like components. Chesterman Beach (b) has higher tyrosine- and tryptophan-like components.

Application of the PARAFAC algorithm identified four operationally-defined fractions with the FEEMs. These were humic-, fulvic-, tryptophan- and tyrosine-like components as illustrated in Figure 3.4. This analysis described 97.7% of the variability within the fluorescent data.

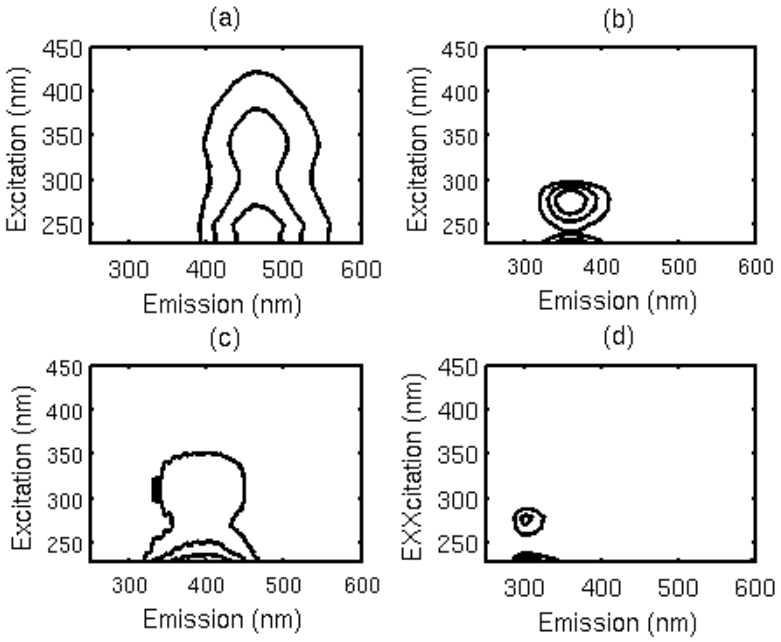

Figure 3.4 Spectra of the four components used to describe fluorescent organic matter quality within the water samples. The spectra represent (a) humic-like, (b) tryptophan-like, (c) fulvic-like, and (d) tyrosine-like fractions.

The relative concentrations of each component, measured as arbitrary fluorescence units (arb), obtained by PARAFAC are shown in Table 3.4. The toxicity assays were performed with the samples that had undergone salinity adjustment and filtration therefore all future correlations to toxicity in this study used the "after" values. The results show a large difference in fluorophore concentrations before and after salinity adjustment ranging from 0 to >1500% change in measured values. Rathtrevor Beach showed the largest change in all fluorophore components with a large increase in all values after salinity adjustment and filtration. These differences can also be viewed in Figure 3.5 which compares before and after measurements for each component compared to a 1:1 line. These plots show that the concentration of each component typically increases after salinity adjustment and filtration with the exception of the tryptophan-like

component however there is random scattering across the 1:1 lines. Humic-(a) and fulvic-like (b) components showed the least amount of change before and after salinity adjustment and filtration as compared to tyrosine- and tryptophan-like components. Note that component concentrations after salinity adjustment and filtration were used to compare to toxicity assays.

Table 3.4 Fluorescent measurements of humic- (HA), fulvic- (FA), tryptophan- (Trp) and tyrosine-like (Tyr) components of water used for toxicity assays. Measurements are from before and after salinity adjustments and filtration.

Sample	**HA (arb)**			**FA (arb)**			**Trp (arb)**			**Tyr (arb)**		
	Before	After	% Change	Before	After	% Change	Before	After	% Change	Before	After	% Change
Bouctouche	2.29	2.12	7.7	0.95	0.84	11.5	0.033	0.000	100.0	0.16	0.10	38.8
Petit Rocher	0.57	0.53	7.6	0.50	0.41	17.5	0.120	0.072	39.6	0.26	0.15	40.6
Major Kollock Creek	4.74	4.51	5.0	1.53	1.49	2.7	0.000	0.000	0.0	0.11	0.08	24.4
Naufrage Harbour	2.89	3.28	13.6	0.92	1.12	21.0	0.000	0.000	0.0	0.03	0.06	69.2
Rathtrevor Beach	0.02	0.17	764.0	0.04	0.42	972.9	0.004	0.079	2037.8	0.01	0.20	1568.8
Hawke's Bay	0.19	0.22	14.7	0.29	0.36	20.9	0.007	0.036	387.0	0.04	0.08	135.1
Blackberry Bay	0.58	0.57	1.8	0.59	0.68	15.6	0.042	0.066	55.4	0.11	0.12	4.4
Chesterman Beach	0.09	0.08	2.8	0.18	0.28	54.4	0.066	0.121	82.1	0.11	0.20	89.9
Jimbo	0.21	0.16	20.8	0.40	0.36	10.2	0.049	0.044	10.8	0.10	0.08	24.1

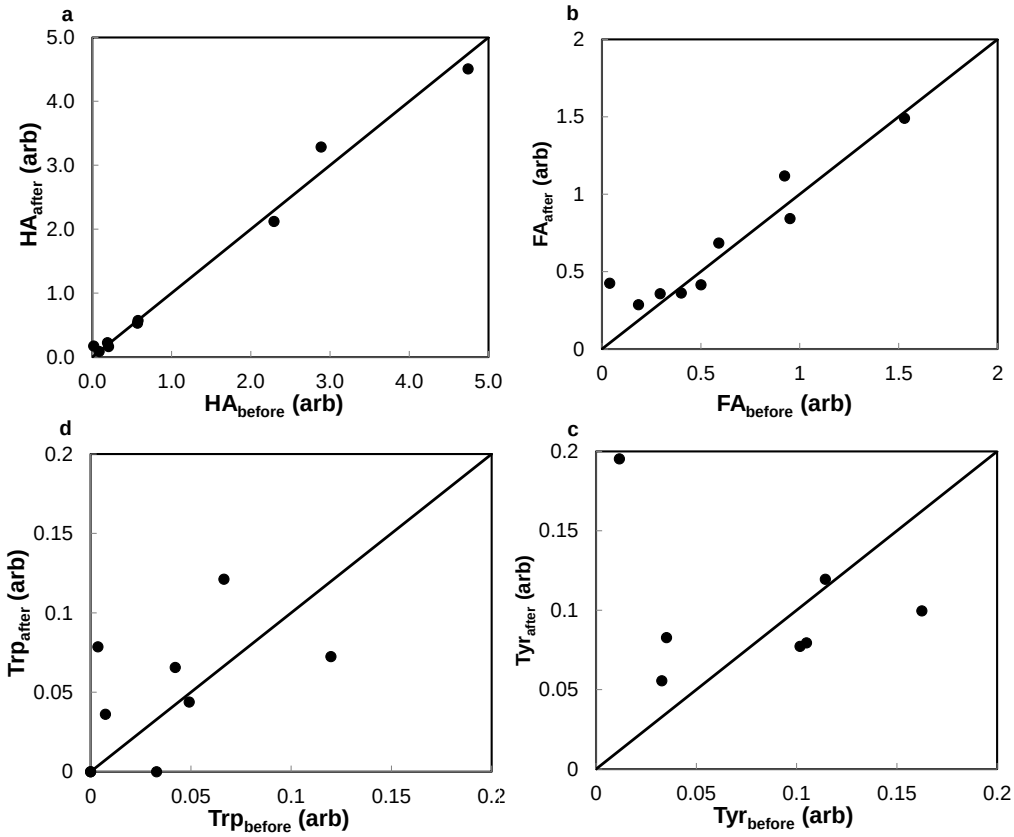

Figure 3.5 Comparison of (a) humic-, (b) fulvic-, (c) tryptophan-, and (d) tyrosine-like components before and after salinity adjustment and filtration. The 1:1 line is represented by the solid line.

The contributions of each of the four components to the total fluorescence are plotted against DOC in Figure 3.6. Both (a) humic- and (b) fulvic-like components are strongly correlated with DOC (r^2 values of 0.90 and 0.87, respectively). The tryptophan-like fraction (c) showed a correlation with DOC with an r^2 of 0.66, however only a very weak correlation was found between DOC and tyrosine (Figure 3.6d, $r^2 = 0.32$).

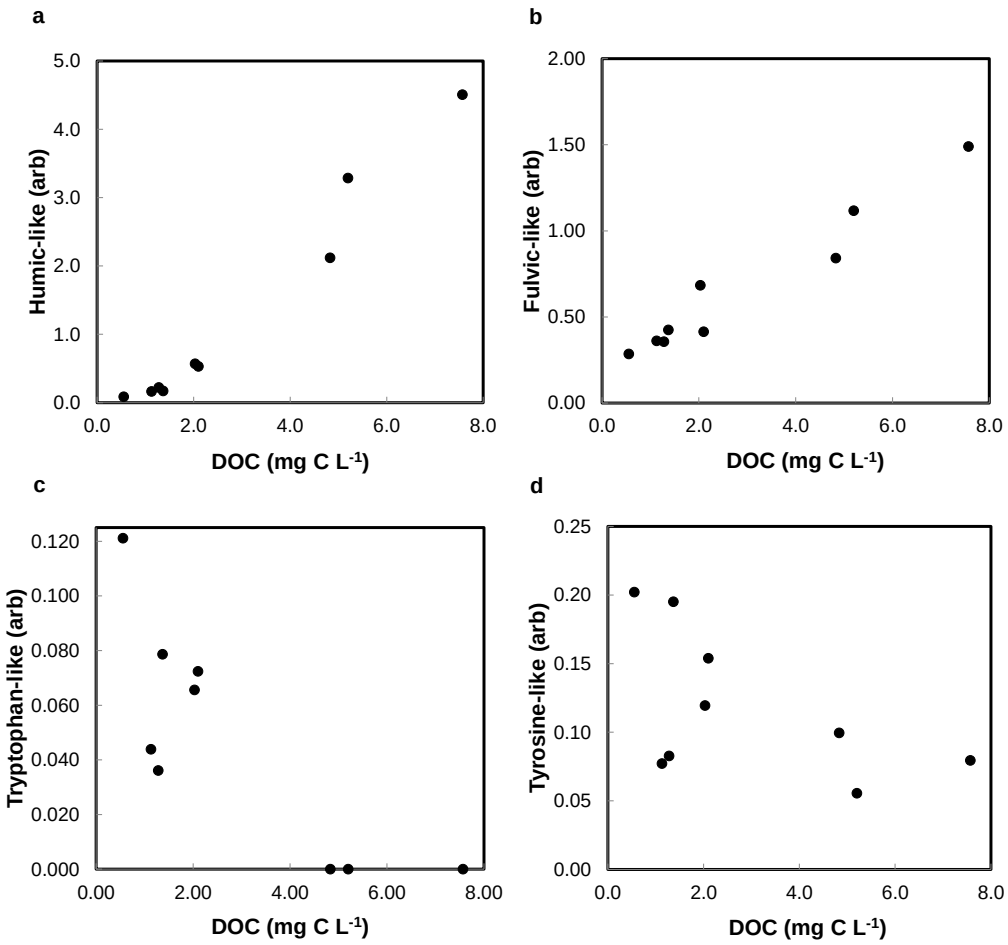

Figure 3.6 Contributions of each component as a function of DOC to the observed fluorescence including (a) humic-like, (b) fulvic like, (c) tryptophan-like and (d) tyrosine-like.

SAC_{340} and FI measurements can be observed in Table 3.5. SAC_{340} measurements of the samples indicated a range from approximately 10 to 40. FI ranged from approximately 1.25 to 1.8 suggesting samples ranged from terrestrially to microbial sources (McKnight et al. 2001). Most sources were terrestrially-derived with FI indexes of 1.25 to 1.45. Jimbo had a FI of 1.64 suggesting both terrestrial and microbial input. Petit Rocher and Chesterman Beach had relatively high FI of 1.76 and 1.77, respectively, indicating microbial sources.

Table 3.5 SAC_{340} and Fluorescence Index (FI) of each water sample used for toxicity assay.

Sample	**SAC_{340}**	**FI**
Bouctouche	21.19	1.33
Petit Rocher	14.89	1.76
Major Kollock Creek	39.37	1.25
Naufrage Harbour	28.46	1.26
Rathtrevor Beach	12.69	1.28
Hawke's Bay	20.75	1.27
Blackberry Bay	26.32	1.43
Chesterman Beach	31.61	1.77
Jimbo	10.06	1.64

3.3.3 DOC Quantity on LC_{50}

The LC_{50} ranged from 333 nM to 980 nM (21.1 µg L^{-1} to 62.3 µg L^{-1}) over a range of DOC from approximately 0.5 to 8.0 mg C L^{-1}. Overall DOC was found to be protective against copper toxicity to *Brachionus plicatilis*. This is consistent with literature for which increased NOM concentrations has been shown to be protective to *Brachionus plicatilis* (Arnold et al. 2010) as well as in other marine organisms such as the blue mussel, *Mytilus sp.* (DePalma et al. 2011; Nadella et al. 2009) and the sea urchin (*Parecentrotus lividus*) (Lorenzo et al. 2006). As well, Arnold et al. (2010b) also found a significant relationship between DOC and EC_{50} values in six different species (the blue mussels, *Mytilus galloprovincialis* and *M. edulis*, the oyster, *Crassostrea virginica*, the sand dollar, *Dendraster excentricus*, the sea urchin, *Strongylocentrotus purpuratus*, and the copepod, *Eurytemora affinis*). However, from this data, two potential trends were observed. The first trend shows a plateauing out of the protective effect of DOC. This

trend can be observed in Figure 3.7. A low DOC (< 0.5 mg C L^{-1}) in ASW sample from Arnold et al. (2010) for *Brachionus plicatilis* using the same ASTM (2004) protocol was added to the data set as a control. The dashed lines represent the trend in the data. A steep increase in LC_{50} is observed when going from zero DOC to approximately 2 mg C L^{-1} DOC. This resulted in a linear correlation with an r^2 of 0.72 and significant *p*-value of 0.016. At DOC concentrations above this point, further increases in DOC did not significantly affect copper toxicity and a plateauing of the line is observed.

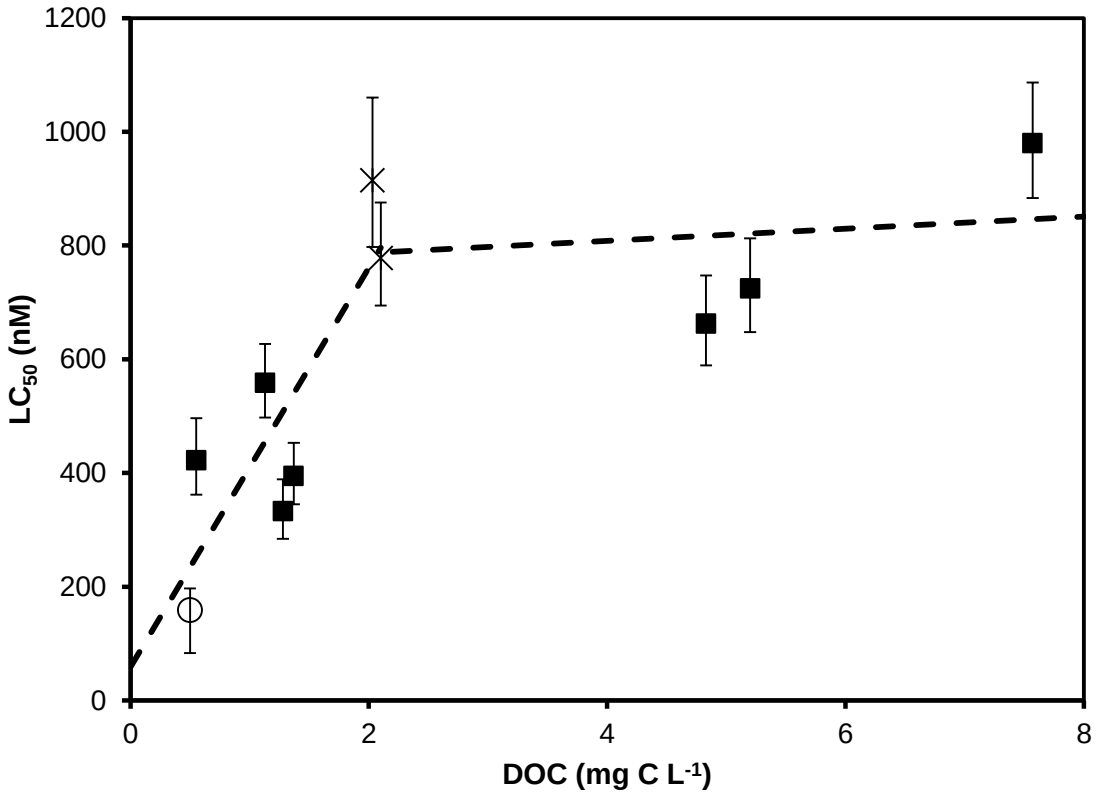

Figure 3.7 Total dissolved copper LC_{50} as a function of DOC representing a salt-induced colloid formation trend. The dash lines show the salting out effect trend of the data. A steep increase in LC_{50} is observed until approximately 2 mg C L^{-1} DOC (r^2 = 0.72, *p*-value = 0.016) then a plateau effect is observed suggesting salt-induced colloid formation. Circle (○) data point represents a control ASW sample from Arnold et al. (2010). Cross (×) data points represent potential outliers.

It was hypothesized that the decrease in protectivity as DOC concentrations increased was due to salt induced colloid formation of DOC particles that could occur at high salinities. This can be described using the Derjanguin-Landau-Verwey-Overbeek (DLVO) theory (Christenson, 1984). The force between two surfaces in liquid is predicted by the continuum theory which predicts this force by the sum of van der Waals force and electrostatic force. Van der Waals force allows for attraction between two similar surfaces while electrostatic forces result in repulsion between surfaces of the same charge. However, at high ionic strength, repulsive forces decrease due to collapse of the electrical double layer. This allows for the possibility of colloidal particles in a liquid medium to form persistent aggregates due to van der Waals force of attraction (Liang et al. 2007). At a constant salinity, DOC-DOC interactions increase at higher DOC. The increased DOC-DOC interactions results in less binding sites available for copper to bind and therefore more copper is bioavailable to cause toxicity. As supported by the data in Figure 3.7 at low DOC a linear trend should be seen and then plateau at high DOC. This trend has been seen in another rotifer toxicity study in which exogenous DOC was added to artificial water (Cooper et al. 2013). At 30 ppt salinity, a plateau effect was seen at DOC concentrations above approximately 5 mg C L^{-1}. Brooks et al. (2007) found a comparable trend in the pacific oyster, *Crassostrea gigas*. In this case, humic acid concentrations great than 1.02 mg C L^{-1} did not provide any further protection against copper toxicity. Similarly, copper toxicity in the marine blue mussel (*Mytilus trossolus*) increased in a linear trend when moving from 0 to 10 mg C L^{-1} with EC_{50} values from 148 nM to 582 nM, respectively. However, when the DOC was doubled to 20 mg C L^{-1}, the EC_{50} plateaued with an EC_{50} value of 614 nM (Nadella et al. 2009). This relationship

has also been observed for lead toxicity. In *M. trossolus* and *M. galloprovincialis* an increase in DOC from 0 to 2 mg C L^{-1} increased the EC_{50} of lead significantly from 217 nM and 304 nM to 564 nM and 738 nM for *M. trossolus* and *M. galloprovincialis*, respectively (Nadella et al. in press). However, above 2 mg C L^{-1} up to 12 mg C L^{-1}, there was no significant change in the EC_{50} of *M. trossolus* (521 nM) and *M. galloprovincialis* (758 nM) (Nadella et al. in press).

The second potential relationship between LC_{50} and DOC is suggested if the two sample sites around 2 mg C L^{-1} (Petit Rocher and Blackberry Bay) are considered outliers. These two sample sites show a large increase in protective effect at low DOC, resulting in the observance of a salt-induced colloid formation trend at increase DOC concentrations. However, if these samples are outliers, then there is less support for the salt-induced colloid formation trend. The suggested reasoning for these sites being outliers may be due to sample location. Both Petit Rocher and Blackberry Bay samples were the only samples obtained from marina waters. As such, the water of the marina may not be representative of the water in the surrounding area resulting in the increased protectivity at these sites compared to the other sites. Differences in water quality resulting from proximity to a marina that would result in an increased protectivity at these locations were not characterized. As well, to further support that these sites are outliers are the results from the free copper measurements at the LC_{50} (see Section *3.3.5*) which shows that free copper measurements for these two sites differ from the other sites. If these two sample sites are considered outliers and do not actually reflect salt-induced colloid formation then the relationship between LC_{50} and DOC can be described by the equation LC_{50} (μg L^{-1}) = $25.15DOC^{0.47}$ including the two outlier sites in statistical

analysis or LC_{50} (µg L^{-1}) = $22.86DOC^{0.45}$ without including the outlier sites. This equation is given in µg L^{-1} units to compare with toxicity equations for other species in and Arnold et al. (2006) and Arnold et al. (2010). The relationship has an r^2 of 0.61 and is significant with a *p*-value of 0.008 including outliers or an r^2 of 0.71 and *p*-value of 0.009 excluding outliers.

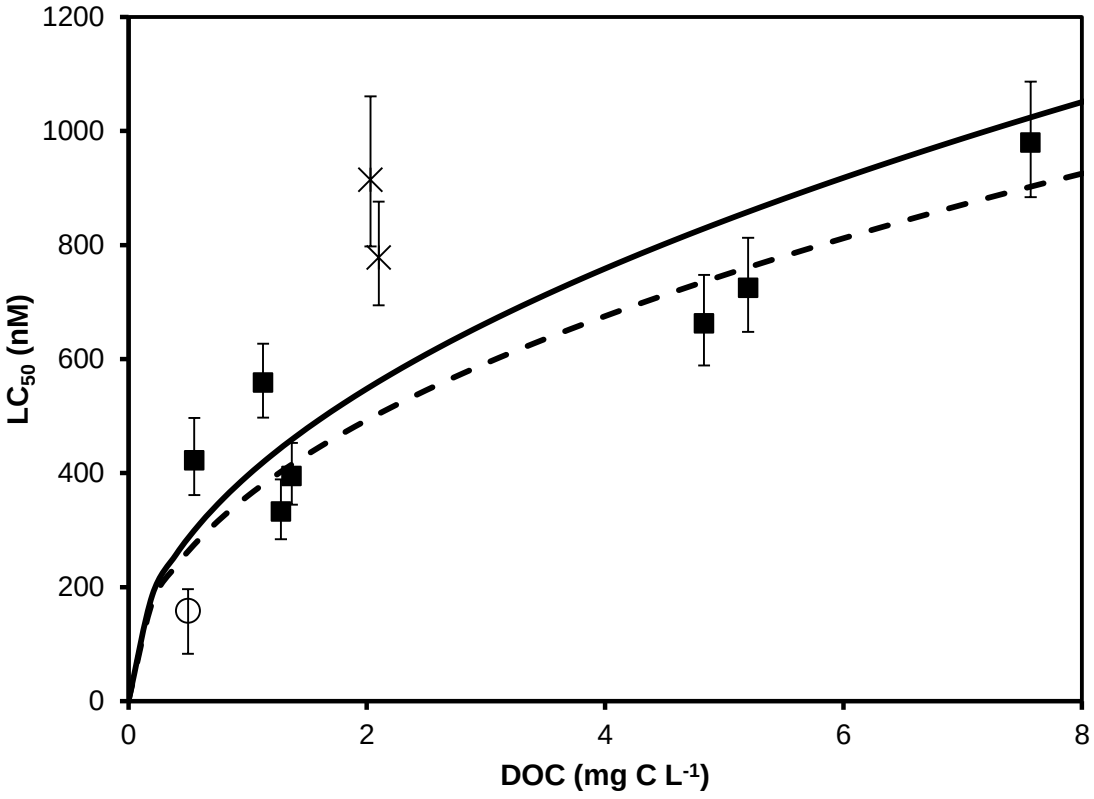

Figure 3.8 Total dissolved copper LC_{50} as a function of DOC. Solid trendline represents the relationship including outliers with LC_{50} (µg L^{-1}) = $25.15DOC^{0.47}$. Dashed trendline represents relationship excluding outliers with LC_{50} (µg L^{-1}) = $22.86DOC^{0.45}$. Circle (○) data point represents a control ASW sample from Arnold et al. (2010). Cross (×) data points represent potential outliers.

The relationship between LC_{50} and DOC for *Brachionus plicatilis* can be compared to the relationship observed in other species in Figure 3.9. This figure shows the relationship between LC_{50} and DOC from this study as well as for Mytilus sp. ($EC_{50}(\mu g\ L^{-1}) = 11.22DOC^{0.6}$; Arnold et al. 2006), the oyster, *Crassostrea virginica* ($EC_{50}(\mu g\ L^{-1}) = 12.7DOC^{0.65}$), the sand dollar, *Dendraster excentricus* ($EC_{50}(\mu g\ L^{-1}) = 18.4DOC^{0.83}$), and the sea urchin, *Strongylocentrotus purpuratus* ($EC_{50}(\mu g\ L^{-1}) = 12.8DOC^{0.76}$) (Arnold et al. 2010). From these comparisons it can be seen that *Brachionus plicatilis* has a similar relationship to other copper-sensitive aquatic organisms. However, *Brachionus plicatilis* appears to have increased protectivity at lower DOC concentrations and decreased protectivity at increased DOC concentrations compared to the other organisms shown here. This is illustrated by the steeper slope at lower DOC concentrations moving to a shallower slope at increasing DOC concentrations as compared to the other model lines.

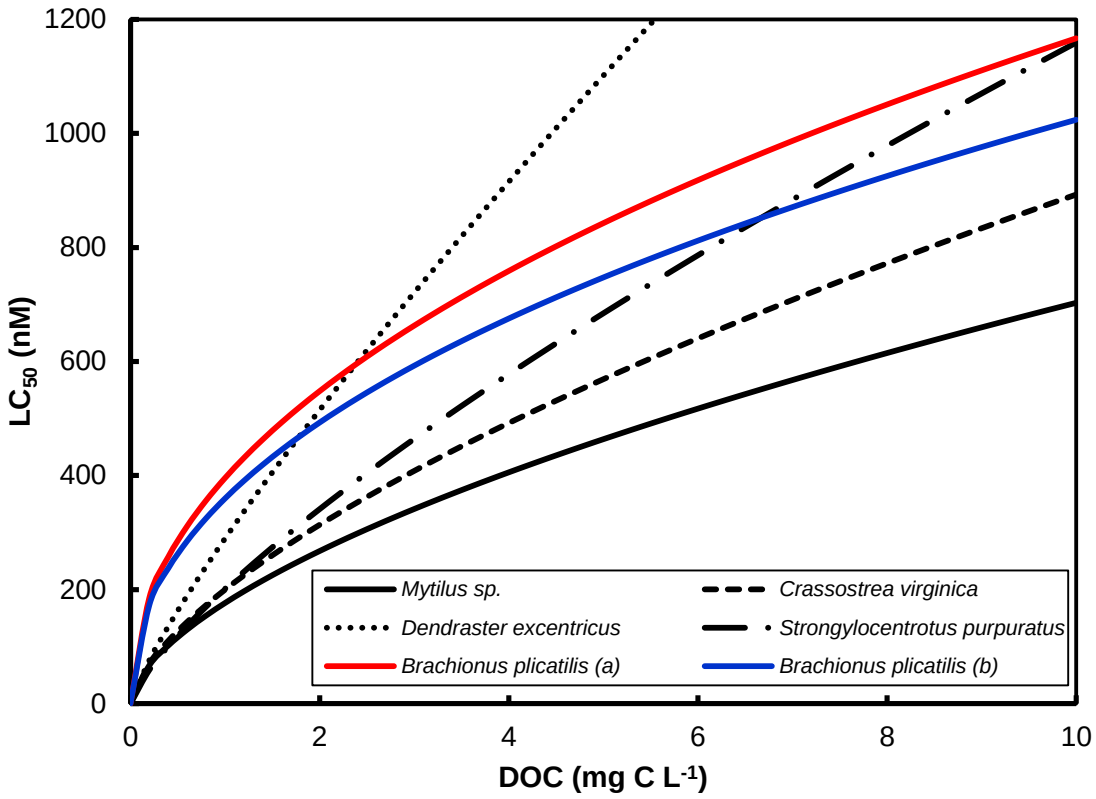

Figure 3.9 Comparison of predictive toxicity equations for *Mytilus sp.*, *Crassostrea virginica*, *Dendraster excentricus*, and S*trongylocentrotis purpuratus*. *Brachionus plicatilis* (a) represents the toxicity equation including the outlier data while (b) represents the toxicity equation excluding the outlier data.

3.3.4 DOC Quality on LC_{50}

SAC_{340} is a measure of colour and has been suggested as a measure of DOM quality (Schwartz et al. 2004). SAC_{340} has shown a good correlation to metal toxicity in freshwater with a higher SAC_{340} (indicating terrigenous C) shown to decrease Cu bioavailability more than organic matter with a lower SAC_{340} (Schwartz et al. 2004). Using the SAC_{340} data from Table 3.5, in the marine samples measured, no correlation was observed between SAC_{340} and LC_{50} normalized to DOC (Figure 3.10a). This is

consistent with De Palma (2009) in which only a very weak correlation (r^2 = 0.28) was observed from ten estuarine and marine samples.

An approximation of NOM origin was determined using fluorescence indices (McKnight et al. 2001). A FI of approximately 1.4 and 1.9 indicates terrestrially-derived and microbially-derived NOM, respectively. Following the idea that terrestrially-derived organic matter is more protective (Schwartz et al. 2004), as FI increases, a decrease in protectivity should be observed. However, the opposite was observed when the FI data from Table 3.5 was plotted with LC_{50} (Figure 3.10b). An increase in LC_{50} normalized for DOC is observed as FI increases. This correlation is significant with a *p*-value of 0.008 and an r^2 of 0.66. This correlation may be due to the fact that samples with higher total DOC were predominantly terrestrially-derived sources. Therefore, when normalized to DOC, the LC_{50} decreased substantially more than microbially-derived sources that contained lower total DOC. This could also mean that microbially-derived sources had stronger ligands than predicted or that terrestrially-derived organic matter copper complexes have the ability to be taken up by an organism resulting in less protectivity.

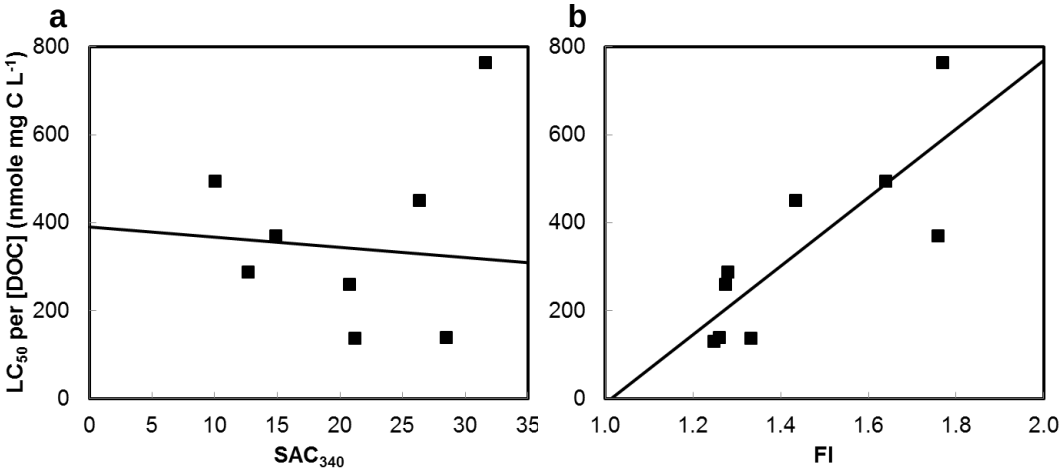

Figure 3.10 Copper LC_{50} as a function of (a) SAC_{340}, and (b) fluorescence index (FI).

It has been found that terrestrial organic material is more protective than microbially-derived organic material (Luider et al. 2004; Pempkowiak et al. 1999; Schwartz et al. 2004). Since terrestrial organic matter is mostly composed of fulvic and humic acids (Birdwell & Engel 2009; McKnight et al. 2001) it was thought that DOC will show more protectiveness when these components are in higher concentrations. The relationship between the four different fluorescent components of DOC and the LC_{50} is shown in Figure 3.11. Both humic- and fulvic-like fractions with LC_{50} show a positive correlation with LC_{50}. For fulvic-like (b) fractions a significant linear increase is observed (r^2 = 0.53, *p*-value = 0.027). Humic-like (a) fractions were just outside the range of significance with a *p*-value of 0.062 and an r^2 of 0.41. Tryptophan (c) and tyrosine (d) show a very weak, slightly negative correlation with LC_{50} with an r^2 of 0.18 and 0.14, respectively. Both tryptophan and tyrosine showed no significance with *p*-values of 0.261 and 0.328, respectively. The very low correlation of tryptophan- and tyrosine- like fluorophores could be due to the low fluorescent intensities that have larger relative errors which may mask any potential correlations. Similar trends were seen in De Palma et al. (2011) where the total contribution of tyrosine- and tryptophan-like components were found to be a constant fraction of the total fluorescence, independent of DOC.

The protective effect of humic- and fulvic-like fractions agree with data presented in Lorenzo et al. in which humic acids (2002) and fulvic acids (2006) proved protective to the sea urchin, *Paracentrotus lividus* against copper toxicity. As well, Nadella et al. (2009) estimated fulvic-like fraction concentrations from three different NOM sources using fluorescence techniques and found a strong protective effect. The most protective

NOM source was found to contain 20% and 40% higher fulvic substance content than the two less protective NOM sources (Nadella et al. 2009).

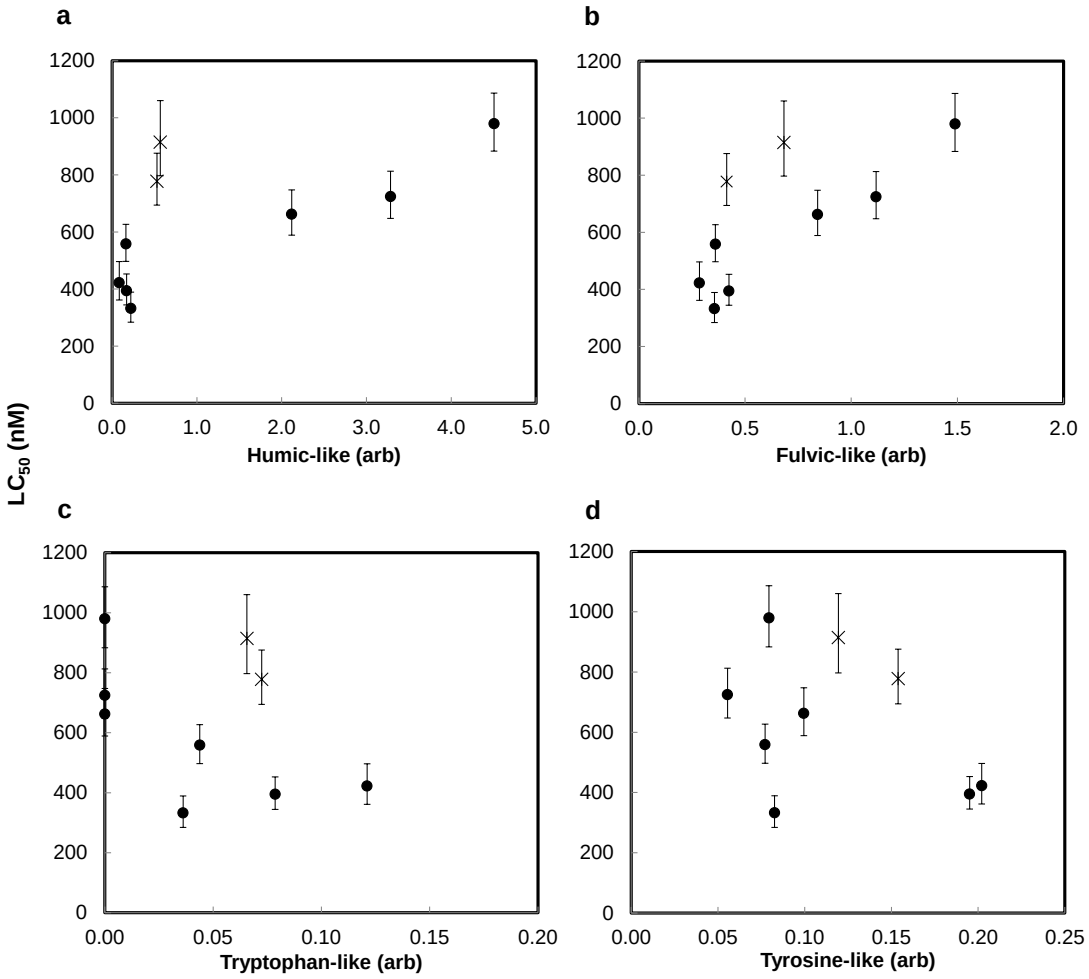

Figure 3.11 Copper LC_{50} as a function of fluorescent (a) humic-, (b) fulvic-, (c), tryptophan-, and (d) tyrosine-like components. Cross (×) data points represent the potential outlier sites.

Figure 3.12 visually illustrates that the marine samples varied in organic matter quality. In this figure, the size of the symbols indicate the percent contribution to total fluorescence of each component within each sample. For both (a) humic-, and (b) fulvic-like components the contributing fluorescence to total fluorescence increases with DOC

values. In contrast, (c) tryptophan-like fractions and (d) tyrosine-like fractions showed a higher percent contribution to total fluorescence in samples with low DOC values compared to high DOC values. This is consistent with the results from Figure 3.11 where tyrosine and tryptophan remained constant within DOC. As DOC increased, the humic- and fulvic-like components increased as well resulting in a larger contribution to total fluorescence causing a relative decrease in the proportion of tyrosine- and tryptophan-like factors.

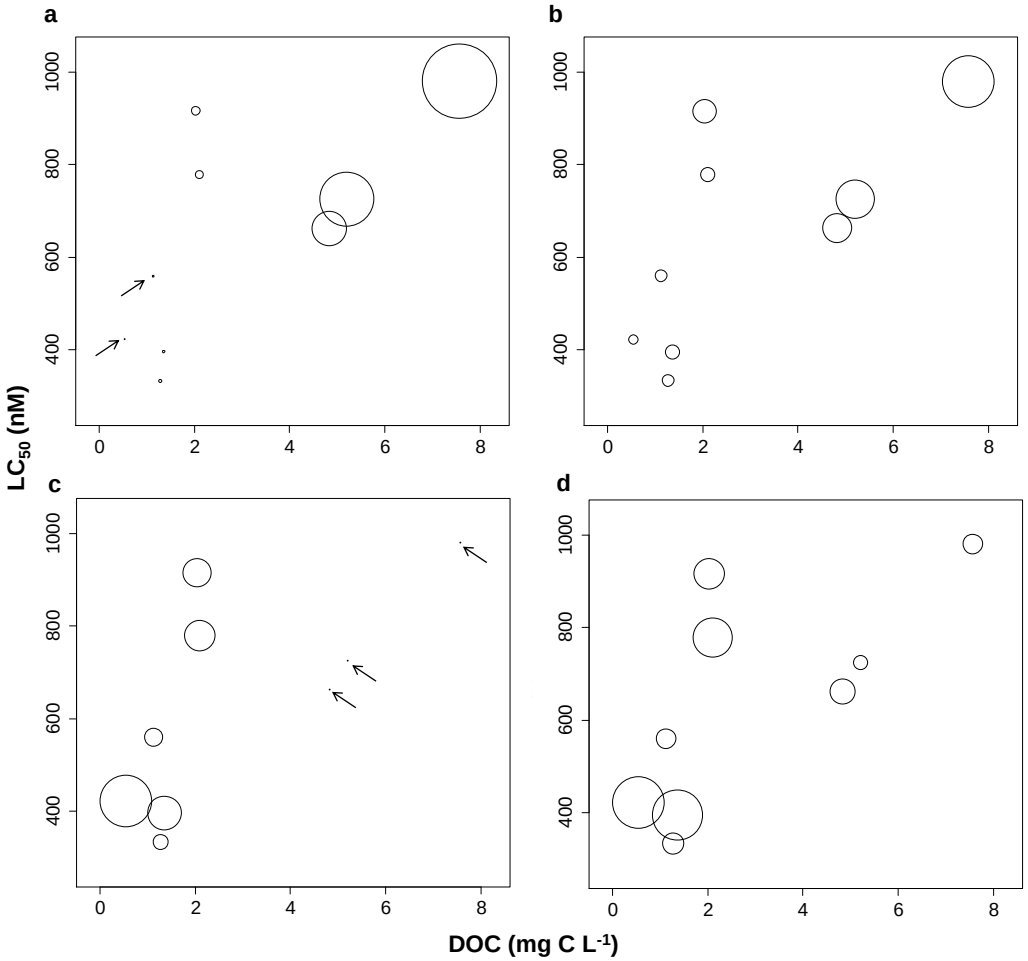

Figure 3.12 Plots of DOC versus LC_{50} weighted by contribution of fluorescence for (a) humic-, (b) fulvic-, (c) tryptophan-, and (d) tyrosine-like components. The larger symbols correspond to the largest contributions and the smallest symbols correspond to the smallest contributions. Arrows indicate position of samples in which there was very little/no component present.

3.3.5 Free Copper and LC_{50}

The free copper at the LC_{50} for each sample was measured using the Cu ISE. The comparison of free copper, reported as pCu ($-\log[Cu^{2+}]$), for each site can be found in Figure 3.13.

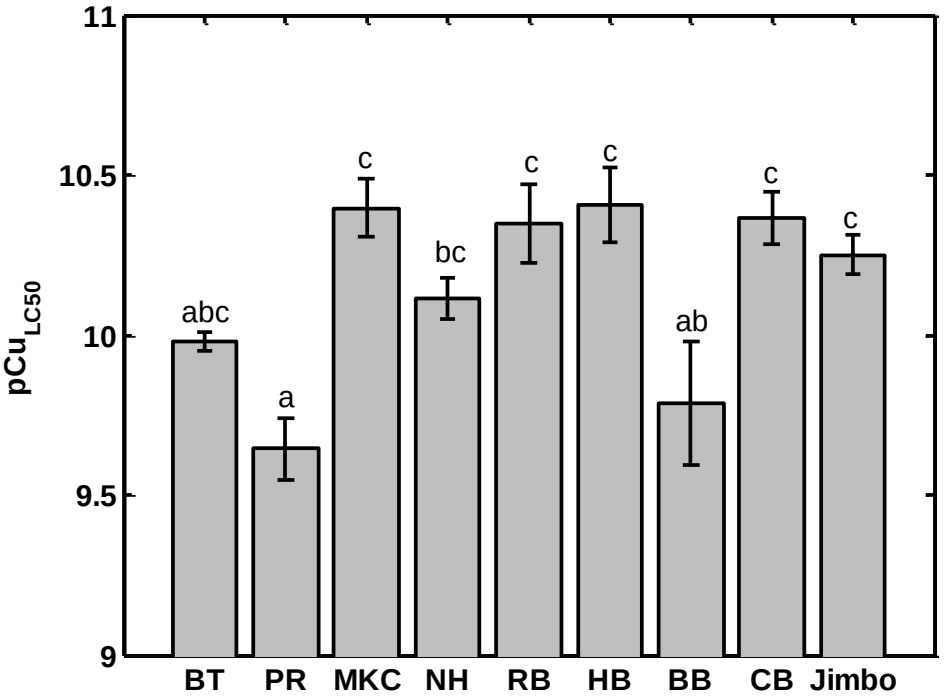

Figure 3.13 Free copper measurements at the LC_{50} for each site (Refer to Table 3.1 for full names of sampling sites). Error bars represent 95% confidence intervals.

Seven of the nine samples measured were found to be statistically similar. Petit Rocher (PR) was found to be significantly different from all sites excluding Bouctouche (BT) and Blackberry Bay (BB). BB was found to be similar to BT, PR and Naufrage Harbour (NH) but significantly different from the other sites. This supports the suggestion that Petit Rocher and Blackberry Bay are outliers as discussed in Section

3.3.3. These results suggest that although differences in free copper are observed, most of these differences are not significant and free copper is statistically similar in these sites.

Another way to look at this data is by plotting the free copper as a function of LC_{50}. This can be seen in Figure 3.14. The solid line represents the mean of the data and the dashed lines represent a factor of two around the data. This factor of two was added since the BLM currently predicts toxicity within a factor of two (Arnold et al. 2010). In this study, all samples, save one (PR), fall within the factor of two about the mean. The LC_{50} for free copper spans a range from 333 nM to 980 nM but as LC_{50} increases, there is no significant increase in free copper with free copper pCu values ranging from 9.64 to 10.4 (2.5 - 14.4 ng L^{-1}). As mentioned above, Petit Rocher and Blackberry Bay measured slightly higher free copper at the LC_{50} than the other samples. Without these measured free copper concentrations, the free copper is very constant ranging from only 9.98 to 10.40 (2.5 – 6.7 ng L^{-1}). The slight increase in free copper of Petit Rocher and Blackberry Bay may be related to differences in DOC that may affect copper uptake. However, these differences were not characterized by the methods used in this study. Future work could apply high performance size exclusion chromatography (HPSEC) (Landry & Tremblay 2012; Wu et al. 2003) or immobilized metal ion affinity chromatography (IMAC) (Midorikawa & Tanoue 1998; Wu & Tanoue 2001) before fluorescence or other NOM characterization to obtain more information on size and composition of the organic matter. For instance, Landry and Tremblay (2012) used HPSEC with Fourier transform infrared spectroscopy (FTIR) and found that low molecular weight (LMW) marine NOM was enriched with sulfate groups as compared to high molecular weight (HMW) marine NOM which was the most amide-rich size

fraction. Using IMAC with absorption and fluorescent techniques, Midorikawa & Tanoue (1998) found that LMW fractions showed weaker ligand sites while HMW fractions had stronger copper-complexing ligand sites. These methods may provide some insight on the relationship of size of NOM and influence on free copper and toxicity that were not examined in this study.

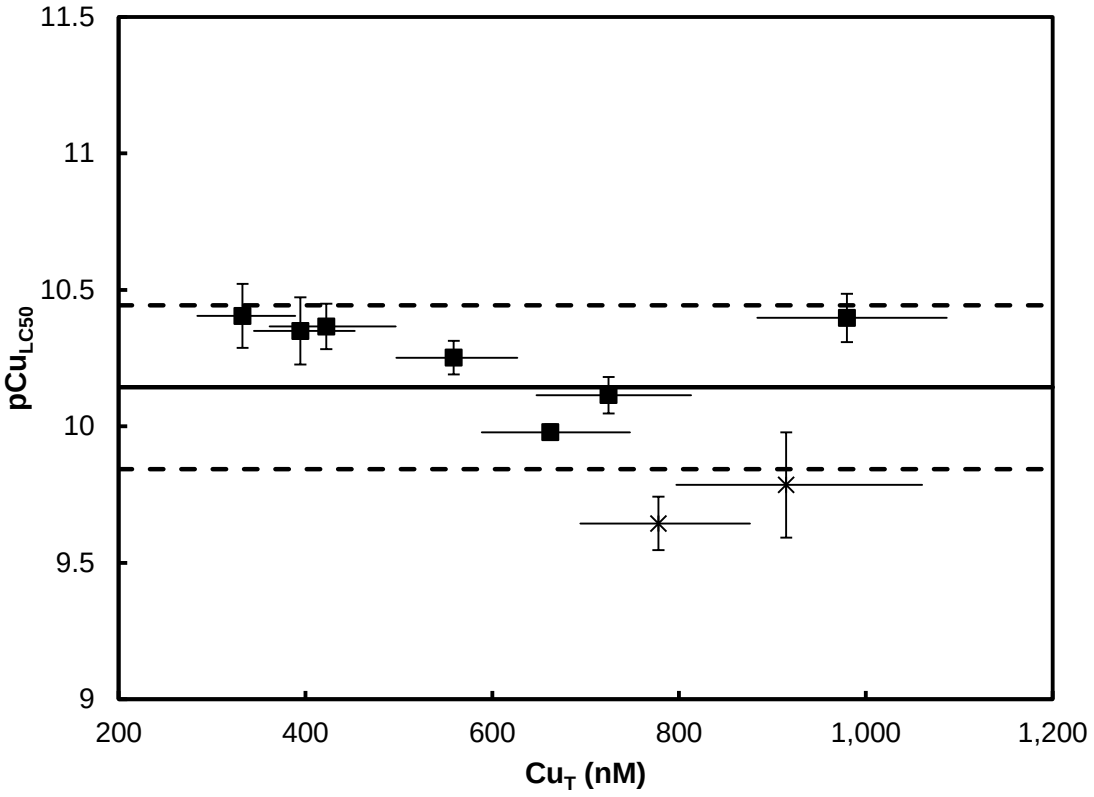

Figure 3.14 Free copper at the LC_{50} as a function of total copper at the LC_{50}. The solid line represents the mean free copper and the dashed lines represent a factor of two of the ISE data. Error bars represent 95% confidence intervals. Cross (×) data points represent the potential outlier sites.

In ambient clean sea water samples, a pCu concentration of 11.9 was found in Macquarie Harbour, Tasmania. As well, a pCu of 11.5 was found for clean marine water off the coast of Peru (Sunda & Ferguson 1983). Toxicity was observed for *Brachionus*

plicatilis at an average pCu of 10.1, which adds strength to these measurements since toxicity was observed at higher free copper concentrations than ambient water samples in which copper toxicity is not observed. In addition, the pCu values found in this study is consistent with pCu values observed in other copper toxicity assays. In Eriksen et al. (2001), the marine alga, *Nitzschia closterium* was found to have decreased growth rates over a pCu range from 11.3 to 8.2. Sunda and Guillard (1976) reported reduced growth rates of the marine diatom, *Thalassiosira pseudonana*, from pCu values of 11.2 to 8.2. As well, reduced growth rates of seven marine diatom species showed reduced growth rates at pCu values from 10.5 to 11.0 (Brand et al. 1986).

Free copper is often considered the best indicator of toxicity due to this species being most available to interact with an organism (Chadwick et al. 2008; Eriksen et al. 2001, Sunda & Hanson 1979). Eriksen et al. (2001) reported that free copper measurements directly correlated to growth rate inhibition of the marine diatom, *Nitzschia closterium*, while anodic stripping voltammetry (ASV) labile copper (free copper + free copper bound to inorganic ligands) significantly overestimated the toxicity. Stauber et al. (1996) also found similar results where ASV measurements predicted growth inhibition to *N. closterium* based on the concentrations measured, however no toxicity was observed. These results lend credence to the theory that free copper is the best estimate of toxicity.

Following this idea, it is proposed that differences in LC_{50} values are due to differences in water chemistry interactions that affect how much total copper is needed to reach the critical free copper concentration required to cause toxicity. For example, in cases where DOC is high, more copper is able to bind and become unavailable for

uptake, thus a higher total copper concentration is needed to reach a free copper concentration that causes toxicity. Constant free copper values are clearly illustrated by the free copper corresponding to the lowest and highest LC_{50} values obtained in this study. Hawke's Bay resulted in the lowest LC_{50} with a value of 333 nM, and Major Kollock Creek had the highest LC_{50} value of 980 nM. However, the free copper measured for both of these sites were identical with a pCu of 10.40. This has also been observed for labile copper in the pacific oyster, *Crassostrea gigas* (Brooks et al. 2007). In this case, the labile copper EC_{50} concentration remained constant at an average concentration of 109 nM, despite total copper EC_{50} ranging from 327 nM to 638 nM.

3.3.6 Effect of DOC on free copper

The relationship between free copper at the LC_{50} and DOC is fairly constant and is illustrated in Figure 3.15. Although Blackberry Bay (DOC = 2.03 mg C L^{-1}) was not statistically different than Bouctouche or Naufrage Harbour (DOC values of 4.83 mg C L^{-1} and 5.20 mg C L^{-1}, respectively), this site along with Petit Rocher (DOC = 2.10 mg C L^{-1}) showed slightly more free copper at the LC_{50} as compared to the other sample sites which showed toxicity at pCu values between 10 and 10.4. The more protective effect at these sites, resulting in higher concentrations of free copper before toxicity occurs, was discussed in Section *3.3.5*. However, overall this figure displays no significant trend in free copper concentrations with DOC. This was expected since free copper at the LC_{50} was similar (within a factor of two) for all sites. This data is consistent with the results from Brooks et al. (2007) in which labile copper at the LC_{50} was constant across a DOC range from 0.12 mg C L^{-1} to 3.13 mg C L^{-1} for the pacific oyster. This data further

supports the theory that a critical concentration of free copper is required to cause toxicity.

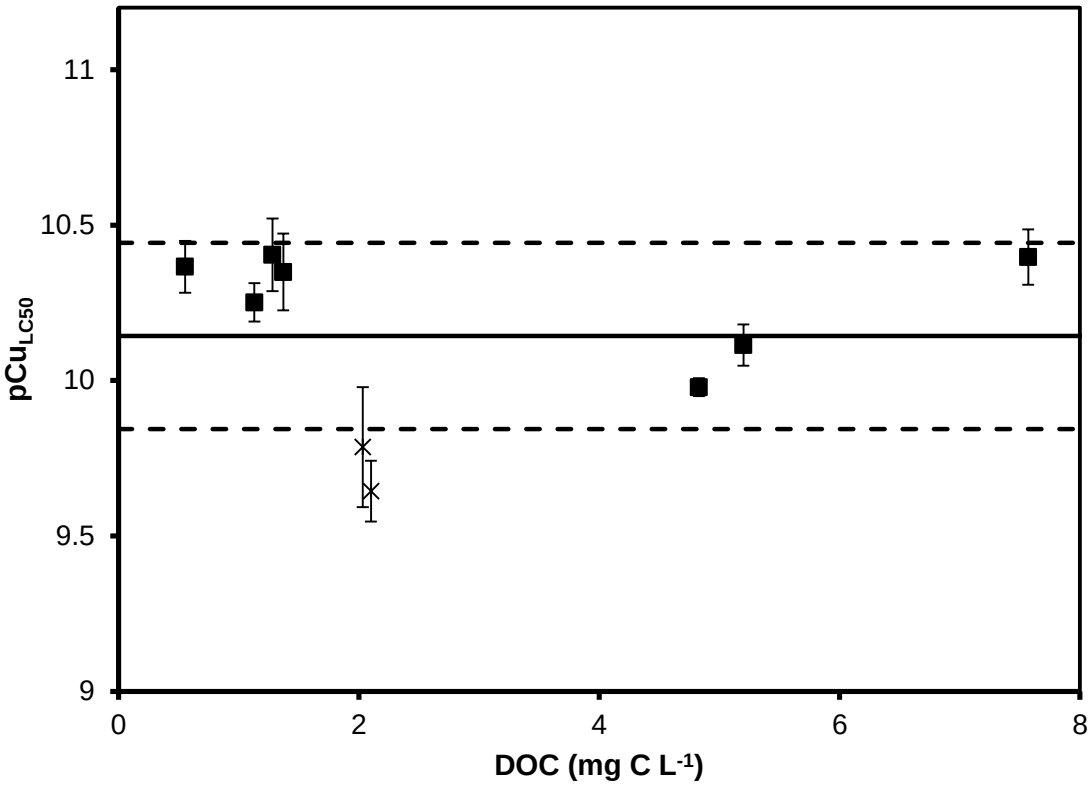

Figure 3.15 Free copper at the LC_{50} as a function of DOC. The mean (solid line) and factor of two (dashed lines) are also included. Error bars represent 95% confidence intervals. Cross (×) data points represent the potential outlier sites.

With respect to the fluorophore components within NOM, there was no significant correlation between the free copper and any of the four components (Figure 3.16).

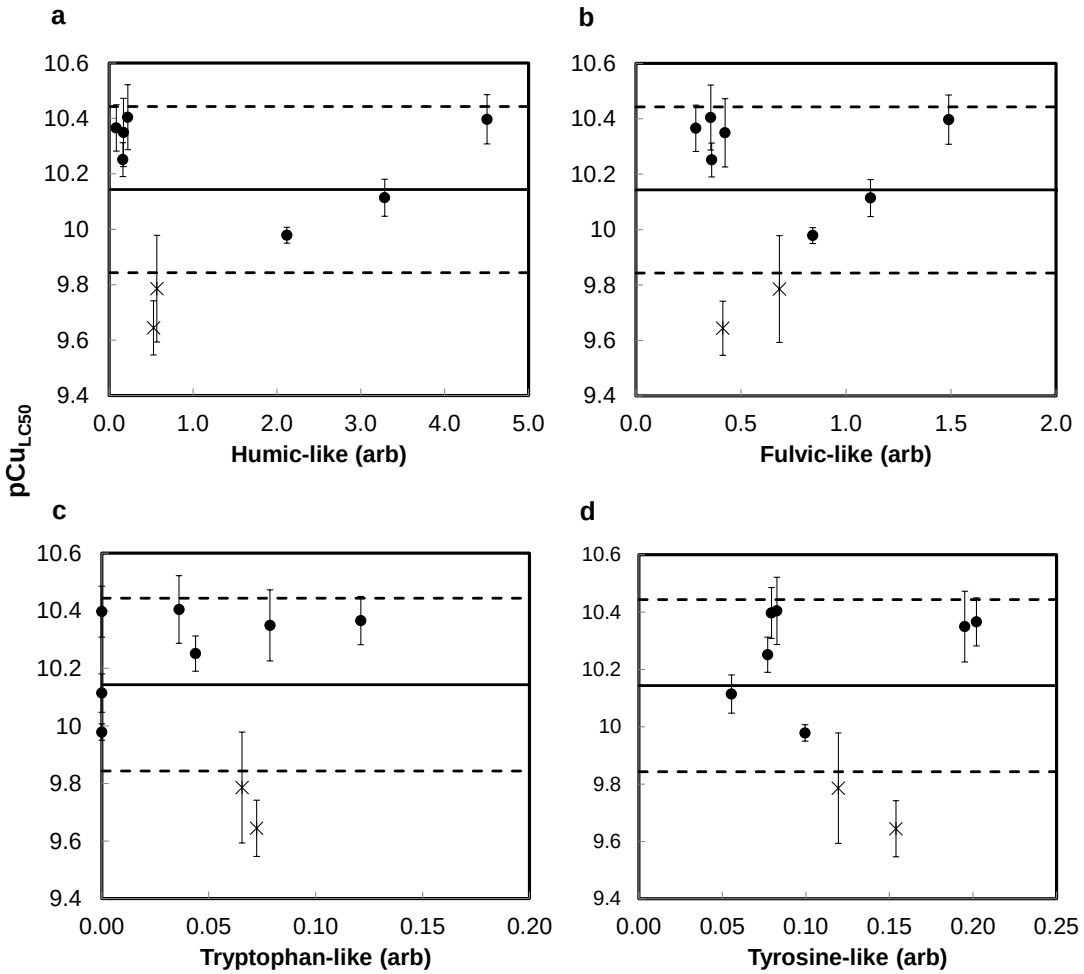

Figure 3.16 Free copper at the LC_{50} as a function of fluorescent (a) humic-, (b) fulvic-, (c), tryptophan-, and (d) tyrosine-like components. The mean is depicted by the solid line and a factor of two is represented by the dashed lines.

Overall, the lack of significant trends of DOC characteristics with free Cu at the LC_{50} add strength to the notion that free copper, within variation, is constant despite the change in total copper LC_{50}. This suggests that free copper is a good predictor of toxicity.

3.4 Conclusions

The findings of this study suggest that DOC is protective against copper toxicity in marine environments independent of DOC source and quality which is consistent with De Palma et al. (2011). DOC was found to be protective to *Brachionus plicatilis.* However, it was shown that two possible relationships between LC_{50} and DOC exist. For the first trend, a plateau effect in which the amount of increased protectivity decreased as DOC increased above 2 mg C L^{-1} was observed. The suggested reasoning for this plateau effect in LC_{50} as DOC increases is due to salt-induced colloid formation. The increase in DOC-DOC interactions at high salinity reduce the available binding sites for copper thereby allowing more copper to be bioavailable to cause toxicity. This is supported by other studies with copper (Brooks et al. 2007; Cooper et al. 2013; Nadella et al. 2009) and lead (Nadella et al. in press) which show the same trend. The second trend showed a relationship where LC_{50} (µg L^{-1}) = $25.15DOC^{0.47}$ including the outlier data or LC_{50} (µg L^{-1}) = $22.86DOC^{0.45}$ excluding the outlier data. Similar relationships between LC_{50} and DOC have been observed in other marine organisms (Arnold 2005; Arnold et al. 2006, Arnold et al. 2010, Arnold et al. 2010a; DePalma et al. 2011).

Free copper has been deemed the best predictor of copper toxicity as it is the species most bioavailable. The data here shows that regardless of water chemistry, free copper concentrations are relatively constant, within a factor of two, at the LC_{50}. This suggests that a critical free copper concentration is required to cause toxicity, however the amount of total copper needed to reach this critical concentration changes depending on the water chemistry.

The overall BLM implication of this study is that a source dependent parameter for DOC is not necessary to include in equilibrium models to predict site specific LC_{50} values. In addition, the free copper data presented here is consistent with the BLM which suggests that bound Cu at the site of the biotic ligand is proportional to toxicity. Future work consists of applying these methods to more natural seawater samples, ideally in samples with DOC ranges between 2 and 4 mg C L^{-1} to determine which trend most accurately represents the correlation between LC_{50} and DOC. As well, future studies will further address the influence of DOC source on free Cu and toxicity. DOC can be further characterized by the use of HPSEC or IMAC as discussed in Section *3.3.5*. Applying accumulation studies to these methods while utilizing a different organism to which copper accumulation can be measured would also be useful. This will give a better understanding of the interactions of copper at the site of the biotic ligand. For instance, some studies have suggested organic-metal complexes increase metal uptake with respect to copper (Lorenzo et al. 2005), lead (Sánchez-Marín et al. 2011) and cadmium (George & Coombs 1977; Kozuch & Pempkowiak 1996; Pempkowiak & Kozuch 1994) in marine water. Current modeling considers only the free metal available for interaction and uptake by an organism so applying accumulation studies specifically in the presence of increased humic and fulvic acid content to determine bioavailability of these copper-organic complexes would also be beneficial.

3.5 References

American Society for the Testing of Materials International (ASTM). 2004. Standard guide for acute toxicity test with the rotifer Brachionus. E 1440-91. Annual book of ASTM standards. Vol 11.05. West Conshohocken, PA, 830-837.

Arnold, W.R., 2005. Effects of dissolved organic carbon on copper toxicity: implications for saltwater copper criteria. *Integrated Environmental Assessment and Management*. **1**, 34-39.

Arnold, W.R., Cotsifas, J., Corneillie, K.M. 2006. Validation and update of a model used to predict copper toxicity to the marine bivalve *Mytilus sp*. *Environmental Toxicology*. **21**, 65-70.

Arnold, W.R., Diamond, R.L., Smith, D.S. 2010. The effects of salinity, pH, and dissolved organic matter on acute copper toxicity to the rotifer, *Brachionus plicatilis* ("L" strain). *Archives of Environmental Contamination and Toxicology*. **59**, 225-234.

Arnold, W.R., Cotsifas, J.S., Ogle, R.S., DePalma, S.G.S., Smith, D.S. 2010a. A comparison of the copper sensitivity of six invertebrate species in ambient salt water of varying dissolved organic matter concentrations. *Environmental Toxicology and Chemistry*. **29**(2), 311-319.

Baker, A., 2001. Fluorescence excitation–emission matrix characterization of some sewage-impacted rivers. *Environmental Science and Technology.* **35**, 948–953.

Benner, R. Chemical composition and reactivity. In: Hansell, D.A., Carlson, C.A. (Eds.), Biogeochemistry of Marine Dissolved Organic Matter. Elsevier, USA, 59–90. 2002.

Birdwell, J.E., Engel, A.S. 2009. Variability in terrestrial and microbial contributions to dissolved organic matter fluorescence in the Edwards Aquifer, central Texas. *Journal of Cave and Karst Studies*. **71**(2), 144-156.

BC MOE (British Columbia Ministry of the Environment). Water Quality Criteria for Copper. Available at http://www.env.gov.bc.ca/wat/wq/BCguidelines/copper/copper.html#toc.

Brand, L.E., Sunda, W.G., Guillard, R.R.L. 1986. Reduction of marine phytoplankton reproduction rates by copper and cadmium. *Journal of Experimental Marine Biology and Ecology* 96, 225–250.

Brooks, S.J., Bolam, T., Tolhurst, L., Bassett, J., La Roche, J., Waldock, M., Barry, J., Thomas, K.V. 2007. Effects of dissolved organic carbon on the toxicity of copper to the developing embryos of the pacific oyster (*Crassostrea gigas*). *Environmental Toxicology and Chemistry*. **26**(8), 1756-1763.

CCREM (Canadian Council of Resource and Environment Ministers). 1987. Canadian Water Quality Guidelines. Prepared by the Task Force on Water Quality Guidelines of the Canadian Council of Resource and Environment Ministers.

Chadwick, D.B., Rivera-Duarte, I., Rosen, G., Wang, P.F., Santore, R.C., Ryan, A.C., Paquin, P.R., Hafner, S.D., Choi, W. 2008. Demonstration of an integrated model for predicting copper fate and effects in DoD harbors. SPAWAR Technical Report 1972. Project ER-0523.

Christenson, H.K. 1984. DLVO (Derjaguin-Landau-Verwey-Overbeek) theory and solvation forces between mica surfaces in polar and hydrogen-bonding liquids. *Journal of the Chemical Society, Faraday Transactions*. 80, 1933-1946.

Coble, P.G. 1996. Characterization of marine and terrestrial DOM in seawater using excitation-emission matrix spectroscopy. *Marine Chemistry*. **51**(4), 325-346.

Cooper, C.A., Tait, T., Gray, H., Cimprich, G., Santore, R.C., McGeer, J.C., Smith, D.S. 2013. Influence of salinity and dissolved organic carbon on acute toxicity to the rotifer *Brachionus plicatilis*. Submitted.

Cory, R.M., McKnight, D.M. 2005. Fluorescence spectroscopy reveals ubiquitous presence of oxidized and reduced quinones in dissolved organic matter. *Environmental Science and Technology*. **39**, 8142–8149.

DePalma, S.G.S. 2009. Characterization of dissolved organic matter and reduced sulfur in coastal marine and estuarine environments: Implications for protective effects on acute copper toxicity. MSc. Thesis. Wilfrid Laurier University. Waterloo, Ontario.

DePalma, S.G.S., Arnold, W.R., McGeer, J.C., Dixon, D.G., Smith, D.S., 2011. Effects of dissolved organic matter and reduced sulphur on copper bioavailability in coastal marine environments. *Ecotoxicology and Environmental Safety*. **74**, 230-237.

De Polo, A., Scrimshaw, M. 2012. Challenges for the development of a biotic ligand model predicting copper toxicity in estuaries and seas. *Environmental Toxicology and Chemistry*. **31** (2), 230-238.

De Schamphelaere, K.A.C., Vasconcelos, F.M., Tack, F.M.G., Allen, H.E., Janssen, C.R. 2004. Effect of dissolved organic matter source on acute copper toxicity to *Daphnia magna*. *Environmental Toxicology and Chemistry*. **23**(5), 1248-1255.

Di Toro, D.M. Allen, H.E., Bergman, H.L., Meyer, J.S., Paquin, P.R., Santore, R.C. 2001. Biotic ligand model of the acute toxicity of metals 1. Technical basis. *Environmental Toxicology and Chemistry*. **20**, 2383-2396.

Donat, J.R., Lao, K.A., Bruland, K.W. 1994. Speciation of dissolved copper and nickel in South San Francisco Bay: a multi-method approach. *Analytica Chimica Acta*, **284**, 547–571.

Eikebrokk B., Juhna, T., Østerhus, S.W. 2006. Water treatment by enhanced coagulation – Operational status and optimization issues. Techneau Report D 5.3.1a.

Eriksen, R.S., Nowak, B., van Dam, R.A. 2001. Copper speciation and toxicity in a contaminated estuary. Supervising Scientist Report 163. Department of Sustainability, Environment, Water, Population and Communities, Canberra, Australia.

Eriksen, R.S., Mackey, D.J., van Dam, R., Nowak, B. 2001a. Copper speciation and toxicity in Macquarie Harbour, Tasmania: an investigation using a copper ion selective electrode. *Marine Chemistry*. **74**, 99-113.

George, S.G., Coombs, T.L., 1977. The effects of chelating agents on the uptake and accumulation of cadmium by *Mytilus edulis*. *Marine Biology*. **39**, 261–268.

Government of Canada. 2003. Water and Canada: Preserving a Legacy for People in the Environment.

Grosell, M., Wood, C.M. 2002. Copper uptake across rainbow trout gills: Mechanisms of apical entry. *The Journal of Experimental Biology*. **205**, 1179-1188.

International Copper Association (ICA). 1995. The biological importance of copper: A literature review. ICA Project No. 223.

Kogut, M.M., Voelker, B.M. 2002. Strong copper-binding behavior of terrestrial humic substances in seawater. *Environmental Science and Technology*. **35**, 1149-1156.

Kozuch, J., Pempkowiak, J. 1996. Molecular weight of humic acids as a major property of the substances influencing the accumulation rate of cadmium by a blue mussel (*Mytilus edulis*). *Environment International*. **22**(5), 585-589.

Landry, C., Tremblay, L. 2012. Compositional differences between size classes of dissolved organic matter from freshwater and seawater revealed by an HPLC-FTIR system. *Environmental Science and Technology*. **46**, 1700-1707.

Larsson, T., Wedborg, M., Turner, D. 2007. Correction of inner-filter effect in fluorescence excitation-emission matrix spectrometry using Raman scatter. *Analytica Chimica Act.,* **583**, 357-363.

Liang, Y., Hilal, N., Langston, P., Starov, V. 2007. Interaction forces between colloidal particles in liquid: Theory and experiment. *Advances in Colloid and Interface Science*. **134-135**, 151-166.

Lorenzo, J.I., Nieto, O., Beiras, R., 2002. Effect of humic acids on speciation and toxicity of copper to Paracentrotus lividus larvae in seawater. *Aquatic Toxicology*. **58**, 27-41.

Lorenzo, J.I., Beiras, R., Mubiana, V.K., Blust, R. 2005. Copper utake by mytilus edulis in the presence of humic acids. *Environmental Toxicology and Chemistry*. **24**(4), 973-980.

Lorenzo, J.I., Nieto, O., Beiras, R., 2006. Anodic stripping voltammetry measures copper bioavailability for sea urchin larvae in the presence of fulvic acids. *Environmental Toxicology and Chemistry*. **25**, 36-44.

Luider, C.D., Crusius, J., Playle, R.C., Curtis, P.J. 2004. Influence of natural organic matter source on copper speciation by Cu binding to fish gills, by ion selective electrode and by DGT gel samles. *Environmental Science and Technology*. **38**, 2865-2872.

Mackey, D.J. 1983. Metal-organic complexes in seawater – An investigation of naturally occurring complexes of Cu, Zn, Fe, Mg, Ni, Cr, Mn and Cd using high-performance liquid chromatography with atomic fluorescence detection. *Marine Chemistry*. **13**, 169-180.

Mantoura, R., Woodward, M., 1983. Conservative behaviour of riverine dissolved organic carbon in the Severn Estuary: chemical and geochemical implications. *Geochimica et Cosmochimica Acta*. **47**, 1293–1309.

McKnight, D.M., Boyer, E.W., Westerhoff, P.K., Doran, P.T., Kulbe, T., Andersen, D.T. 2001. Spectrofluorometric characterization of dissolved organic matter for indication of precursor organic material and aromaticity. *Limnology and Oceanography*. **46** (1), 38-48.

Midorikawa, T., Tanoue, E. 1998. Molecular masses and chromophoric properties of dissolved organic ligands for copper (II) in oceanic water. *Marine Chemistry*. **62**, 219-239.

Millero, F.J., Woosley, R. Ditrolio, B., Waters, J. 2009. Effect of ocean acidification on the speciation of metals in seawater. *Oceanography*. **22**, 72-85.

Nadella, S.R., Fitzpatrick, J.L., Franklin, N., Bucking, C., Smith, D.S., Wood, C.M., 2009. Toxicity of Cu, Zn, Ni and Cd to developing embryos of the blue mussel (Mytilis trossolus) and the protective effect of dissolved organic carbon. *Comparative Biochemistry and Physiology Part C.* **149**, 340-348.

Nadella, S.R.,Tellis, M., Diamond, R., Smith, S., Bianchini, A., Wood, C.M. 2013. Toxicity of lead and zinc to developing mussel an sea urchin embryos: Critical tissue residues and effects of dissolved organic matter and salinity. *Comparative Biochemistry and Physiology*. In press.

NOAA. 2004. Population trends along the coastal united states: 1980–2008. Technical report, National Oceanic and Atmospheric Administration, National Ocean Service.

Ohno, T. 2002. Fluorescence inner-filtering correction for determining the humification index of dissolved organic matter. *Environmental Science and Technology*. **36**, 742–746.

Paquin, P.R., Santore, R.C., We, K.B., Kavvadas, C.D., Di Toro, D.M. 2000. The biotic ligand model: a model of the acute toxicity of metals to aquatic life. *Environmental Science and Policy*. **3**, 175-182.

Paquin, P.R., Gorsuch, J.W., Apte, S., Batley, G.E., Bowles, K.C., Campbell, P.G.C., Delos, C, G., Di toro, D.M., Dwyer, R.L., Galvez, F., Gensemer, R.W., Goss, G.G., Hogstrand, C., Janseen, C.R., McGeer, J.C., Naddy, R.B, Playle, R.C., Santore, R.C., Schneider, U., Stubblefield, W.A., Wood, C.M., Wu, J.B. 2002. The biotic ligand model: a historical overview. *Comparative Biochemistry and Physiology Part C*. **133**, 3-35.

Pempkowiak, J., Kozuch, J. 1994. The influence of structural features of marine humic substances on the accumulation rates of cadmium by a blue mussel *Mytilus edulis*. *Environment International*. **20**(3), 391-395.

Pempkowiak, J., Kozuch, J., Grzegowska, H., Gjessing, E.T. 1999. Biological vs. chemical properties of natural organic matter isolated from selected Norwegian lakes. *Environment International*. **25**(2/3), 357-366.

Sánchez-Marín, P., Bellas, J., Mubiane, V.K., Lorenzo, J.I., Blust, R., Beiras, R. 2011. Pb uptake by the marine mussel *Mytilus sp.* interactions with dissolved organic matter. *Aquatic Toxicology*. **102**, 48-57.

Santore, R.C., Di Toro, D.M., Paquin, P.R., Allen, H.E., Meyer, J.S. 2001. Biotic ligand model of the acute toxicity of metals 2. Application to acute copper toxicity in freshwater fish and *daphnia*. *Environmental Toxicology and Chemistry*. **20**, 2397-2402.

Schwartz, M.L., Curtis, P.J., Playle, R.C. 2004. Influence of natural organic matter source on acute copper, lead, and cadmium toxicity to rainbow trout oncorhynchus mykiss. *Environmental Toxicology and Chemistry*. **23**, 2889-2899.

Smith, D.S., Kramer, J.R. 1999. Fluorescence analysis for multi-site aluminum binding to natural organic matter. *Environment International*. **25**. 295–306.

Stauber, J.L., Ahsanulluh, M, Nowak, B., Eriksen, R., Florence, T.M. 1996. Toxicity assessment of waters from Macquarie Harbour, western Tasmania, using algae, invertebrates and fish. Supervising Scientist Report 112. Department of Environment and Land Management, Tasmania.

Stedmon, C.A., Bro, R. 2008. Characterizing dissolved organic matter fluorescence with parallel factor analysis: a tutorial. *Limnology and Oceanography: Methods.* **6**. 572–579.

Stedmon, C.A., Markager, S. 2005. Resolving the variability in dissolved organic matter fluorescence in a temperate estuary and its catchment using PARAFAC analysis. *Limnology and Oceanography.* **50**. 686–697.

Sunda, W.G., Ferguson, R.L. 1983. Sensitivity of natural bacterial communities to additions of copper and to cupric ion activity: A bioassay of copper complexation in seawater. In CS Wong, E Boyle, K Bruland & JD Burton (Editors). *Trace metals in seawater*. Plenum Press, New York, 871–891.

Sunda, W.G., Guillard, R.R.L. 1976. The relationship between cupric ion activity and the toxicity of copper to phytoplankton. *Journal of Marine Research.* **34**, 511.

Sunda, W.G., Hanson, P.J. 1979. Chemical speciation of copper in river water. In Jenne, E. Editor. *Chemical modeling in aqueous systems*. ACS Symposium Series; American Chemical Society: Washington, DC, 147-180.

U.S. EPA. 2007. National recommended water quality criteria. Available at http://water.epa.gov/scitech/swguidance/standards/current/index.cfm.

Winter, A., Fish, T., Playle, R., Smith, D.S., Curtis, P. 2007. Photodegradation of natural organic matter from diverse freshwater sources. *Aquat. Toxicol.* **84**, 215–222.

Wu, F.C., Evans, R.D., Dillon, P.J. 2003. Separation and characterization of NOM by high-performance liquid chromatography and on-line three-dimensional excitation emission matrix fluorescence detection. *Environmental Science and Technology.* **37**, 3687–3693.

Wu, F., Tanoue, E. 2001. Geochemical characterization of organic ligands for copper (II) in difference molecular size fractions in Lake Biwa, Japan. *Organic Geochemistry*. **32**, 1311-1318.

Xie, W.-H., Shiu, W.-Y., Mackay, D., 1997. A review of the effect of salts on the solubility of organic compounds in seawater. *Marine Environmental Research*. **44**, 429–444.

Chapter 4 Characterization of NOM interactions with copper in natural sea water using fluorescence quenching: Influence on toxicity

4.0 Abstract

Speciation of copper in marine systems strongly influences the ability of copper to cause toxicity. Natural organic matter (NOM) contains many binding sites for copper which provides a protective effect on copper toxicity. Fluorescence quenching techniques to characterize NOM in marine systems is limited but has recently been validated in artificial seawater. The purpose of this study was to characterize copper binding with NOM using fluorescence quenching techniques. Fluorescence quenching of NOM with copper was performed on nine sea water samples. Ligands for copper binding ranged from one to three ligands. The resulting stability constants and binding capacities were consistent with literature values of marine NOM, showing strong binding with log*K* values from 9.33 to 11.22 and binding capacities for ligands ranged from 4 to 1614 nmole mg C^{-1}. Binding capacities were strongly correlated with the LC_{50} for rotifer (*Brachionus plicatilis*) acute toxicity assays (r^2 = 0.67, *p*-value = 0.008). Free copper concentrations calculated using fluorescence quenching were compared to previously measured free copper using a copper ion-selective electrode. There was strong agreement between free copper values with a less than 0.3 pCu difference between methods with free copper concentrations remaining constant within the generally accepted factor of two for Biotic Ligand Model (BLM) predictions. These results support the theory that water chemistries affect the amount of total copper needed to be added to a system to reach a critical free copper concentration required to cause toxicity. As well, this data confirms the applicability of fluorescence spectroscopy techniques for NOM and copper speciation characterization in sea water.

4.1 Introduction

Trace metals, such as copper, are essential to life yet at increased concentrations toxicity can result. Anthropogenic release of copper has made it a common contaminant in marine waters (Chadwick et al. 2008). As such, there is an increased concern of the fate and bioavailability of copper in marine systems.

The Biotic Ligand Model (BLM) is a predictive tool used to estimate site-specific bioavailability and toxicity of metals. The BLM is able to predict toxicity at the biotic ligand (ex. the gill of a fish) based on equilibration calculations of metal speciation using bulk water chemistries, such as pH, salinity and natural organic matter (NOM) as input parameters (Di Toro et al. 2001; Santore et al. 2001; Paquin et al. 2002). The BLM has been adopted as a regulatory tool for freshwater by the U.S. EPA (2007) for copper however there is need for a BLM in saltwater environments. Investigations pertaining to saltwater are currently underway for application of a marine BLM; however more information is needed before being accepted for regulatory use (Arnold 2005). The focus of this study is to characterizate marine dissolved organic carbon (DOC) binding characteristics with copper using fluorescence spectroscopy techniques.

The speciation of copper plays a strong role on copper bioavailability and toxicity (Chadwick et al. 2008; Eriksen et al. 2001; Eriksen et al. 2001a; Sunda & Hanson 1979). In particular, natural organic matter (NOM) is a heterogenous mixture of organic

compounds that contain many potential binding sites for metals such as copper. Copper can form complexes with NOM at binding sites such as amino (Cu-NHR, $[Cu\text{-}NH_2R]^+$), carboxyl ($Cu\text{-}CO_2H$), phenolic (Cu-OAr) and sulfide or thiol groups (Cu-SH) (Smith et al. 2002). NOM can be broadly categorized into two groups, allochthonous and autochthonous. Allochthonous, or terrestrially-derived organic matter comes from the decomposition and leaching of soil and plant materials such as lignin, tannins and detritus and typically contains a higher humic and fulvic substance content. Autochthonous, or microbially-derived organic matter comes from bacterial and algal processes occurring within the water column and typically contains a higher proteinaceous content (Birdwell & Engel 2009; McKnight et al. 2001).

Due to the wide variety of binding sites within NOM, the determination of metal binding constants is difficult. Typical stability constants for copper-NOM have been found to range from a log*K* of 4 to 15 (Playle et al. 1993). However, NOM fluoresces due to the presence of aromatic structural groups with electron-donating functional groups. This quality allows fluorescence techniques to be used to characterize NOM and metal speciation (Chen et al. 2003; da Silva et al. 1998; Mackey 1983; Smith & Kramer 2000). The fluorescence of NOM is known to be quenched in the presence of metals such as copper and have been used to determine conditional stability constants (log*K*) and binding capacities (L_T) for fluorescent NOM (da Silva et al. 1998). Initial efforts for this characterization were performed by Ryan and Weber (1982), resulting in the well-known Ryan-Weber equation (Equation 4.1)

$$I = \left(\frac{(I_{ML}-100)}{2KC_L}\right)\left[(KC_L + KC_M + 1) - \sqrt{(KC_L + KC_M + 1)^2 - 4K^2C_LC_M}\right]$$ Equation 4.1

Since then, fluorescence quenching has been used to determine binding characteristics for copper in a variety of media (Chen et al. in press; da Silva et al. 1998; Hernández et al. 2006; Smith & Kramer 2000; Wu and Tanoue 2001). Wu and Tanoue (2001) determined conditional stability constants for two different molecular sized fractions of NOM with respect to copper, however did not solve for binding capacities. Fulvic acid binding characteristics with copper have also been studied using fluorescence techniques (da Silva et al. 1998; Smith & Kramer 2000). Smith and Kramer (2000) validated copper fluorescence quenching in freshwater by its ability to predict free copper using Suwannee River fulvic acid (SRFA) titrations with copper. da Silva et al. (1998) isolated fulvic acid from three different sources and solved for conditional stability constants and binding capacities with copper, however in two cases no reasonable values were obtained for binding capacities (da Silva et al. 1998). In addition, Hernández et al. (2006) were able to solve for log*K* and binding capacity of copper with humic acids in pig slurries and amended soils. Preliminary work using fluorescence quenching techniques has validated fluorescence quenching methods for copper in marine environments using Luther Marsh organic matter, containing both humic and fulvic components, in artificial seawater (Diamond et al. 2012). In addition, Diamond (2012) also determined the stability constants and binding capacities for two ligands found within a natural sea water sample.

The objectives of this study were to (1) Determine conditional stability constants and binding capacities of copper with DOC in nine natural seawater samples, (2) Relate DOC binding characteristics to observed copper toxicity of these nine samples. Copper toxicity in these samples were previously measured and discussed in Chapter 3.

4.2 Methods

4.2.1 Experimental protocol

The method for storage, selection and preparation of samples is given in Chapter 3. For a brief description of sampling site locations and characteristics please refer to Table 4.1. A full description of sampling sites and characteristics are given in Chapter 3. The samples used in this study were the prepared samples for the toxicity assays (after salinity adjustments and filtration) in order to compare the results to the toxicity assay results from Chapter 3.

Table 4.1 Characteristics of water samples

Sample	Coordinates (lat / long)	LC_{50}* (nM)	DOC† (mg C L^{-1})	Salinity‡ (ppt)
Bouctouche (BT)	46.471532 / -64.717283	662	4.83	30.1
Petit Rocher (PR)	47.783534 / -65.708606	778	2.10	30.2
Major Kollock Creek (MKC)	46.813469 / -64.912441	980	7.57	29.9
Naufrage Harbour (NH)	46.46763 / -62.417343	725	5.20	29.9
Rathtrevor Beach (RB)	49.321793 / -124.264684	395	1.37	30.1
Hawke's Bay (HB)	50.616142 / -57.182465	333	1.28	30.0
Blackberry Bay (BB)	49.151791 / -125.89802	915	2.03	29.9
Chesterman Beach (CB)	49.11336 / -125.88692	422	0.55	30.1
Jimbo	25.77471 / -80.1454	559	1.13	30.1

* 48h static acute LC_{50} to the rotifer, *Brachionus plicatilis* following ASTM (2004) guidelines with modifications from Arnold et al. (2010).
† DOC measurements after salinity adjustment and filtration through a 0.45 µm filter.
‡ Adjusted salinity using a mixture of artificial seawater salts (ASTM 2004).

The copper titrant solution was prepared at 157 µM from a 1000 mg L^{-1} copper standard solution (Assurance grade, SPEXCertiPrep, New Jersey). The sample was pH adjusted to pH 8.01 ± 0.01 using dilute NaOH or HCl, as required. Smith and Kramer (2000) determined stabilization of the fluorescence signal within 10 minutes after Cu addition. Thus, the solution was allowed to equilibrate for 15 minutes after each copper addition between fluorescent measurements. Three titrations were performed for each sample with three replicate fluorescent measurements per addition of titrant.

The sample was contained within a beaker with constant stirring. Aliquots were taken from the beaker and measured in a 1 cm quartz cuvette using a Varian Cary Eclipse Fluorescence Spectrophotometer (Varian, Mississauga, ON). Fluorescence emission wavelengths were measured from 300 nm to 700 nm at an excitation wavelength of 270 nm. Depending on the sample the excitation and emission monochromator slit widths were set from 5 to 20 nm and the photomultiplier tube (PMT) was set to between 800 V and 1000 V. The excitation and emission monochromator slit widths and PMT were varied between the given ranges in order to optimize the fluorescence intensity of the sample. After measurement, the aliquot was returned to the beaker and the next addition of titrant was added. This process was repeated until the decrease in maximum intensity plateaued or until the total copper added to the sample was double the LC_{50} value.

4.2.2 Data processing

All data processing was performed using MATLAB™ (MathWorks Inc., MA, USA). The fluorescent components are resolved using the total fluorescence excitation versus emission surface. Fluorescence for the *p*th fluorescent component can be represented as

$$F_p = k_{L_p}[L_p] + k_{ML_p}[ML_p] \qquad \text{Equation 4.2}$$

Where,

$$[L_p] = f(K_p, L_{pT}, MT) \quad \text{Equation 4.3}$$

$$[ML_p] = f(K_p, L_{pT}, MT)$$

Ultimately, fluorescence can be solved as a function of four parameters,

$$F_p = f(K_p, L_{pT}, k_{L_p} k_{ML_p}) \quad \text{Equation 4.4}$$

For these equations p=1,…, P for a total of P different fluorescent components, L_p corresponds to the pth free ligand and ML_p to the pth bound ligand (M:L_p = 1:1), and k is the respective proportionality constants. The components for each sample resolved using PARAFAC performed in Chapter 3 (See Chapter 3 Section *3.2.3*) are used to constrain the quenching data to four different fluorescent components: humic-, fulvic-, tryptophan- and tyrosine-like. A 'slice' of the contour spectra at 270 nm excitation is taken, as this is the excitation wavelength used for all the fluorescence quenching titrations. It is assumed that the fluorescence response is linear with concentration (Smith & Kramer 2000) so a linear model is used to interpolate the contribution of each fluorophore to the total fluorescence curve, constrained to the four components resolved using PARAFAC. An initial guess of the contribution of each fluorophore is used and then optimized to a final constant (k) for each component. This results in the equation for total fluorescence (F_T):

$$F_T = k_1 humic + k_2 fulvic + k_3 tryptophan + k_4 tyrosine \quad \text{Equation 4.5}$$

Where each component (i.e. *humic*, *fulvic*, *tryptophan* and *tyrosine*) is the PARAFAC resolved emission at 270 nm excitation. The model is applied to the quenching data for

each copper addition. An example of the resulting spectra showing the contributions of each fluorophore to total fluorescence can be seen for Bouctouche before any addition of copper in Figure 4.1. The solid black line represents the modeled fluorescence curve which compares well to the measured fluorescence (black circles). In this example, the humic-like fraction (blue) contributes the most to total fluorescence, followed by the fulvic-like fraction (red). Tryptophan- (magenta) and tyrosine- (green) like fractions show very little contribution to total fluorescence. The MATLAB script used to determine these contributions can be found in Appendix C1. Appendix C2 has the plots showing the contribution of fluorophores to the total fluorescence for all sites.

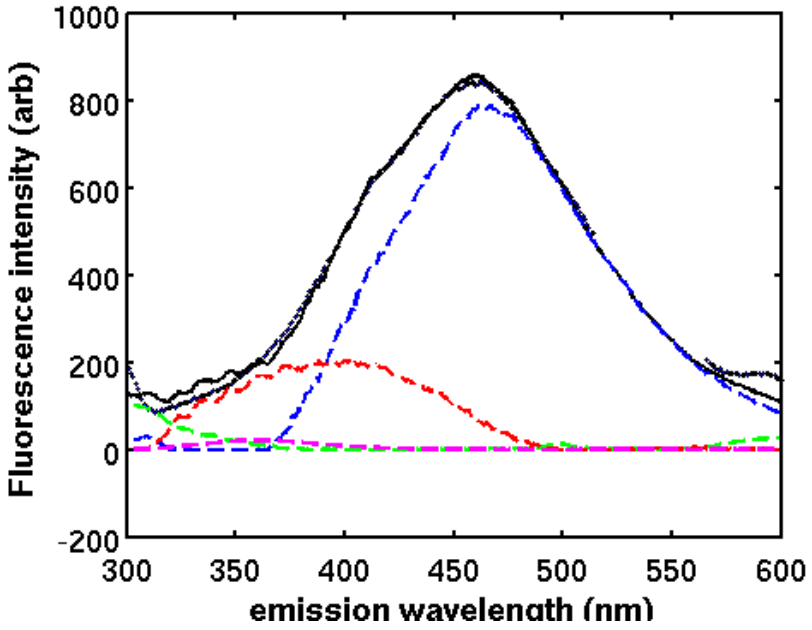

Figure 4.1 Contribution of humic- (blue), fulvic- (red), tryptophan- (pink), and tyrosine-like (green) fractions to total fluorescence in Bouctouche. Dotted black line is the measured fluorescence while the solid black line is the modeled curve to determine fluorophore contributions.

After obtaining the contribution to fluorescence for each component, a multi-site Ryan-Weber model was applied to the data to allow for determination of stability constants (reported as logK') and binding capacities (L_T) of the fluorophores within each sample (Smith and Kramer 2000). Components which remained constant or increased in contribution with copper additions were excluded from this fitting. It is assumed that components in which fluorescence intensity increased with copper additions may have been due to displacement of a more efficient quencher causing an increase in fluorescence.

For all calculations concentrations were used rather than activities and a one to one metal-ligand stoichiometry was assumed. From *Section 4.2.1*, it can be noted that a fixed pH was used for all metal titrations therefore the results are only valid for the specified pH. The speciation distribution for the metal and the ligand between free and bound can be calculated using the P+1 mass balance expressions for total metal (*MT*) and total ligand (L_{T_p})

$$\begin{aligned} M_T &= [M] + \sum_{p=1}^{P} [ML_p] \\ L_{T_1} &= [L_1] + [ML_p] \\ &\vdots \\ L_{T_p} &= [L_p] + [ML_p] \end{aligned} \qquad \text{Equation 4.6}$$

The above expressions can be expanded and after susbstitution of each of the *P* stability constant expressions, the result is expressed as a polynomial in [*M*] of degree P+1. For one and two ligands, the result is a quadratic and cubic expression, respectively and can be solved explicitly. For greater than two ligands numerical techniques for root finding must be performed to determine [*M*]. Once [*M*] is determined then the result can

be substituted back in to the expression to determine the concentration of free and bound ligand (Smith & Kramer 2000).

The fluorescence at all identified fluorescent sites can be expressed as a function of 3*P* parameters. The parameters include *K'*, L_T and a proportionality constant for *ML* for each of the *P* sites. In this case, the proportionality constant for *L* was determined from the measured data in order to decrease the number of adjustable parameters. These parameters are fit using the multiresponse parameter fitting, as a function of total metal added (M_T) and the observed fluorescence responses (Smith & Kramer 2000). In multiresponse fitting the error criteria to be minimized is det($\mathbf{Z}^T\mathbf{Z}$), where det stands for determinant and T is for the matrix transpose. The *N*x*P* matrix Z is a matrix of residuals, with a column of 'observed - calculated' for each of the N fluorescence responses. A general example of the matrix of residuals ($\mathbf{Z}$) can be shown in full for the *i*th addition of titrant and the *i*th fluorescent response for *i*=1,…,*N* and *j*=1,…,*P*

$$Z = \begin{bmatrix} F_{obs_{11}} - F_{calc_{11}} & \cdots & F_{obs_{1P}} - F_{calc_{1P}} \\ \vdots & \vdots & \vdots \\ F_{obs_{N1}} - F_{calc_{N1}} & \cdots & F_{obs_{NP}} - F_{calc_{NP}} \end{bmatrix} \qquad \text{Equation 4.7}$$

For *P* fluorescent responses corresponding to *P* proposed fluorescent sites and for *N* additions of titrant. Using this criteria, it is assumed that the errors are distributed as a *P*-dimensional normal distribution, and that there are correlations between responses, but not between metal additions (Smith & Kramer 2000). An initial guess of *K'* and L_T is then optimized in this way to determine the final fit. This guess is important in order to obtain practical and realistic stability constants and binding capacities as well as to avoid the chance of fitting local minima which is common in nonlinear regression. An example

of the MATLAB script used for the multiresponse fitting combined with the free copper modeling is found in Appendix C3.

4.3 Results and Discussion

An example of the resolved quenching curves for two fluorophores are shown for Bouctouche in Figure 4.2. In this example, Figure 4.2a represents the humic-like component and Figure 4.2b represents the fulvic-like component. Resolved quenching curves with Ryan Weber fitting for all sample sites can be found in Appendix C4.

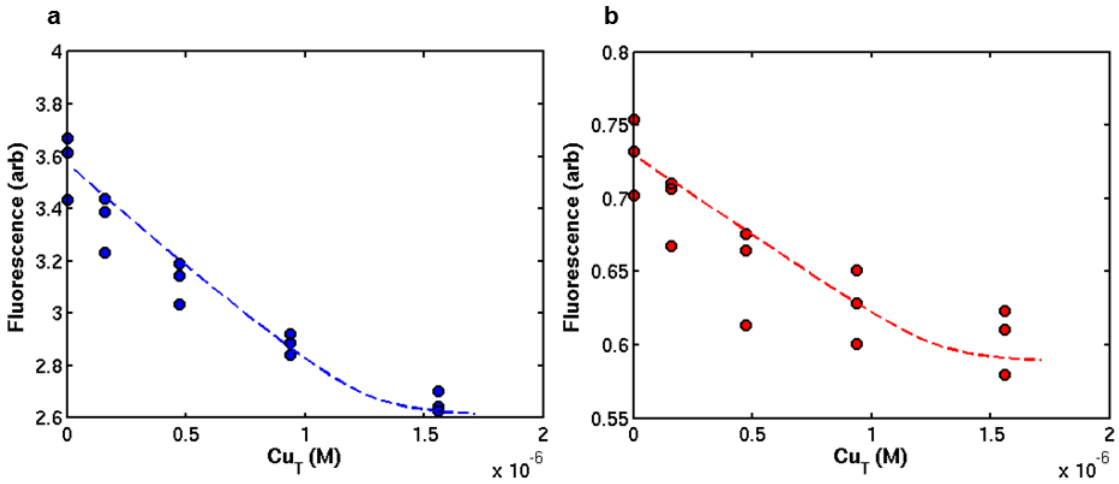

Figure 4.2 Ryan Weber fitting of the resolved fluorophores for Bouctouche. The humic-like fraction is represented in a, and b displays the fulvic-like fraction.

Using the fluorescence quenching data and applying a multiresponse Ryan-Weber model, the log*K* and binding capacities were determined for each site and are tabulated in Table 4.2. The binding capacities are expressed as per milligram of carbon as it is assumed that the abundance of these sites would change with DOC concentration. For all fluorophores, the binding is relatively strong for all sites ranging from 9.33 to 11.22. This is consistent with the results from Chadwick et al. (2008) in San Diego Bay in which log*K* values for three different ligands ranged from 9.14 to 12.9. As well the binding capacities shown here covers a broad range from 4 to 1614 nmole mg C^{-1} which encompasses the range seen in Chadwick et al. (2008) from 33.5 – 878 nmole mg C^{-1}. This is also consistent with binding parameter values found in other literature for marine DOC in which log*K* values range from 10.0 to 14.3 and binding capacities have been found from approximately 2.5 to >150 nmole mg C^{-1} (Buck & Bruland 2005; Hurst & Bruland 2005; Kogut & Voelker 2001).

The Jimbo site was previously measured using fluorescence quenching techniques in Diamond (2012). In this case, the humic-like fraction had a log*K* of 9.20 and a binding capacity of 890 nmole mg C^{-1}. The fulvic-like fraction displayed stronger binding with a log*K* of 10.38 and a binding capacity of 78 nmole mg C^{-1}. The results of this study show stronger binding for both fluorophore fractions with a log*K* of 10.34 and 10.41 for humic- and fulvic-like fractions respectively. For humic-like fractions the binding capacity was similar with 998 nmole mg C^{-1}, however binding capacity of the humic-like fraction was reduced by a factor 16 at 5 nmole mg C^{-1}. The differences in binding parameters may have been due to differences in the sampling site between times of collection. The sample collection of Jimbo for Diamond (2012) occurred January 2011 while collection for this

study occurred two years later in January 2013. During the time between sampling dates, remediation efforts in the area had begun and so changes in DOC characteristics were not necessarily unexpected.

Table 4.2 Binding characteristics (stability constant, Log*K* and binding capacity, L_T) of nine sea water samples with copper.

Site	Humic-like		Fulvic-like		Tryptophan-like	
	Log*K*	L_T (nmole mg C^{-1})	Log*K*	L_T (nmole mg C^{-1})	Log*K*	L_T (nmole mg C^{-1})
BT	9.86	47	9.82	220	-	-
PR	9.94	21	9.33	1340	-	-
MKC	9.74	15	9.59	154	9.74	151
NH	10.10	189	10.18	20	-	-
RB	11.22	373	-	-	-	-
HB	9.89	885	9.99	29	-	-
BB	10.07	33	9.63	1614	-	-
CB	10.63	965	-	-	11.20	4
Jimbo	10.34	998	10.41	5	-	-

The sum of the binding capacities of the DOC fractions (not normalized for DOC concentration) was compared to the LC_{50} values for each site and the results are shown in Figure 4.3. It was expected that binding capacity would increase with LC_{50} to support the findings in Chapter 3; that more total copper is added to obtain the same free copper concentration required to cause toxicity. A fairly strong significant positive correlation (r^2 = 0.67 and *p*-value of 0.007) was found between binding capacity and LC_{50} thus adding strength to the findings from Chapter 3. An increase in binding capacity would result in an increase of total copper needed to be added to the system in order to reach the

same free copper concentration required to cause toxicity as another site with a smaller binding capacity.

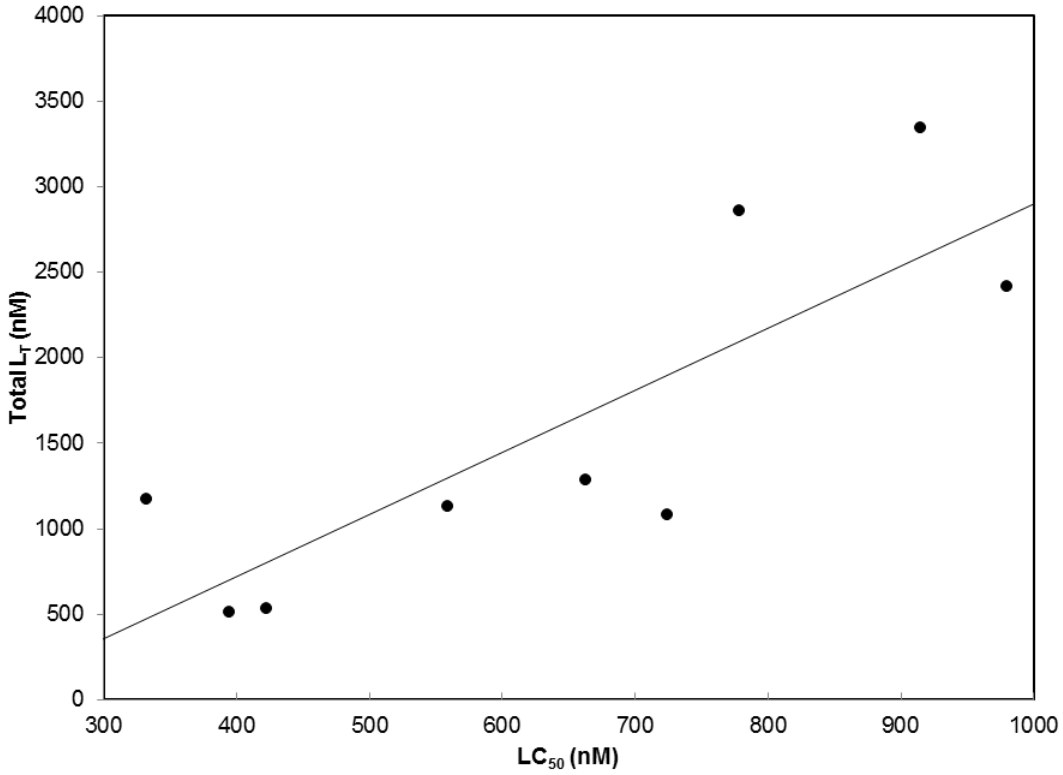

Figure 4.3 Total binding capacity (L_T) as a function of LC_{50} for the binding sites found in each sample (r^2 = 0.67, *p*-value = 0.007).

To further support this theory, free copper at the LC_{50} was calculated for each site using the fluorescence quenching data. These results are compared to the free copper at the LC_{50} measured using the copper ion-selective electrode (ISE), shown as pCu ($-\log[Cu^{2+}]$) in Table 4.3. For details on measuring free copper at the LC_{50} using the copper ISE refer to Chapter 3 Section *3.2.6*. Plots comparing the free copper modeled via the fluorescence data compared to the measured ISE data can be found in Appendix C5. For each sample, the free copper results agree with differences between the ISE measured data and fluorescence quenching calculated free copper at the LC_{50} within a factor of two

(no more than a 0.3 pCu difference). As well, compared internally all measurements, save one (Rathtrevor Beach), are within a factor of two about the mean of all fluorescence determined pCu values. This factor of two comes from the current criteria for the BLM in which predictions are considered acceptable within a factor of two. This is similar to the free copper measured in Chapter 3 in which free copper was relatively constant. The strong agreement between the free copper results from the two methods further validates the fluorescence quenching method for application in marine water.

Table 4.3 Comparison of free Cu at the LC_{50} measured using the copper ion-selective electrode and calculated using the fluorescence data. The values in brackets denote a factor of two about the mean.

Site	**ISE Free Cu (pCu)**	**Fluorescence Free Cu (pCu)**
BT	9.98	9.82
PR	9.64	9.94
MKC	10.40	10.10
NH	10.11	9.83
RB	10.35	10.56
HB	10.40	10.30
BB	9.79	10.06
CB	10.37	10.10
Jimbo	10.25	10.36
Ave	10.14 (9.84 – 10.44)	10.12 (9.82 – 10.42)

This free copper data can also be compared using a 1:1 line as shown in Figure 4.4. As can be seen from this plot, the data is randomly scattered across the 1:1 line. As well, all data are found within a factor of two from the 1:1 line. This illustrates the strong agreement between methods.

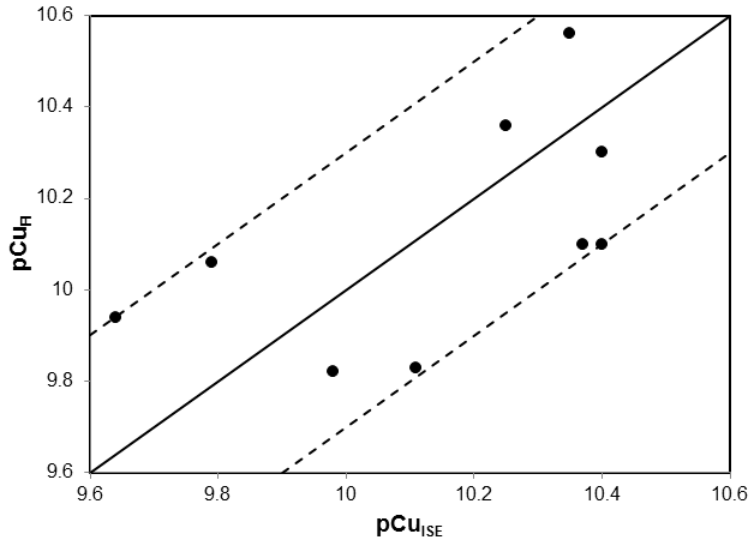

Figure 4.4 Comparison of free copper measured using the ion-selective electrode (pCu_{ISE}) and fluorescence quenching data (pCu_{Fl}). Solid line represents 1:1 and dashed lines are a factor of two from the 1:1 line.

Overall, the linear correlation between binding capacity and LC_{50} and the constant free copper measured is consistent with the free copper and toxicity results found in Chapter 3. This adds strength to the theory that differences in water chemistry, such as binding capacities of the waters, alter the total amount of copper required to reach a critical free copper concentration that results in toxicity.

4.4 Conclusions

Fluorescence quenching techniques have been widely used to characterize NOM interactions with copper in a variety of media (da Silva et al. 1998; Hernández et al. 2006; Smith & Kramer 2000; Wu and Tanoue 2001). However there has been limited use of these techniques in sea water. Previous validation of fluorescence quenching techniques to characterize NOM and copper binding in artificial seawater was performed by Diamond et al. (2012) and suggested good applicability in marine waters. In this

study, Diamond et al. (2012) recovered known tryptophan speciation from fluorescence quenching titrations with copper in ASW. The findings of this study further validate the use of these methods in marine water. Binding sites ranged from one to three ligands with all ligands displaying strong log*K* values ranging from 9.33 to 11.22. Binding capacity of these ligands broadly ranged from 4 to 1614 nmole mg C^{-1}. These values are consistent with literature data for marine NOM. A positive correlation was found between binding capacity and LC_{50}. Along with the free copper values determined via the fluorescence data that showed constant free copper concentrations at the various LC_{50} values, these findings agree with, and support the results from Chapter 3. The data presented here supports the theory that a critical free copper concentration is required to cause toxicity, however differences in water chemistry, such as binding capacity, alter the total amount of copper needed to be added to a system to reach this critical concentration. Comparison between free copper concentrations calculated from the fluorescence data and ISE measured free copper also agree strongly. Overall, the results demonstrate the strong influence of binding characteristics on copper speciation, bioavailability and toxicity to aquatic organisms upon copper exposure and confirm the applicability of fluorescence quenching techniques in marine waters.

4.5 References

American Society for the Testing of Materials International (ASTM). 2004. Standard guide for acute toxicity test with the rotifer Brachionus. E 1440-91. Annual book of ASTM standards. Vol 11.05. West Conshohocken, PA, 830-837.

Arnold, W.R., 2005. Effects of dissolved organic carbon on copper toxicity: implications for saltwater copper criteria. *Integrated Environmental Assessment and Management*. **1**, 34-39.

Arnold, W.R., Diamond, R.L., Smith, D.S. 2010. The effects of salinity, pH, and dissolved organic matter on acute copper toxicity to the rotifer, *Brachionus plicatilis* ("L" strain). *Archives of Environmental Contamination and Toxicology*. **59**, 225-234.

Birdwell, J.E., Engel, A.S. 2009. Variability in terrestrial and microbial contributions to dissolved organic matter fluorescence in the Edwards Aquifer, central Texas. *Journal of Cave and Karst Studies*. **71**(2), 144-156.

Buck, K.N., Bruland, K.W. 2005. Copper speciation in San Francisco Bay: A novel approach using multiple analytical windows. *Marine Chemistry*. **96**, 185-198.

Chadwick, D.B., Rivera-Duarte, I., Rosen, G., Wang, P.F., Santore, R.C., Ryan, A.C., Paquin, P.R., Hafner, S.D., Choi, W. 2008. Demonstration of an integrated model for predicting copper fate and effects in DoD harbors. SPAWAR Technical Report 1972. Project ER-0523.

Chen, J., LeBoeuf, E.J., Dai, S., Gu, B. 2003. Fluorescence spectroscopic studies of natural organic matter fractions. *Chemosphere*. **50**, 639-647.

Chen, W., Smith, D.S., Guéguen, C. 2013. Influence of water chemistry and dissolved organic matter (DOM) molecular size on copper and mercury binding determined by multiresponse fluorescence quenching. *Chemosphere*. In press.

da Silva, J.C.G.E, Machado, A.A.S.C., Oliveira, C.J.S., Pinto, M.S.S.D.S. 1998. Fluorescence quenching of anthropogenic fulvic acids by Cu(II), Fe(III) and UO^{2+}_2. *Talanta*. **45**, 1155-1165.

Diamond, R.L. 2012. Characterizing dissolved organic matter and Cu^{2+}, Zn^{2+}, Ni^{2+}, and Pb^{2+} binding in salt water and implications for toxicity. MSc. Thesis. Wilfrid Laurier University. Waterloo, Ontario.

Di Toro, D.M. Allen, H.E., Bergman, H.L., Meyer, J.S., Paquin, P.R., Santore, R.C. 2001. Biotic ligand model of the acute toxicity of metals 1. Technical basis. *Environmental Toxicology and Chemistry*. **20**, 2383-2396.

Eriksen, R.S., Nowak, B., van Dam, R.A. 2001. Copper speciation and toxicity in a contaminated estuary. Supervising Scientist Report 163. Department of Sustainability, Environment, Water, Population and Communities, Canberra, Australia.

Eriksen, R.S., Mackey, D.J., van Dam, R., Nowak, B. 2001a. Copper speciation and toxicity in Macquarie Harbour, Tasmania: an investigation using a copper ion selective electrode. *Marine Chemistry*. **74**, 99-113.

Hernández, D., Plaza, C., Senesi, N., Polo, A. 2006. Detection of copper (II) and zinc (II) binding to humic acids from pig slurry and amended soils by fluorescence spectroscopy. *Environmental Pollution*. **143**, 212-220.

Hurst, M.P., Bruland, K.W. 2005. The use of Nafion-coated thin mercury film electrodes for the determination of the dissolved copper speciation in estuarine water. *Analytica Chimica Acta*. **546**, 68-78.

Kogut, M.M., Voelker, B.M. 2001. Strong copper-binding behavior of terrestrial humic substances in seawater. *Environmental Science and Technology*. **35**, 1149-1156.

Mackey, D.J. 1983. Metal-organic complexes in seawater – An investigation of naturally occurring complexes of Cu, Zn, Fe, Mg, Ni, Cr, Mn and Cd using high-performance liquid chromatography with atomic fluorescence detection. *Marine Chemistry*. **13**, 169-180.

McKnight, D.M., Boyer, E.W., Westerhoff, P.K., Doran, P.T., Kulbe, T., Andersen, D.T. 2001. Spectrofluorometric characterization of dissolved organic matter for indication of precursor organic material and aromaticity. *Limnology and Oceanography*. **46** (1), 38-48.

Paquin, P.R., Gorsuch, J.W., Apte, S., Batley, G.E., Bowles, K.C., Campbell, P.G.C., Delos, C, G., Di toro, D.M., Dwyer, R.L., Galvez, F., Gensemer, R.W., Goss, G.G., Hogstrand, C., Janseen, C.R., McGeer, J.C., Naddy, R.B, Playle, R.C., Santore, R.C., Schneider, U., Stubblefield, W.A., Wood, C.M., Wu, J.B. 2002. The biotic ligand model: a historical overview. *Comparative Biochemistry and Physiology Part C*. **133**, 3-35.

Playle, R.C., Dixon, D.G., Burnison, K. 1993. Copper and cadmium binding to fish gills: Modification by dissolved organic carbon and synthetic ligands. *Canadian Journal of Fisheries and Aquatic Sciences*. **50**, 2667-2677.

Ryan, D.K., Weber, J.H. 1982. Fluorescence quenching titration for determination of complexing capacities and stability constants of fulvic acid. *Analytical Chemistry*. **54**, 986-990.

Santore, R.C., Di Toro, D.M., Paquin, P.R., Allen, H.E., Meyer, J.S. 2001. Biotic ligand model of the acute toxicity of metals 2. Application to acute copper toxicity in freshwater fish and *daphnia*. *Environmental Toxicology and Chemistry*. **20**, 2397-2402.

Smith, D.S., Kramer, J.R. 1999. Fluorescence analysis for multi-site aluminum binding to natural organic matter. *Environment International.* **25**. 295–306.

Smith, D.S., Kramer, J.R. 2000. Multisite metal binding to fulvic acid determined using multiresponse fluorescence. *Analytica Chimica Acta*. **416**, 211-220.

Smith, D.S., Bell, R.A., Kramer, J.R. 2002. Metal speciation in natural waters with emphasis on reduced sulfur groups as strong metal binding sites. 2002. *Comparative Biochemistry and Physiology Part C.* **133**, 65-74.

Sunda, W.G., Hanson, P.J. 1979. Chemical speciation of copper in river water. In Jenne, E. Editor. Chemical modeling in aqueous systems. ACS Symposium Series; American Chemical Society: Washington, DC, 147-180.

U.S. EPA. 2007. National recommended water quality criteria. Available at http://water.epa.gov/scitech/swguidance/standards/current/index.cfm.

Wu, F., Tanoue, E. 2001. Geochemical characterization of organic ligands for copper (II) in different molecular size fractions in Lake Biwa, Japan. *Organic Geochemistry*. **32**, 1311-1318.

Chapter 5 Conclusions and Future Work

5.1 Conclusions and Future Work

The following chapter is a brief summary of the findings and conclusions from the experimental chapters of this thesis. In each section the original objectives will be addressed and ideas for future work will be shared.

5.1.1 Objective 1 and 2

Objective 1 and 2 were as follows:

Objective 1: To determine true copper speciation in seawater using literature methods and new techniques to determine which techniques offer the most accurate measurement of copper speciation.

Objective 2: To validate a new method for determining free copper using a Cu ISE in seawater.

These objectives were met by Chapter 2: Internal calibration flow-through ISE method for determining Free Cu in salt water. In this chapter a literature flow-through Cu ISE method (Eriksen et al. 1999) was used to measure free copper of four marine grab samples. The free copper measurements compared well to literature measurements, however both literature and experimental measurements showed up to two orders of magnitude variability. This resulted in the question as to whether or not this variability was due to sample differences or from instrumental variability. To answer this question a

new flow-through internal calibration Cu ISE method was developed and validated using a model system of artificial seawater and tryptophan. Titration of the model system with copper resulted in measured free copper measurements that strongly agreed with modeled free copper using NIST binding constants. In addition variability between measurements was reduced to within an order of magnitude. These results fulfilled Objective 2.

After the successful validation of the new method, two of the marine grab samples measured using the external calibration literature method were measured using the new method. Results showed similar measured free copper with each copper addition, however reproducibility improved to within an order of magnitude. These results suggest that the variability seen in the literature between measurements were due to instrumental method variability rather than sample differences. The new method provides more reliable speciation results, thus fulfilling Objective 1. Chapter 3: Influence of DOC source on free copper and toxicity to *Brachionus Plicatilis,* measured free copper at the LC_{50} for different water samples using the new Cu ISE method. It was found that free copper remained relatively constant (within a factor of two), independent of total copper LC_{50} values. This is consistent with the Biotic Ligand Model (BLM) assumption that bound metal at the biotic ligand is constant. These results also contribute to Objective 1. In the future, this method will be applied to measure free copper in marine samples due to the increased reliability of this method.

Chapter 4: Characterization of NOM interactions with copper in natural sea water using fluorescence quenching: Influence on toxicity, also fulfilled objective 1. Free copper concentrations determined via fluorescence quenching techniques showed the same free value copper concentrations at the LC_{50} as free copper values measured using

the Cu ISE method validated in Chapter 2. The free copper results presented in Chapter 4 further support the applicability of fluorescence spectroscopy for accurate determination of copper speciation in sea water.

5.1.2 Objective 3

Objective 3 is as follows:

Objective 3: To apply an integrated approach to investigate the effect of DOC source on copper speciation and toxicity in aquatic organisms.

The majority of this objective was fulfilled by Chapter 3: Influence of DOC source on free copper and toxicity to *Brachionus Plicatilis*. In this chapter DOC was characterized using fluorescence contour plots that showed the water samples collected for toxicity assays were different at a molecular level. Four components (humic-, fulvic-, tryptophan- and tyrosine-like fractions of NOM) were identified within each of the nine samples. As well, qualitative indices of DOC source were determined via SAC_{340} and fluorescence indices. Toxicity assays using the rotifer, *Brachionus plicatilis*, were then performed for each of the water samples. The influence of DOC quality on rotifer toxicity and copper speciation were then discussed with two trends found. A linear trend (r^2 = 0.72, *p*-value = 0.016) was observed until approximately 2 mg C L^{-1} DOC and then a plateau effect was observed. This trend was suggested to be due to salt-induced colloid formation. In this case, at high salinity, DOC-DOC interactions are more frequent resulting in less copper binding and a plateauing out of the linear trend. Thus, there is no significant increase in protective effect with increasing DOC concentrations above

approximately 2 mg C L^{-1}. This trend has also been observed in the literature (Brooks et al. 2007; Cooper et al. 2013; Nadella et al. in press). The second trend resulting in a correlation between LC_{50} and DOC where LC_{50} (µg L^{-1}) = $25.15DOC^{0.47}$ including outlier data or LC_{50} (µg L^{-1}) = $22.86DOC^{0.45}$ excluding outlier data. Similar relationships between LC_{50} and DOC have been observed in other marine organisms (Arnold 2005; Arnold et al. 2006, Arnold et al. 2010, Arnold et al. 2010a; DePalma et al. 2011). Overall, these results stress the need for more toxicity assays to be performed, particularly between 2 – 4 mg C L^{-1} in order to determine which trend most accurately represents the correlation between LC_{50} and DOC.

It was found in Chapter 3 that the relationship between LC_{50} and humic- and fulvic-like components were significantly correlated (p = 0.030 and p = 0.013) with LC_{50} values while proteinaceous components were not (p = 0.39 and 0.53 for tryptophan and tyrosine, respectively). In addition, humic- and fulvic-like fractions both exhibited a positive correlation with LC_{50} although only the fulvic-like fraction showed a significant p-value. Overall, it was found that DOC quality does not need to be added as input models to current prediction models. Within the acceptable factor of two for BLM toxicity predictions, total DOC is sufficient to predict toxicity.

The free copper at the LC_{50} for each site was measured using the new Cu ISE method developed in Chapter 2. As mentioned above, the mean free copper value remained constant within the BLM prediction factor of two. These results suggest that a critical free copper concentration is required to cause toxicity however differences in water chemistry affect how much total copper is required to reach this threshold. This theory is supported by the findings of Chapter 4. In Chapter 4, fluorescence quenching of

NOM with copper was performed for each site. From this data the stability constants and binding capacities of the binding sites in NOM could be determined and the amount of free copper present could be calculated. It was found that one to three ligands for copper binding were available for the sample sites measured and that all ligands had relatively strong binding with stability constants ranging from a log*K* from 9.33 to 11.22 and binding capacities ranging from 4 to 1614 nmole mg C^{-1}. This data is consistent with binding parameters found in other marine NOM. It was also found that the sum of the binding capacities had a significant linear correlation with LC_{50} (r^2 = 0.67, *p*-value = 0.007). This supports the theory that free copper is constant to cause toxicity. An increase in total copper LC_{50} is due to water parameters, such as a larger binding capacity, which allows more copper to bind thereby reducing bioavailability. This means that more copper needs to be added to the system to reach a critical concentration of free copper that is available to interact with the organism to cause toxicity.

Future work related to this aspect of the data is to apply accumulation studies to these DOC characterization and copper speciation methods, especially in the presence of increased humic and fulvic acid content, to determine bioavailability of these copper-organic complexes. In addition, more NOM characterization techniques such as high performance size exclusion chromatography (HPSEC) or immobilized metal ion affinity chromatography (IMAC) could be included to better identify size and composition of NOM.

5.1.3 Implications of Research

Currently, national water quality guidelines for copper may be over- or under-protective at sites with unique conditions (CCME 2003). For example, chemical characteristics (e.g. pH, salinity, DOC etc.) at a site may alter the bioavailability and toxicity of copper. It is crucial that water quality guidelines for copper accurately reflect the toxicity of copper under these various conditions to ensure protection of each aquatic environment while being economically practical. This can result in the development of site-specific criteria for copper. Models, such as the Biotic Ligand Model (BLM), can be used as predictive tools to estimate site-specific bioavailability and toxicity in an environment based on chemistry characteristics. The results from this research help to supplement a marine BLM for copper.

One of the crucial elements in developing a reliable BLM is the ability to accurately measure copper speciation in sea water. This was achieved by the development of a new flow-through ion-selective electrode (ISE) method that utilized an internal calibration method in order to improve reproducibility of free copper measurements. As well, fluorescence quenching techniques were utilized to determine free copper concentrations in marine waters and agreed well with the internal calibration flow-through ISE measurements. The result is two methods that can be used to reliably measure free copper in sea water.

Using the two methods for determining free copper in seawater, toxicity assays using the rotifer, *Brachionus plicatilis*, were performed to investigate the influence of DOC source on copper speciation and toxicity. Through these toxicity assays it was found that free copper was constant at the LC_{50}, despite changes in LC_{50} and DOC

concentrations. This has significant impacts for toxicity modeling as this supports the current assumptions of the BLM. A constant free copper concentration, despite changing LC_{50} values implies that there is a constant concentration of copper bound to the biotic ligand. This concentration would be a critical concentration required to cause toxicity. The change in total copper LC_{50} values would be due to differences in water chemistry that affect how much total copper is needed to be added to a system to reach a critical free copper concentrations required for toxicity. This was supported by fluorescence quenching techniques which showed that copper binding capacity of the different sea water samples used for the toxicity assays increased with increasing LC_{50} values.

Interestingly, the relationship between LC_{50} and DOC showed two potential trends. The first was a salt-induced colloid formation trend in which DOC concentrations above 2 mg C L^{-1} showed no increase in a protective effect against coper toxicity. The second trend resulted in an LC_{50} model equation for rotifer toxicity where LC_{50} ($\mu g\ L^{-1}$) = $25.15DOC^{0.47}$ (including outlier data) or LC_{50} ($\mu g\ L^{-1}$) = $22.86DOC^{0.45}$ (excluding outlier data). However, there was no significant effect of DOC source/composition on LC_{50} which suggests that total DOC concentrations alone are a sufficient parameter for toxicity modeling without the need for DOC quality parameters. Overall, a summary of the chemical effects on copper toxicity in marine environments using the results from this reaserch only can be seen in Figure 5.1.

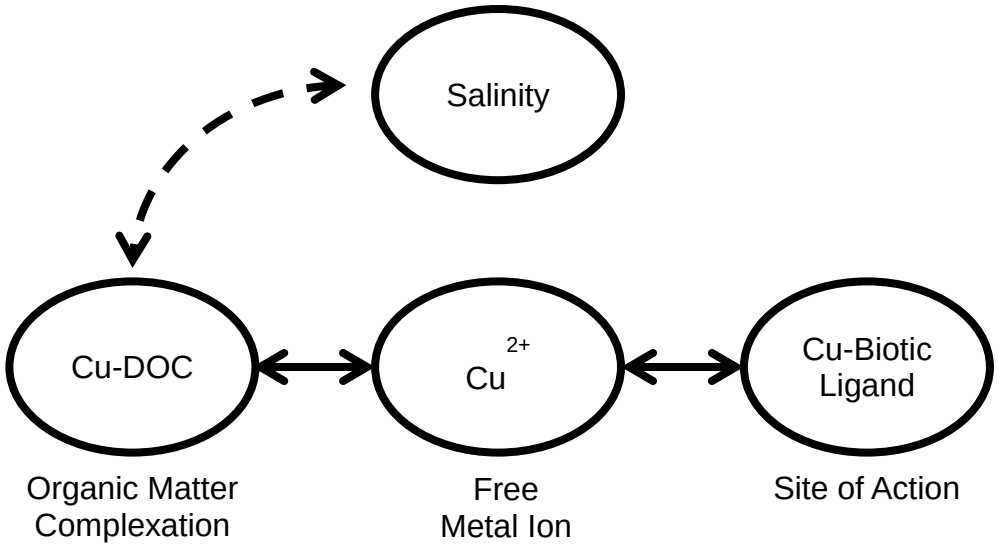

Figure 5.1 Summary schematic of the interaction of DOC on free copper and toxicity to the rotifer, Brachionus plicatilis. Dashed line represents the potential influence of salinity on DOC (salt-induced colloid formation).

In this figure, the dashed line represents the influence of salt-induced colloid formation on DOC. In this case, salinity reduces the capacity of DOC to bind copper, thereby reducing the ability of DOC to have a protective effect on copper toxicity. If salt-induced colloid formation is not occurring then, based from this research alone, there is no relationship between salinity and DOC. Instead there is only a direct relationship between DOC, free copper and toxicity of the organism. In either case, the major assumption of the BLM is supported in which toxicity is proportional to the amount of copper bound to the biotic ligand.

5.2 References

Arnold, W.R., 2005. Effects of dissolved organic carbon on copper toxicity: implications for saltwater copper criteria. *Integrated Environmental Assessment and Management*. **1**, 34-39.

Arnold, W.R., Cotsifas, J., Corneillie, K.M. 2006. Validation and update of a model used to predict copper toxicity to the marine bivalve *Mytilus sp*. *Environmental Toxicology*. **21**, 65-70.

Arnold, W.R., Diamond, R.L., Smith, D.S. 2010. The effects of salinity, pH, and dissolved organic matter on acute copper toxicity to the rotifer, *Brachionus plicatilis* ("L" strain). *Archives of Environmental Contamination and Toxicology*. **59**, 225-234.

Arnold, W.R., Cotsifas, J.S., Ogle, R.S., DePalma, S.G.S., Smith, D.S. 2010a. A comparison of the copper sensitivity of six invertebrate species in ambient salt water of varying dissolved organic matter concentrations. *Environmental Toxicology and Chemistry*. **29**(2), 311-319.

Brooks, S.J., Bolam, T., Tolhurst, L., Bassett, J., La Roche, J., Waldock, M., Barry, J., Thomas, K.V. 2007. Effects of dissolved organic carbon on the toxicity of copper to the developing embryos of the pacific oyster (*Crassostrea gigas*). *Environmental Toxicology and Chemistry*. **26**(8), 1756-1763.

CCME (Canadian Council of Ministers of the Environment). 2003. Canadian Water Quality Guidelines for the Protection of Aquatic Life: Site-Specific Guidance. Available at ceqg-rcqe.ccme.ca/download/en/221/.

Cooper, C.A., Tait, T., Gray, H., Cimprich, G., Santore, R.C., McGeer, J.C., Smith, D.S. 2013. Influence of salinity and dissolved organic carbon on acute toxicity to the rotifer *Brachionus plicatilis*. Submitted.

DePalma, S.G.S., Arnold, W.R., McGeer, J.C., Dixon, D.G., Smith, D.S., 2011. Effects of dissolved organic matter and reduced sulphur on copper bioavailability in coastal marine environments. *Ecotoxicology and Environmental Safety*. **74**, 230-237.

Eriksen R.S., Mackey, D.J., Alexander, P., De Marco, R., Wang, X.D. 1999. Continuous flow methods for evaluating the response of a copper ion selective electrode to total free copper in seawater. *Journal of Environmental Monitoring*. **1**, 483-487.

Nadella, S.R.,Tellis, M., Diamond, R., Smith, S., Bianchini, A., Wood, C.M. 2013. Toxicity of lead and zinc to developing mussel an sea urchin embryos: Critical tissue residues and effects of dissolved organic matter and salinity. *Comparative Biochemistry and Physiology*. In press.

APPENDIX A

A1. Solving for chemical equilibrium using MATLAB™

Modelling experimental data requires simultaneously solving for the chemical equilibria in solution while subject to the constraints of mass balance and mass action. Mass balance and mass action can be represented in Tableau notation (Morel & Hering 1993). The tableau notation defines the chemical equilibria and the stoichiometric coefficients required for the formation of each species are input into the columns (Smith 2010). An example of a basic tableau is given in Figure A1.

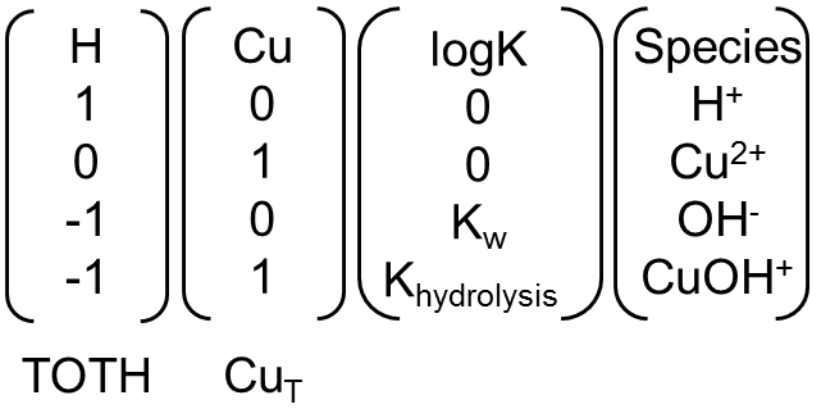

Figure A1. Example of tableau notation for basic copper system.

Multiplication across each row will determine the respective species concentration while summation down each column will determine total concentrations (mass balance) (Smith 2010). The species present in the tableau are dependent on each other and therefore components from the tableau can be selected to solve for the chemical equilibria. Four vectors are created labeled C, T, K and A. C contains the species

concentrations and T comprises the total concentrations. The vector, K includes the logK values and A containes the stoichiometric coefficients. These vectors are then solves for using the equation:

$$R = A'x\ (10^{C}) - T$$

Where,

$$C = \ 10^{(K+A\ x\ X')}$$

The Newton-Raphson method is used to minimize the sum of the residuals of the species concentrations determined. Using an initial guess, the residual vector and Jacobian (gradient matrix) is calculated for each iteration. The Jacobian finds the direction of decrease for the sum of the residuals. This process is then repeated to produce a new estimate that refines the guess until sum of the residuals is minimized (Smith 2010).

References

Morel, F.M.M., Hering, J.G. 1993 Principles and applications of aquatic chemistry. Wiley-Interscience.

Smith, DS. Solution of simultaneous chemical equilibria in heterogenous systems: implementation in Matlab. Waterloo, Ontario: Wilfrid Laurier University; 2010.

A2. MATLAB script for modeling free Cu over a pH range

```
function II=Internal_calib_Trp_Cu_varypH2
 figure(1); clf
 % determine free Cu
 CuTppb=25; %ug/L
CuT=(CuTppb*1e-6)/63.5;
TrpT=10e-6; %mol/L
ClT=0.6; KCuCl=10^0.3;
NaHCO3=200; %mg/L from recipe
NaHCO3AW=100; %g/mol
DIC=(NaHCO3*1e-3)/NaHCO3AW;

pH=[8.15 7.43 6.78 6.05 4.87 3.46];
%H=10.^(-1*pH); H=(1/0.74)*H; pH=-log10(H);

CumV=[-24.65 3.3 31.7 41.7 51.7 50.5];

%plot(pH,CumV,'ko','markersize',10,'markerfacecolor','b')

% one point calibration
% E=Eo+mlogCu
% Eo=E-mlogCu assume m=59.2/2 = 29.6;
% free Cu just determined by Cl complexation

CuTadjust=CuT./(1+KCuCl*ClT);

CumVend=mean([51.7 50.5]); m=29.6;
logCucalpoint=log10(CuTadjust); Eo=CumVend-m*logCucalpoint;

% apply calibration

logCu=(CumV-Eo)./m;

% plot it

plot(pH,logCu,'ko','markersize',12,'markerfacecolor','b')
set(gca,'linewidth',2,'fontsize',16)
xlabel('pH','fontsize',16, 'fontweight', 'bold')
ylabel('log[Cu^{2+}]','fontsize',16, 'fontweight', 'bold')
%title('25 ppb Cu and 10 uM Trp in seawater','fontsize',12)

print internal_calib.png -dpng
```

```
hold on
CuTppb=25; %ug/L
CuT=(CuTppb*1e-6)/63.5;
TrpT=10e-6; %mol/L
ClT=0.6; KCuCl=10^0.3;
NaHCO3=200; %mg/L from recipe
NaHCO3AW=100; %g/mol
DIC=(NaHCO3*1e-3)/NaHCO3AW;

pH=[8.00 4.94 3.37];
%H=10.^(-1*pH); H=(1/0.74)*H; pH=-log10(H);

CumV=[-50.6 43.65 51.6];

% one point calibration

CuTadjust=CuT./(1+KCuCl*ClT);

CumVend=mean([43.65 51.6]); m=29.6;
logCucalpoint=log10(CuTadjust); Eo=CumVend-m*logCucalpoint;

% apply calibration

logCu=(CumV-Eo)./m;

% plot it

plot(pH,logCu,'ko','markersize',12,'markerfacecolor','b')

print internal_calib.eps -depsc2

hold on
CuTppb=25; %ug/L
CuT=(CuTppb*1e-6)/63.5;
TrpT=10e-6; %mol/L
ClT=0.6; KCuCl=10^0.3;
NaHCO3=200; %mg/L from recipe
NaHCO3AW=100; %g/mol
DIC=(NaHCO3*1e-3)/NaHCO3AW;

pH=[8.28 7.36 6.56 5.79 4.59 3.44];
%H=10.^(-1*pH); H=(1/0.74)*H; pH=-log10(H);

CumV=[-33.3 1.3 32.2 49.9 54.8 54.1];

% one point calibration
```

```
CuTadjust=CuT./(1+KCuCl*ClT);

CumVend=54.1; m=29.6;
logCucalpoint=log10(CuTadjust); Eo=CumVend-m*logCucalpoint;

% apply calibration

logCu=(CumV-Eo)./m;

% plot it

plot(pH,logCu,'ko','markersize',12,'markerfacecolor','b')

hold on
CuTppb=10; %ug/L
CuT=(CuTppb*1e-6)/63.5;
TrpT=10e-6; %mol/L
ClT=0.6; KCuCl=10^0.3;
NaHCO3=200; %mg/L from recipe
NaHCO3AW=100; %g/mol
DIC=(NaHCO3*1e-3)/NaHCO3AW;

pH=[8.10 7.34 6.70 5.94 4.78 3.29];
%H=10.^(-1*pH); H=(1/0.74)*H; pH=-log10(H);

CumV=[-45.6 -6.0 3.2 8.7 25.3 24.1];


% one point calibration

CuTadjust=CuT./(1+KCuCl*ClT);

CumVend=mean([25.3 24.1]); m=29.6;
logCucalpoint=log10(CuTadjust); Eo=CumVend-m*logCucalpoint;

% apply calibration

logCu=(CumV-Eo)./m;

% plot it

plot(pH,logCu,'ko','markersize',12,'markerfacecolor','r')

print internal_calib.eps -depsc
```

```
hold on
CuTppb=10; %ug/L
CuT=(CuTppb*1e-6)/63.5;
TrpT=10e-6; %mol/L
ClT=0.6; KCuCl=10^0.3;
NaHCO3=200; %mg/L from recipe
NaHCO3AW=100; %g/mol
DIC=(NaHCO3*1e-3)/NaHCO3AW;

pH=[8.06 4.70 3.34];
%H=10.^(-1*pH); H=(1/0.74)*H; pH=-log10(H);

CumV=[-43.8 56.6 55.5];


% one point calibration

CuTadjust=CuT./(1+KCuCl*ClT);

CumVend=mean([56.6 55.5]); m=29.6;
logCucalpoint=log10(CuTadjust); Eo=CumVend-m*logCucalpoint;

% apply calibration

logCu=(CumV-Eo)./m;

% plot it

plot(pH,logCu,'ko','markersize',12,'markerfacecolor','r')

print internal_calib.eps -depsc

hold on
CuTppb=10; %ug/L
CuT=(CuTppb*1e-6)/63.5;
TrpT=10e-6; %mol/L
ClT=0.6; KCuCl=10^0.3;
NaHCO3=200; %mg/L from recipe
NaHCO3AW=100; %g/mol
DIC=(NaHCO3*1e-3)/NaHCO3AW;

pH=[8.00 4.64 3.22];
%H=10.^(-1*pH); H=(1/0.74)*H; pH=-log10(H);

CumV=[-32.5 54.4 51.6];
```

```
% one point calibration

CuTadjust=CuT./(1+KCuCl*ClT);

CumVend=mean([54.4 51.6]); m=29.6;
logCucalpoint=log10(CuTadjust); Eo=CumVend-m*logCucalpoint;

% apply calibration

logCu10=(CumV-Eo)./m;

% plot it

plot(pH,logCu10,'ko','markersize',12,'markerfacecolor','r')

print internal_calib.eps -depsc

hold on
CuTppb=10; %ug/L
CuT=(CuTppb*1e-6)/63.5;
TrpT=10e-6; %mol/L
ClT=0.6; KCuCl=10^0.3;
NaHCO3=200; %mg/L from recipe
NaHCO3AW=100; %g/mol
DIC=(NaHCO3*1e-3)/NaHCO3AW;

pH=[8.48 7.59 6.95 5.91 4.53 3.29];
%H=10.^(-1*pH); H=(1/0.74)*H; pH=-log10(H);

CumV=[-28.2 -10.4 -3.5 -8.75 9.5 14.3];

% one point calibration

CuTadjust=CuT./(1+KCuCl*ClT);

CumVend=mean([14.3 9.5]); m=29.6;
logCucalpoint=log10(CuTadjust); Eo=CumVend-m*logCucalpoint;

% apply calibration

logCu=(CumV-Eo)./m;

% plot it

plot(pH,logCu,'ko','markersize',12,'markerfacecolor','b')
```

```
Hold on
CuTppb=5; %ug/L
CuT=(CuTppb*1e-6)/63.5;
TrpT=10e-6; %mol/L
ClT=0.6; KCuCl=10^0.3;
NaHCO3=200; %mg/L from recipe
NaHCO3AW=100; %g/mol
DIC=(NaHCO3*1e-3)/NaHCO3AW;

pH=[8.21  4.60 3.61];
%H=10.^(-1*pH); H=(1/0.74)*H; pH=-log10(H);

CumV=[-30.3 66.7 65.2];

% one point calibration

CuTadjust=CuT./(1+KCuCl*ClT);

CumVend=mean([66.7 65.2]); m=29.6;
logCucalpoint=log10(CuTadjust); Eo=CumVend-m*logCucalpoint;

% apply calibration

logCu=(CumV-Eo)./m;

% plot it

plot(pH,logCu,'ko','markersize',12,'markerfacecolor','c')

hold on
CuTppb=5; %ug/L
CuT=(CuTppb*1e-6)/63.5;
TrpT=10e-6; %mol/L
ClT=0.6; KCuCl=10^0.3;
NaHCO3=200; %mg/L from recipe
NaHCO3AW=100; %g/mol
DIC=(NaHCO3*1e-3)/NaHCO3AW;

pH=[7.93 4.72 3.38];
%H=10.^(-1*pH); H=(1/0.74)*H; pH=-log10(H);

CumV=[-47.2 60.05 60.15];

% one point calibration
```

```
CuTadjust=CuT./(1+KCuCl*ClT);

CumVend=mean([60.05 60.15]); m=29.6;
logCucalpoint=log10(CuTadjust); Eo=CumVend-m*logCucalpoint;

% apply calibration

logCu=(CumV-Eo)./m;

% plot it

plot(pH,logCu,'ko','markersize',12,'markerfacecolor','c')

hold on
CuTppb=5; %ug/L
CuT=(CuTppb*1e-6)/63.5;
TrpT=10e-6; %mol/L
ClT=0.6; KCuCl=10^0.3;
NaHCO3=200; %mg/L from recipe
NaHCO3AW=100; %g/mol
DIC=(NaHCO3*1e-3)/NaHCO3AW;

pH=[8.07 4.90 3.30];
%H=10.^(-1*pH); H=(1/0.74)*H; pH=-log10(H);

CumV=[-38.8 50.0 55.5];

% one point calibration

CuTadjust=CuT./(1+KCuCl*ClT);

CumVend=mean([50.0 55.5]); m=29.6;
logCucalpoint=log10(CuTadjust); Eo=CumVend-m*logCucalpoint;

% apply calibration

logCu=(CumV-Eo)./m

% plot it

plot(pH,logCu,'ko','markersize',12,'markerfacecolor','c')

Hold on
CuTppb=50; %ug/L
CuT=(CuTppb*1e-6)/63.5;
TrpT=10e-6; %mol/L
```

```
ClT=0.6; KCuCl=10^0.3;
NaHCO3=200; %mg/L from recipe
NaHCO3AW=100; %g/mol
DIC=(NaHCO3*1e-3)/NaHCO3AW;

pH=[7.98 7.5 6.74 5.82 4.60 3.44];
%H=10.^(-1*pH); H=(1/0.74)*H; pH=-log10(H);

CumV=[-19.3 -16.1 29.3 44.4 57.1 48];

% one point calibration
CuTadjust=CuT./(1+KCuCl*ClT);

CumVend=mean([57 48]); m=29.6;
logCucalpoint=log10(CuTadjust); Eo=CumVend-m*logCucalpoint;

% apply calibration

logCu=(CumV-Eo)./m;

% plot it

plot(pH,logCu,'ko','markersize',12,'markerfacecolor','m')

hold on
CuTppb=50; %ug/L
CuT=(CuTppb*1e-6)/63.5;
TrpT=10e-6; %mol/L
ClT=0.6; KCuCl=10^0.3;
NaHCO3=200; %mg/L from recipe
NaHCO3AW=100; %g/mol
DIC=(NaHCO3*1e-3)/NaHCO3AW;

pH=[4.74 3.28];
%H=10.^(-1*pH); H=(1/0.74)*H; pH=-log10(H);

CumV=[66.1 63.5];

CuTadjust=CuT./(1+KCuCl*ClT);

CumVend=mean([66.1 63.5]); m=29.6;
logCucalpoint=log10(CuTadjust); Eo=CumVend-m*logCucalpoint;

% apply calibration

logCu=(CumV-Eo)./m;
```

```
% plot it

plot(pH,logCu,'ko','markersize',12,'markerfacecolor','m')

hold on
CuTppb=50; %ug/L
CuT=(CuTppb*1e-6)/63.5;
TrpT=10e-6; %mol/L
ClT=0.6; KCuCl=10^0.3;
NaHCO3=200; %mg/L from recipe
NaHCO3AW=100; %g/mol
DIC=(NaHCO3*1e-3)/NaHCO3AW;

pH=[8.01 5.20 3.39];
%H=10.^(-1*pH); H=(1/0.74)*H; pH=-log10(H);

CumV=[-27.1 41.1 50.4];

% one point calibration

CuTadjust=CuT./(1+KCuCl*ClT);

CumVend=mean([41.1 50.4]); m=29.6;
logCucalpoint=log10(CuTadjust); Eo=CumVend-m*logCucalpoint;

% apply calibration

logCu=(CumV-Eo)./m

% plot it

plot(pH,logCu,'ko','markersize',12,'markerfacecolor','m')

% model calc no ppte

c=0; pHplot=[3:0.2:9];

for i=1:size(pHplot,2)


[species,names]=Cumodel_highIS_Cl_DIC_Trp_ppte(CuT,pHplot(i),DIC,ClT,TrpT,3);
   % flag=2 malachite only
   % flag=1 tenorite only
   % flag=3 no ppte
```

```
   c=c+1;
   for j=1:size(species,2)
      txt=[names(j,:),'(c)=species(:,j);'];  eval(txt)
   end
   species_summary(i,:)=species;
end

figure(1); hold on;  plot(pHplot,log10(Cu),'r','linewidth',4);

print internal_calib2.eps -depsc2

hold on; Internal_calib_Trp_Cu_varypH

print internal_calib3.eps -depsc2

Internal_calib_Trp_Cu_varypH_5ppb
Internal_calib_Trp_Cu_varypH_50ppb
Internal_calib_Trp_Cu_varypH_10ppb2

print internal_calib4.eps -depsc2

end

% subfunctions %

function [II,GG]=Cumodel_highIS_Cl_DIC_Trp_ppte(CuT,pH,DIC,ClT,TrpT,flag)

warning('off')

[KSOLUTION,KSOLID,ASOLUTION,ASOLID,SOLUTIONNAMES,SOLIDNAMES]
=get_equilib_defn(flag);

%CuT=3.9592e-7;

%pH=[6:0.1:9]; % fixed pH
numpts=size(pH,2);
Ncp=size(ASOLID,1);
solid_summary=zeros(numpts,Ncp);

for i=1:size(SOLIDNAMES,1)
   txt=[SOLIDNAMES(i,:),'=zeros(numpts,1);']; eval(txt)
end

for i=1:size(pH,2)
   %H=10.^(-1*pH(i)); Ka1=10^(-6.3); Ka2=10.^(-10.3); Kh=10.^(-1.47);
   %CT=Kh*PCO2+(Kh*PCO2*Ka1)./H+(Kh*PCO2*Ka1*Ka2)./(H.^2);
```

```
   CT=DIC;
   CTrun(i)=CT;

   % adjust for fixed pH


[Ksolution,Ksolid,Asolution,Asolid]=get_equilib_fixed_pH(KSOLUTION,KSOLID,AS
OLUTION,ASOLID,pH(i));

   Asolid_SI_check=Asolid; Ksolid_SI_check=Ksolid;

   % number of different species
   Nx=size(Asolution,2); Ncp=size(Asolid,1); Nc=size(Asolution,1);

   % initial guess
   Cu_guess=[-10.5]; CuOH2s_guess=0.1*CuT;  CuCO3s_guess=0.1*CT;
   guess=[10.^Cu_guess CT./10 CuOH2s_guess CuCO3s_guess]; iterations=1000;
criteria=1e-16;
   T=[CuT CT ClT TrpT]; guess=T./10;

   % calculate species using NR

   solids=zeros(1,Ncp);

   if i==1;
[species,err,SI]=NR_method_solution(Asolution,Asolid,Ksolid,Ksolution,T',[guess(1:Nx
)]',iterations,criteria); end
   if i>1;

[species,err,SI]=NR_method_solution(Asolution,Asolid,Ksolid,Ksolution,T',[species(2:N
x+1)],iterations,criteria);
   end

   for qq=1:Ncp

      [Y,I]=max(SI);

      if Y>1.000000001
         Iindex(qq)=I;
         Asolidtemp(qq,:)=Asolid_SI_check(I,:);
         Ksolidtemp(qq,:)=Ksolid_SI_check(I,:);
         solidguess(qq)=T(I)*0.5;
        % solidguess(qq)=min(T)*0.015;
         if i>1;
            %if max(solids)>0
            txt=['solidguess(qq)=',SOLIDNAMES(I,:),'(i-1);']; eval(txt);
```

```
            %end
          end
          guess=[species(2:Nx+1)' solidguess];

[species,err,SItst,solids]=NR_method(Asolution,Asolidtemp',Ksolidtemp,Ksolution,T',gu
ess',iterations,criteria);
           for q=1:size(solids,1);
             txt=[SOLIDNAMES(Iindex(q),:),'(i)=solids(q);']; eval(txt)
           end
       end

       Q=Asolid*log10(species(2:Nx+1)); SI=10.^(Q+Ksolid); Ifirst=I;

   end

   Q=Asolid*log10(species(2:Nx+1)); SI=10.^(Q+Ksolid);
   SI_summary(i,:)=SI;

   species_summary(i,:)=species;
   mass_err_summary(i,:)=(err(1));

   Asolidtemp=[]; Ksolidtemp=[];

end

for i=1:size(species_summary,2)
   txt=[SOLUTIONNAMES(i,:),'=species_summary(:,i);']; eval(txt)
end

II=[species_summary tenorite malachite CuCO3s CuOH2s];
GG=strvcat(SOLUTIONNAMES,'tenorite','malachite','CuCO3s','CuOH2s');

end

% -------------------- NR method solids present

function
[species,err,SI,solids]=NR_method(Asolution,Asolid,Ksolid,Ksolution,T,guess,iterations,
criteria)

Nx=size(Asolution,2); Ncp=size(Asolid,2); Nc=size(Asolution,1); X=guess;

for II=1:iterations

   Xsolution=X(1:Nx); Xsolid=[]; if Ncp>0; Xsolid=X(Nx+1:Nx+Ncp); end
```

```
logC=(Ksolution)+Asolution*log10(Xsolution); C=10.^(logC); % calc species

if Ncp>0;
   Rmass=Asolution'*C+Asolid*Xsolid-T;
end


if Ncp==0; Rmass=Asolution'*C-T; end % calc residuals in mass balance

Q=Asolid'*log10(Xsolution); SI=10.^(Q+Ksolid);
RSI=ones(size(SI))-SI;

% calc the jacobian

z=zeros(Nx+Ncp,Nx+Ncp);

for j=1:Nx;
   for k=1:Nx;
         for i=1:Nc; z(j,k)=z(j,k)+Asolution(i,j)*Asolution(i,k)*C(i)/Xsolution(k); end
   end
end

if Ncp>0;
for j=1:Nx;
   for k=Nx+1:Nx+Ncp;
         t=Asolid';
         z(j,k)=t(k-Nx,j);
   end
end
end

if Ncp>0
for j=Nx+1:Nx+Ncp;
   for k=1:Nx
         z(j,k)=-1*Asolid(k,j-Nx)*(SI(j-Nx)/Xsolution(k));
   end
end
end

if Ncp>0
for j=Nx+1:Nx+Ncp
   for k=Nx+1:Nx+Ncp
      z(j,k)=0;
   end
end
end
```

```
    R=[Rmass; RSI]; X=[Xsolution; Xsolid];

    deltaX=z\(-1*R);
    %deltaX=-1*inv(z)*(R);
    one_over_del=max([1, -1*deltaX'./(0.5*X')]);
    del=1/one_over_del;
    X=X+del*deltaX;

    %X=X+deltaX;

    tst=sum(abs(R));
    if tst<=criteria; break; end

end

logC=(Ksolution)+Asolution*log10(Xsolution); C=10.^(logC); % calc species
RSI=ones(size(SI))-SI;

if Ncp>0; Rmass=Asolution'*C+Asolid*Xsolid-T; end % calc residuals in mass balance
if Ncp==0; Rmass=Asolution'*C-T; end % calc residuals in mass balance

err=[Rmass];

species=[C];
solids=Xsolid;

end

% ---------- NR method just solution species

function
[species,err,SI]=NR_method_solution(Asolution,Asolid,Ksolid,Ksolution,T,guess,iteratio
ns,criteria)

Nx=size(Asolution,2); Ncp=size(Asolid,1); Nc=size(Asolution,1); X=guess;

for II=1:iterations

    Xsolution=X(1:Nx);

    logC=(Ksolution)+Asolution*log10(Xsolution); C=10.^(logC); % calc species

    Rmass=Asolution'*C-T;

    Q=Asolid*log10(Xsolution); SI=10.^(Q+Ksolid);
```

```
   RSI=ones(size(SI))-SI;

   % calc the jacobian

   z=zeros(Nx,Nx);

   for j=1:Nx;
      for k=1:Nx;
            for i=1:Nc; z(j,k)=z(j,k)+Asolution(i,j)*Asolution(i,k)*C(i)/Xsolution(k); end
      end
   end

   R=[Rmass]; X=[Xsolution];

   deltaX=z\(-1*R);
   %deltaX=-1*inv(z)*(R);
   one_over_del=max([1, -1*deltaX'./(0.5*X')]);
   del=1/one_over_del;
   X=X+del*deltaX;

   %X=X+deltaX;

   tst=sum(abs(R));
   if tst<=criteria; break; end

end

logC=(Ksolution)+Asolution*log10(Xsolution); C=10.^(logC); % calc species
RSI=ones(size(SI))-SI;

Q=Asolid*log10(Xsolution); SI=10.^(Q+Ksolid);
RSI=ones(size(SI))-SI;

Rmass=Asolution'*C-T;

err=[Rmass];

species=[C];

end

% ----- equilib definition ----------

function
[KSOLUTION,KSOLID,ASOLUTION,ASOLID,SOLUTIONNAMES,SOLIDNAMES]
=get_equilib_defn(flag);
```

```
logKw=-14.082;
logKh1=-7.982;
logKh1=-7.182;
logBh2=-15.2;
logBh2=-14.8;
logBh3=-27.2;
logBh4=-40.4;
logBh22=-10.98;
pKa1=6.3;
pKa2=10.3;
logKCuCO3=6.77;
%logKCuCO3=6.47;
logKCuCO32=10.2;
logKCuHCO3=1.03;
logKCuCl=0.3;
logKCuTrp=8.29;
pKa1Trp=2.1; %2.35;
pKa2Trp=9.33; %9.33;
logKCuTrp2=15.5;
logKCuHTrp=2.47;

KSOLUTION=[...
    0
    0
    0
    0
    0
    logKw
    logKh1
    logBh2
    logBh3
    logBh4
    logBh22
    pKa2
    pKa2+pKa1
    logKCuCO3
    logKCuCO32
    logKCuHCO3
    logKCuCl
    logKCuTrp
    pKa2Trp
    pKa2Trp+pKa1Trp
    logKCuTrp2
    logKCuHTrp];
```

```
ASOLUTION=[...
   %H     M    CO3   Cl  Trp
    1     0    0     0   0
    0     1    0     0   0
    0     0    1     0   0
    0     0    0     1   0
    0     0    0     0   1
    -1    0    0     0   0
    -1    1    0     0   0
    -2    1    0     0   0
    -3    1    0     0   0
    -4    1    0     0   0
    -2    2    0     0   0
    1     0    1     0   0
    2     0    1     0   0
    0     1    1     0   0
    0     1    2     0   0
    1     1    1     0   0
    0     1    0     1   0
    0     1    0     0   1
    1     0    0     0   1
    2     0    0     0   1
    0     1    0     0   2
    1     1    0     0   1];

SOLUTIONNAMES=strvcat('H','Cu','CO3','Cl','Trp','OH','CuOH','CuOH2','CuOH3','Cu
OH4','Cu2OH2','HCO3','H2CO3','CuCO3aq','CuCO32aq','CuHCO3','CuCl','CuTrp','HTrp
','H2Trp','CuTrp2','CuHTrp');

   % ---------- solid values

   logKsp=-18.7;
   logKcuoh2s=-logKsp+2*logKw;
   logKCuCO3s=11.5;
   logKmalachite=33.18+2*logKw;
   logKmalachite=32.0+2*logKw;
   logKtenorite=20.48+2*logKw;
   if flag==1; logKmalachite=1; end
   if flag==2; logKtenorite=-100; end
   if flag==3; logKtenorite=-100; logKmalachite=1; end

   logKcuoh2s=-10;
   logKCuCO3s=1;
   %logKtenorite=-100;
   %logKmalachite=1;
```

```
   KSOLID=[...
   logKtenorite
   logKmalachite
   logKcuoh2s
   logKCuCO3s];

   ASOLID=[...
    -2     1   0      0  0
    -2     2   1      0  0
    -2     1   0      0   0
    0      1   1      0   0];

 SOLIDNAMES=strvcat('tenorite','malachite','CuOH2s','CuCO3s');

end

% ----------- for fixed pH ----------------

function
[Ksolution,Ksolid,Asolution,Asolid]=get_equilib_fixed_pH(KSOLUTION,KSOLID,AS
OLUTION,ASOLID,pH)

   [N,M]=size(ASOLUTION);
   Ksolution=KSOLUTION-ASOLUTION(:,1)*pH;
   Asolution=[ASOLUTION(:,2:M)];
   [N,M]=size(ASOLID);
   Ksolid=KSOLID-ASOLID(:,1)*pH;
   Asolid=[ASOLID(:,2:M)];

end
```

A3. MATLAB script for free copper at a constant pH

```
function II=Internal_calib_Trp_Cu_varypH_multiCu

figure(1); clf

CuTppb=5; %ug/L
CuT=(CuTppb*1e-6)/63.5;
TrpT=10e-6; %mol/L
ClT=0.6; KCuCl=10^0.3;
NaHCO3=200; %mg/L from recipe
NaHCO3AW=100; %g/mol
DIC=(NaHCO3*1e-3)/NaHCO3AW;

pH=[4:1:9];

% model calc no ppte

c=0; pHplot=[3:0.2:9]; pHplot=8.2;

for i=1:size(pHplot,2)


[species,names]=Cumodel_highIS_Cl_DIC_Trp_ppte(CuT,pHplot(i),DIC,ClT,TrpT,3);
   % flag=2 malachite only
   % flag=1 tenorite only
   % flag=3 no ppte

   c=c+1;
   for j=1:size(species,2)
      txt=[names(j,:),'(c)=species(:,j);'];  eval(txt)
   end
   species_summary(i,:)=species;
end
Cuplot(1)=Cu;
%figure(1); hold on;  plot(pHplot,log10(Cu),'b','linewidth',2);
%set(gca,'linewidth',2,'fontsize',12)
%xlabel('pH','fontsize',12)
%ylabel('log[Cu^{2+}]','fontsize',12)
%title('Trp modelled Cu in seawater','fontsize',12)

CuTppb=10; %ug/L
CuT=(CuTppb*1e-6)/63.5;
c=0;

for i=1:size(pHplot,2)
```

```
[species,names]=Cumodel_highIS_Cl_DIC_Trp_ppte(CuT,pHplot(i),DIC,ClT,TrpT,3);
   % flag=2 malachite only
   % flag=1 tenorite only
   % flag=3 no ppte

   c=c+1;
   for j=1:size(species,2)
      txt=[names(j,:),'(c)=species(:,j);'];  eval(txt)
   end
   species_summary(i,:)=species;
end
Cuplot(2)=Cu;
%figure(1); hold on;  plot(pHplot,log10(Cu),'r','linewidth',2);

CuTppb=25; %ug/L
CuT=(CuTppb*1e-6)/63.5;
c=0;

for i=1:size(pHplot,2)


[species,names]=Cumodel_highIS_Cl_DIC_Trp_ppte(CuT,pHplot(i),DIC,ClT,TrpT,3);
   % flag=2 malachite only
   % flag=1 tenorite only
   % flag=3 no ppte

   c=c+1;
   for j=1:size(species,2)
      txt=[names(j,:),'(c)=species(:,j);'];  eval(txt)
   end
   species_summary(i,:)=species;
end
Cuplot(3)=Cu;
%figure(1); hold on;  plot(pHplot,log10(Cu),'m','linewidth',2);

CuTppb=50; %ug/L
CuT=(CuTppb*1e-6)/63.5;
c=0;

for i=1:size(pHplot,2)


[species,names]=Cumodel_highIS_Cl_DIC_Trp_ppte(CuT,pHplot(i),DIC,ClT,TrpT,3);
   % flag=2 malachite only
```

```
    % flag=1 tenorite only
    % flag=3 no ppte

    c=c+1;
    for j=1:size(species,2)
        txt=[names(j,:),'(c)=species(:,j);'];  eval(txt)
    end
    species_summary(i,:)=species;
end
Cuplot(4)=Cu;
%figure(1); hold on;  plot(pHplot,log10(Cu),'g','linewidth',2);
CuT=(([5 10 25 50])/63.55) ;

figure(1);
%h = (plot([5 10 25 50],log10(Cuplot),'ko-',[5 10 25 50],[-10.7 -9.6 -9.6 -9.3],'k<', [5 10
25 50], [-10.4 -9.8 -9.3 -8.8], 'k<'))

h = (plot(CuT,log10(Cuplot),'ko-',CuT,[-10.7 -9.6 -9.6 -9.3],'k<', CuT, [-10.4 -9.8 -9.3 -
8.8], 'k<'))
set (h(1), 'markerfacecolor', 'k','markersize',12, 'LineWidth', 4)
set (h(2), 'markerfacecolor', 'b', 'markersize', 12)
set (h(3), 'markerfacecolor', 'g', 'markersize', 12)
set(gca,'linewidth',2,'fontsize',16)
xlabel('Cu_T (\mumol L^{-1})','fontsize',16, 'fontweight', 'bold')
ylabel('log[Cu^{2+}]','fontsize',16, 'fontweight', 'bold')
axis([0 0.8 -11 -8.5])
end

% subfunctions %

function [II,GG]=Cumodel_highIS_Cl_DIC_Trp_ppte(CuT,pH,DIC,ClT,TrpT,flag)

warning('off')

[KSOLUTION,KSOLID,ASOLUTION,ASOLID,SOLUTIONNAMES,SOLIDNAMES]
=get_equilib_defn(flag);

%CuT=3.9592e-7;

%pH=[6:0.1:9]; % fixed pH
numpts=size(pH,2);
Ncp=size(ASOLID,1);
solid_summary=zeros(numpts,Ncp);

for i=1:size(SOLIDNAMES,1)
    txt=[SOLIDNAMES(i,:),'=zeros(numpts,1);']; eval(txt)
```

```
end

for i=1:size(pH,2)
   %H=10.^(-1*pH(i)); Ka1=10^(-6.3); Ka2=10.^(-10.3); Kh=10.^(-1.47);
   %CT=Kh*PCO2+(Kh*PCO2*Ka1)./H+(Kh*PCO2*Ka1*Ka2)./(H.^2);
   CT=DIC;
   CTrun(i)=CT;

   % adjust for fixed pH


[Ksolution,Ksolid,Asolution,Asolid]=get_equilib_fixed_pH(KSOLUTION,KSOLID,AS
OLUTION,ASOLID,pH(i));

   Asolid_SI_check=Asolid; Ksolid_SI_check=Ksolid;

   % number of different species
   Nx=size(Asolution,2); Ncp=size(Asolid,1); Nc=size(Asolution,1);

   % initial guess
   Cu_guess=[-10.5]; CuOH2s_guess=0.1*CuT;  CuCO3s_guess=0.1*CT;
   guess=[10.^Cu_guess CT./10 CuOH2s_guess CuCO3s_guess]; iterations=1000;
criteria=1e-16;
   T=[CuT CT ClT TrpT]; guess=T./10;

   % calculate species using NR

   solids=zeros(1,Ncp);

   if i==1;
[species,err,SI]=NR_method_solution(Asolution,Asolid,Ksolid,Ksolution,T',[guess(1:Nx
)]',iterations,criteria); end
   if i>1;

[species,err,SI]=NR_method_solution(Asolution,Asolid,Ksolid,Ksolution,T',[species(2:N
x+1)],iterations,criteria);
   end

   for qq=1:Ncp

      [Y,I]=max(SI);

      if Y>1.000000001
         Iindex(qq)=I;
         Asolidtemp(qq,:)=Asolid_SI_check(I,:);
         Ksolidtemp(qq,:)=Ksolid_SI_check(I,:);
```

```
          solidguess(qq)=T(I)*0.5;
         % solidguess(qq)=min(T)*0.015;
          if i>1;
             %if max(solids)>0
             txt=['solidguess(qq)=',SOLIDNAMES(I,:),'(i-1);']; eval(txt);
             %end
          end
          guess=[species(2:Nx+1)' solidguess];

[species,err,SItst,solids]=NR_method(Asolution,Asolidtemp',Ksolidtemp,Ksolution,T',gu
ess',iterations,criteria);
           for q=1:size(solids,1);
             txt=[SOLIDNAMES(Iindex(q),:),'(i)=solids(q);']; eval(txt)
           end
       end

       Q=Asolid*log10(species(2:Nx+1)); SI=10.^(Q+Ksolid); Ifirst=I;

   end

   Q=Asolid*log10(species(2:Nx+1)); SI=10.^(Q+Ksolid);
   SI_summary(i,:)=SI;

   species_summary(i,:)=species;
   mass_err_summary(i,:)=(err(1));

   Asolidtemp=[]; Ksolidtemp=[];

end

for i=1:size(species_summary,2)
   txt=[SOLUTIONNAMES(i,:),'=species_summary(:,i);']; eval(txt)
end

II=[species_summary tenorite malachite CuCO3s CuOH2s];
GG=strvcat(SOLUTIONNAMES,'tenorite','malachite','CuCO3s','CuOH2s');

end

% ---------- NR method solids present

function
[species,err,SI,solids]=NR_method(Asolution,Asolid,Ksolid,Ksolution,T,guess,iterations,
criteria)

Nx=size(Asolution,2); Ncp=size(Asolid,2); Nc=size(Asolution,1); X=guess;
```

```
for II=1:iterations

   Xsolution=X(1:Nx); Xsolid=[]; if Ncp>0; Xsolid=X(Nx+1:Nx+Ncp); end

        logC=(Ksolution)+Asolution*log10(Xsolution); C=10.^(logC); % calc species

   if Ncp>0;
      Rmass=Asolution'*C+Asolid*Xsolid-T;
   end


   if Ncp==0; Rmass=Asolution'*C-T; end % calc residuals in mass balance

   Q=Asolid'*log10(Xsolution); SI=10.^(Q+Ksolid);
   RSI=ones(size(SI))-SI;

        % calc the jacobian

        z=zeros(Nx+Ncp,Nx+Ncp);

        for j=1:Nx;
                for k=1:Nx;
                                for i=1:Nc;
z(j,k)=z(j,k)+Asolution(i,j)*Asolution(i,k)*C(i)/Xsolution(k); end
        end
   end

   if Ncp>0;
   for j=1:Nx;
                for k=Nx+1:Nx+Ncp;
          t=Asolid';
                                z(j,k)=t(k-Nx,j);
        end
   end
   end

   if Ncp>0
   for j=Nx+1:Nx+Ncp;
                for k=1:Nx
                                z(j,k)=-1*Asolid(k,j-Nx)*(SI(j-Nx)/Xsolution(k));
        end
   end
   end

   if Ncp>0
```

```
   for j=Nx+1:Nx+Ncp
      for k=Nx+1:Nx+Ncp
         z(j,k)=0;
      end
   end
   end

   R=[Rmass; RSI]; X=[Xsolution; Xsolid];

   deltaX=z\(-1*R);
   %deltaX=-1*inv(z)*(R);
         one_over_del=max([1, -1*deltaX'./(0.5*X')]);
         del=1/one_over_del;
         X=X+del*deltaX;

   %X=X+deltaX;

         tst=sum(abs(R));
         if tst<=criteria; break; end

end

logC=(Ksolution)+Asolution*log10(Xsolution); C=10.^(logC); % calc species
RSI=ones(size(SI))-SI;

if Ncp>0; Rmass=Asolution'*C+Asolid*Xsolid-T; end % calc residuals in mass balance
if Ncp==0; Rmass=Asolution'*C-T; end % calc residuals in mass balance

err=[Rmass];

species=[C];
solids=Xsolid;

end

% ---------- NR method just solution species

function
[species,err,SI]=NR_method_solution(Asolution,Asolid,Ksolid,Ksolution,T,guess,iteratio
ns,criteria)

Nx=size(Asolution,2); Ncp=size(Asolid,1); Nc=size(Asolution,1); X=guess;

for II=1:iterations

   Xsolution=X(1:Nx);
```

```
        logC=(Ksolution)+Asolution*log10(Xsolution); C=10.^(logC); % calc species

    Rmass=Asolution'*C-T;

    Q=Asolid*log10(Xsolution); SI=10.^(Q+Ksolid);
    RSI=ones(size(SI))-SI;

        % calc the jacobian

        z=zeros(Nx,Nx);

        for j=1:Nx;
            for k=1:Nx;
                for i=1:Nc;
z(j,k)=z(j,k)+Asolution(i,j)*Asolution(i,k)*C(i)/Xsolution(k); end
        end
    end

    R=[Rmass]; X=[Xsolution];

    deltaX=z\(-1*R);
    %deltaX=-1*inv(z)*(R);
        one_over_del=max([1, -1*deltaX'./(0.5*X')]);
        del=1/one_over_del;
        X=X+del*deltaX;

    %X=X+deltaX;

        tst=sum(abs(R));
        if tst<=criteria; break; end

end

logC=(Ksolution)+Asolution*log10(Xsolution); C=10.^(logC); % calc species
RSI=ones(size(SI))-SI;

Q=Asolid*log10(Xsolution); SI=10.^(Q+Ksolid);
RSI=ones(size(SI))-SI;

Rmass=Asolution'*C-T;

err=[Rmass];

species=[C];
```

```
end

% ----- equilib definition ----------

function
[KSOLUTION,KSOLID,ASOLUTION,ASOLID,SOLUTIONNAMES,SOLIDNAMES]
=get_equilib_defn(flag);

logKw=-14.082;
logKh1=-7.982;
logKh1=-7.182;
logBh2=-15.2;
logBh2=-14.8;
logBh3=-27.2;
logBh4=-40.4;
logBh22=-10.98;
pKa1=6.3;
pKa2=10.3;
logKCuCO3=6.77;
%logKCuCO3=6.47;
logKCuCO32=10.2;
logKCuHCO3=1.03;
logKCuCl=0.3;
logKCuTrp=8.29;
pKa1Trp=2.1; %2.35;
pKa2Trp=9.33; %9.33;
logKCuTrp2=15.5;
logKCuHTrp=2.47;

KSOLUTION=[...
    0
    0
    0
    0
    0
    logKw
    logKh1
    logBh2
    logBh3
    logBh4
    logBh22
    pKa2
    pKa2+pKa1
    logKCuCO3
    logKCuCO32
    logKCuHCO3
```

```
    logKCuCl
    logKCuTrp
    pKa2Trp
    pKa2Trp+pKa1Trp
    logKCuTrp2
    logKCuHTrp];

ASOLUTION=[...
   %H     M     CO3   Cl  Trp
    1     0     0     0   0
    0     1     0     0   0
    0     0     1     0   0
    0     0     0     1   0
    0     0     0     0   1
    -1    0     0     0   0
    -1    1     0     0   0
    -2    1     0     0   0
    -3    1     0     0   0
    -4    1     0     0   0
    -2    2     0     0   0
    1     0     1     0   0
    2     0     1     0   0
    0     1     1     0   0
    0     1     2     0   0
    1     1     1     0   0
    0     1     0     1   0
    0     1     0     0   1
    1     0     0     0   1
    2     0     0     0   1
    0     1     0     0   2
    1     1     0     0   1];

SOLUTIONNAMES=strvcat('H','Cu','CO3','Cl','Trp','OH','CuOH','CuOH2','CuOH3','Cu
OH4','Cu2OH2','HCO3','H2CO3','CuCO3aq','CuCO32aq','CuHCO3','CuCl','CuTrp','HTrp
','H2Trp','CuTrp2','CuHTrp');


   % ---------- solid values

   logKsp=-18.7;
   logKcuoh2s=-logKsp+2*logKw;
   logKCuCO3s=11.5;
   logKmalachite=33.18+2*logKw;
   logKmalachite=32.0+2*logKw;
   logKtenorite=20.48+2*logKw;
   if flag==1; logKmalachite=1; end
```

```
    if flag==2; logKtenorite=-100; end
    if flag==3; logKtenorite=-100; logKmalachite=1; end

    logKcuoh2s=-10;
    logKCuCO3s=1;
    %logKtenorite=-100;
    %logKmalachite=1;

    KSOLID=[...
    logKtenorite
    logKmalachite
    logKcuoh2s
    logKCuCO3s];

    ASOLID=[...
     -2     1   0       0  0
     -2     2   1       0  0
     -2     1   0      0   0
     0      1   1      0   0];

  SOLIDNAMES=strvcat('tenorite','malachite','CuOH2s','CuCO3s');


end

% ----------- for fixed pH ----------------

function
[Ksolution,Ksolid,Asolution,Asolid]=get_equilib_fixed_pH(KSOLUTION,KSOLID,AS
OLUTION,ASOLID,pH)

    [N,M]=size(ASOLUTION);
    Ksolution=KSOLUTION-ASOLUTION(:,1)*pH;
    Asolution=[ASOLUTION(:,2:M)];
    [N,M]=size(ASOLID);
    Ksolid=KSOLID-ASOLID(:,1)*pH;
    Asolid=[ASOLID(:,2:M)];

end
```

APPENDIX B

B1. DOC quality of water samples collected

Table B1. Dissolved organic carbon and fluorescent measurements in arbitrary fluorescent units (arb) of humic- (HA), fulvic- (FA), tryptophan- (Trp) and tyrosine-like (Tyr) components of ambient water samples.

Sample Site	Location	DOC (mg C L^{-1})	HA (arb)	FA (arb)	Trp (arb)	Tyr (arb)
Bouctouche	NB	4.36	2.29	0.95	0.033	0.16
Petit Rocher	NB	2.13	0.57	0.50	0.120	0.26
Major Kollock Creek	NB	7.86	4.74	1.53	0.000	0.11
Naufrage Harbour	PEI	5.5	2.89	0.92	0.000	0.03
Rathtrevor Beach	BC	1.52	0.02	0.04	0.004	0.01
Hawke's Bay	NFLD	1.54	0.19	0.29	0.007	0.04
Blackberry Bay	BC	1.45	0.58	0.59	0.042	0.11
Chesterman Beach	BC	0.82	0.09	0.18	0.066	0.11
Jimbo	Miami, FL	1.34	0.21	0.40	0.049	0.10
Bathurst #1	NB	2.21	0.74	0.58	0.031	0.17
Bathhurst #2	NB	3.72	1.76	1.20	0.030	0.23
Shippaggan	NB	2.05	0.59	0.54	0.022	0.13
Salt Marsh S of Shippaggan	NB	3.96	1.46	1.03	0.008	0.15
Neguac	NB	3.93	1.71	1.13	0.000	0.15
Loggiecroft (KB Park)	NB	5.17	3.09	1.60	0.000	0.11
Escuminac	NB	3.41	1.45	0.95	0.000	0.12
Baie Sainte Anne	NB	3.91	2.44	1.56	0.000	0.14
St Peters Harbour	PEI	2.42	0.76	0.59	0.060	0.15
St Peters Bay	PEI	2.39	1.11	0.84	0.021	0.13
North Lake	PEI	2.43	1.32	0.73	0.000	0.12

Ryan’s (KB Park)	NB	2.96	1.82	1.05	0.000	0.10
Richibucto	NB	2.59	1.26	0.91	0.056	0.17
Bouchtouche (BT)	NB	3.27	1.30	1.04	0.016	0.14
Little BT River	NB	2.84	1.12	0.88	0.022	0.13
Cocagne	NB	2.90	1.42	1.07	0.000	0.12
Grande Digue	NB	4.29	2.16	1.62	0.000	0.11
Port Alberni	BC	0.62	0.09	0.19	0.027	0.10
Longbeach Incinerator Rock	BC	2.08	0.12	0.28	0.009	0.10

B2. Effects of salinity adjustment on LC_{50}

Three water samples were chosen to measure toxicity at ambient salinity and after salinity adjustment to observe whether the LC_{50} is significantly affected by salinity adjustment to 30 ppt. These samples were chosen to represent low, mid and high salinity before adjustment. The results of the toxicity assays are shown Table B1. For Bouctouche and Naufrage Harbour which represented the low and high ambient salinities, there was no significant difference in LC_{50} before and after salinity adjustment. Major Kollock Creek, with a mid-range ambient salinity of 12.8 ppt did show a significant difference in LC_{50} values before and after salinity adjustment. The ambient salinity was significantly more protective than the salted up sample. These results suggest LC_{50} may be influenced by the salting up of the water samples to 30 ppt. However, the data shown here suggest a site-specific influence on salting up and change in LC_{50}.

Table B2. Copper LC_{50} to *Brachionus plicatilis* before and after salinity adjustment.

Sample	**Salinity (ppt)**		**LC_{50} (nM)**	
	Before	After	Before	After
Bouctouche	19.1	30.1	686 (602-785)	662 (589-748)
Major Kollock Creek	12.8	29.9	1247 (1104-1416)	980 (883-1087)
Naufrage Harbour	4.3	30.1	862 (740-1013)	725 (647-813)

B3. Contour plots for sampling sites used in toxicity assays

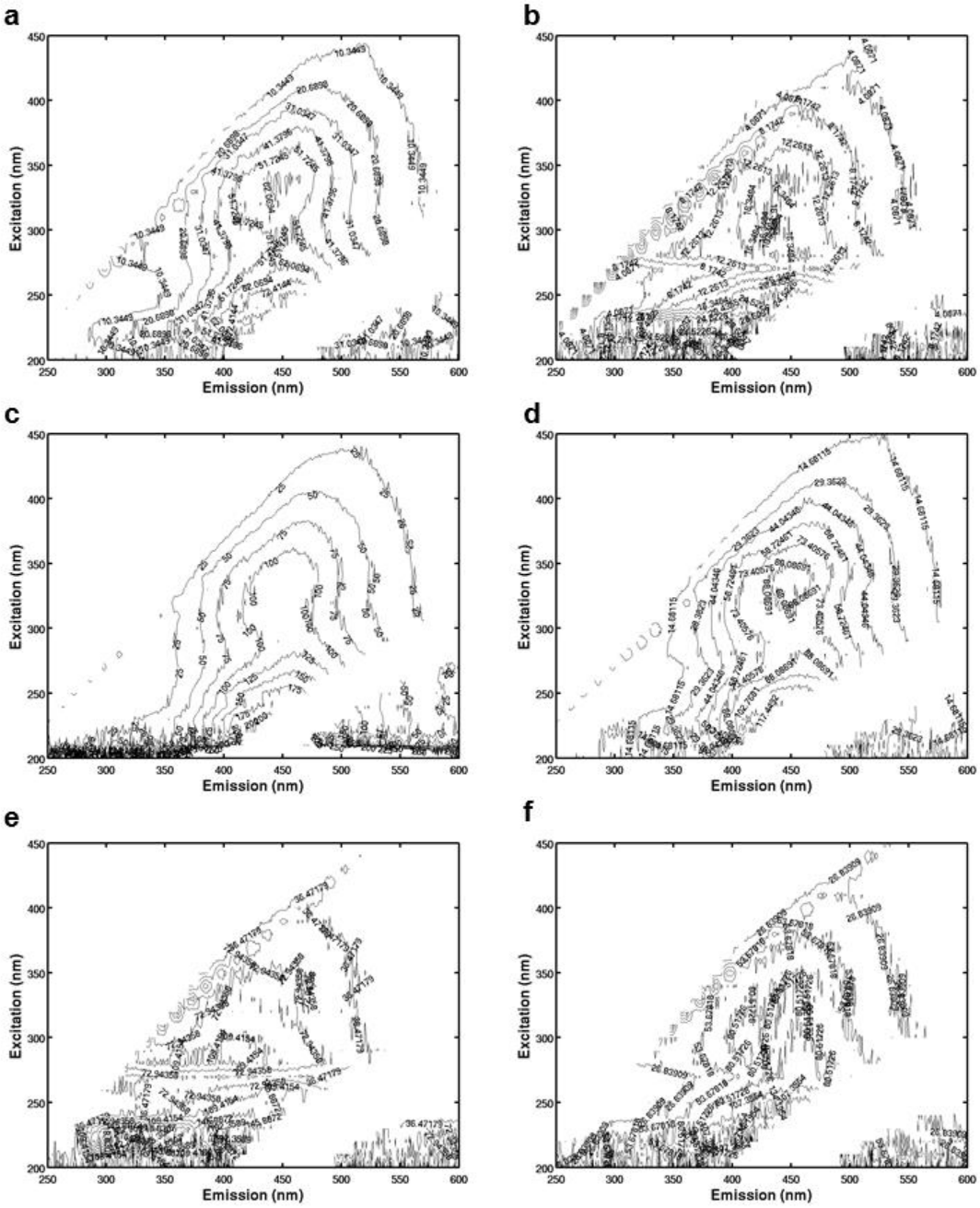

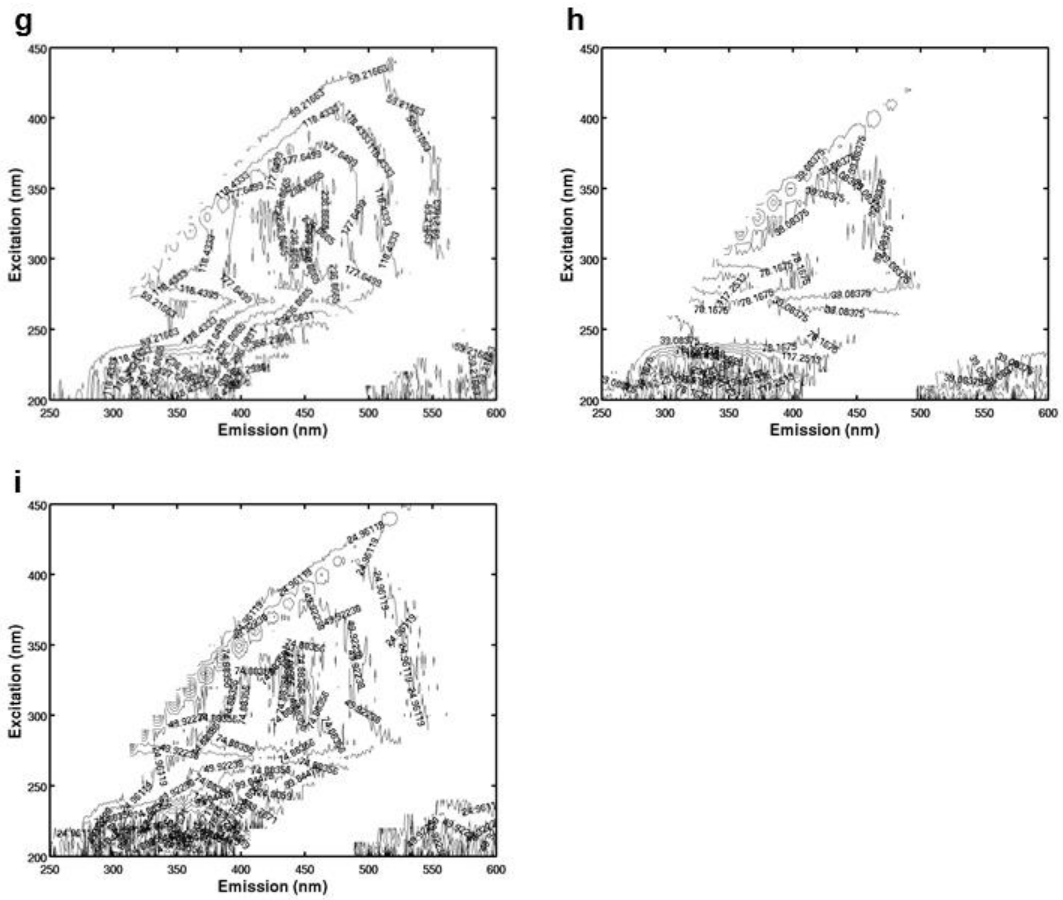

Figure B1. Fluorescence excitation-emission contour plots for a. Bouctouche, b. Petit Rocher, c. Major Kollock Creek, d. Naufrage Harbour, e. Rathtrevor Beach, f. Hawke's Bay, g. Blackberry Bay, h. Chesterman Beach, and i. Jimbo.

APPENDIX C

C1. MATLAB script for determining contribution of fluorophores to total fluorescence during fluorescence quenching titrations with copper

```
function II=Quenching_fitting_HB_4_components

global humicspeci Tyrspeci Trpspeci fulvicspeci

figure(1); clf;

load /home/clear/Desktop/Tara_PARAFAC_and_Quenching/TaraFinalfour.mat

%ex of 270 nm is the 8th excitation wavelength in the surfaces for each component

humicspec=surf1(8,:); % determined which is which by looking at spec
Tyrspec=surf4(8,:); % determined which is which by looking at spec
Trpspec=surf3(8,:);% determined which is which by looking at spec
fulvicspec=surf2(8,:);

plot(em,humicspec,'b',em,Tyrspec,'g',em,Trpspec,'r',em,fulvicspec,'m','linewidth',2)
set(gca,'fontsize',14,'linewidth',2)
xlabel('emission wavelength (nm)','fontsize',14)
ylabel('Fluorescence intensity (arb)','fontsize',14)

print fourcomponentEMspec.eps -depsc2
print fourcomponentEMspec.png -dpng

% now want to load the data from the quenching expt.

lowEM=250; highEM=600; % need to specify range of data
scatter=270*2; scatterwidth=25; % need to specify the scatter data to NaN

[CuT,EM,F]=getquenchingdata(lowEM,highEM,scatter,scatterwidth);

%plot(EM,F)

% need to interpolate so same em for model spec components as for
% measurements

humicspeci=interp1(em,humicspec,EM,'spline',0);
Tyrspeci=interp1(em,Tyrspec,EM,'spline',0);
Trpspeci=interp1(em,Trpspec,EM,'spline',0);
fulvicspeci=interp1(em,fulvicspec,EM,'spline',0);
```

```
beta0=log10([20000 5000 5000 20000]); % initial guess and log so force positive values
betatst=10.^beta0;
%
Ftst=betatst(1)*humicspeci+betatst(2)*Tyrspeci+betatst(3)*Trpspeci+betatst(4)*fulvicsp
eci;
%
figure(1); clf;
plot(EM,F(:,1),'ko','markersize',4)
hold on
plot(EM,Ftst,'k','linewidth',2)
plot(EM,betatst(1)*humicspeci,'b--','linewidth',2)
plot(EM,betatst(2)*Tyrspeci,'g--','linewidth',2)
plot(EM,betatst(3)*Trpspeci,'r--','linewidth',2)
plot(EM,betatst(4)*fulvicspeci,'m--','linewidth',2)

[beta,resid,J,Sigma,mse] = nlinfit(EM,F(:,1),@linearmodel,beta0);

rBETA=10.^beta;

Ftst=rBETA(1)*humicspeci+rBETA(2)*Tyrspeci+rBETA(3)*Trpspeci+rBETA(4)*fulvi
cspeci;

figure(1); clf;
plot(EM,F(:,1),'ko','markersize',2,'markerfacecolor','b')
hold on
plot(EM,Ftst,'k','linewidth',2)
plot(EM,rBETA(1)*humicspeci,'b--','linewidth',2)
plot(EM,rBETA(2)*Tyrspeci,'g--','linewidth',2)
plot(EM,rBETA(3)*Trpspeci,'r--','linewidth',2)
plot(EM,rBETA(4)*fulvicspeci,'m--','linewidth',2)

set(gca,'fontsize',14,'linewidth',2)
xlabel('emission wavelength (nm)','fontsize',14)
ylabel('Fluorescence intensity (arb)','fontsize',14)

print example4fit.eps -depsc2
print example4fit.png -dpng

% now fit them all

for i=1:size(CuT,2)
   [beta,resid,J,Sigma,mse] = nlinfit(EM,F(:,i),@linearmodel,beta0);
   betas(i,:)=10.^beta;
end

figure(1); clf
```

```
subplot(221); plot(CuT,betas(:,1),'ko','markersize',8,'markerfacecolor','b')
hold on;
subplot(222); plot(CuT,betas(:,2),'ko','markersize',8,'markerfacecolor','g')
subplot(223); plot(CuT,betas(:,3),'ko','markersize',8,'markerfacecolor','r')
subplot(224); plot(CuT,betas(:,4),'ko','markersize',8,'markerfacecolor','m')

set(gca,'fontsize',14,'linewidth',2)
xlabel('emission wavelength (nm)','fontsize',14)
ylabel('CuT (ppb)','fontsize',14)

print RW4plot.png -dpng

display=[betas]

II=1; % to complete syntax of the function

end



function II=linearmodel(beta,EM)

global humicspeci Tyrspeci Trpspeci fulvicspeci

k1=10^beta(1); k2=10^beta(2); k3=10^beta(3); k4=10^beta(4);

Fmodel=humicspeci*k1+Tyrspeci*k2+k3*Trpspeci+k4*fulvicspeci;

II=Fmodel;

end


function [CuT,EM,F]=getquenchingdata(EMlow,EMhigh,scatter,scatterwidth)

data=[...
```

Quenching Data inserted here

```
];

[N,M]=size(data); c=0;

CuT=data(1,2:M);
EM=data(2:N,1);
```

```
F=data(2:N,2:M);

for i=1:size(EM,1)
  EMtst=EM(i);
  if EMtst>=EMlow;
     if EMtst<=EMhigh;
        c=c+1;
        EMM(c)=EM(i);
        f(c,:)=F(i,:);
     end
  end
end

EM=EMM'; F=f;

for i=1:size(EM,1)
   EMtst=EM(i);
   if EMtst>=scatter-scatterwidth
      if EMtst<=scatter+scatterwidth
         F(i,:)=NaN*ones(size(F(i,:)))
      end
   end
end

end
```

C2. MATLAB script for Ryan-Weber fitting combined with modeling free copper

```
function II=testBT_2D

figure(1); clf;
pH=8.0;
p2run=[ 9.8558    9.8213   -6.6461   -5.9737   -0.1394   -0.0954]
% error -3.6348 delta -0.1597

logK1=p2run(1); logK2=p2run(2);
LT1=10^p2run(3); LT2=10^p2run(4);
lessefficient1=10^p2run(5); lessefficient2=10^p2run(6);

flag=2;
%lessefficient1=0.5; lessefficient2=0.702; flag=3; % flag for solid species
% flag=2 malachite only
% flag=1 tenorite only
% flag=3 no ppte

[CuT,F1meas, F2meas]=returndata; % note CuT=0 replaced by 0.01 ppb.  can't have zero
value in equilib solver.
% need to replace with measured CuT.

CuTplot=[1e-8:0.05e-6:max(CuT)*1.1]; CuT=CuT';

[L1,CuL1,L2,CuL2,Cu]=Cu_seawater_calculate_fluorescence_two_ligand(CuTplot,pH,l
ogK1,logK2,LT1,LT2,flag);

n=size(F1meas,1); constantF=0; %constantF=1.4;
k11=mean(F1meas(1:3)-constantF)/LT1; %k12=mean(F1meas(n-2:n)-constantF)/LT1;
%k12=0;
k12=lessefficient1*k11;
F1calc=k11*L1+k12*CuL1+constantF;

n=size(F2meas,1); constantF=0; %constantF=0.64;
k21=mean(F2meas(1:3)-constantF)/LT2; %k22=mean(F2meas(n-2:n)-constantF)/LT2;
%k22=0;
k22=lessefficient2*k21;
F2calc=k21*L2+k22*CuL2+constantF;

figure(1); %subplot(221)
plot(CuT,F1meas,'ko',CuTplot,F1calc,'b--
','markersize',8,'markerfacecolor','b','linewidth',2)
set (gca, 'linewidth', 2, 'fontsize', 16)
xlabel ('Cu_T (M)', 'fontsize', 16, 'fontweight', 'bold')
```

```
ylabel ('Fluorescence (arb)', 'fontsize', 16, 'fontweight', 'bold')

figure(2); %subplot(222)
plot(CuT,F2meas,'ko',CuTplot,F2calc,'r--
','markersize',8,'markerfacecolor','r','linewidth',2)
set (gca, 'linewidth', 2, 'fontsize', 16)
xlabel ('Cu_T (M)', 'fontsize', 16, 'fontweight', 'bold')
ylabel ('Fluorescence (arb)', 'fontsize', 16, 'fontweight', 'bold')

figure(3); %subplot(223)
plot(CuTplot,log10(Cu),'k--','linewidth',2)
LC50=662e-9; freeCuatLC50=10^(-9.98);
hold on
plot(LC50,log10(freeCuatLC50),'ko','markersize',10,'markerfacecolor','b')
set (gca, 'linewidth', 2, 'fontsize', 16)
xlabel ('Cu_T (M)', 'fontsize', 16, 'fontweight', 'bold')
ylabel ('log[Cu^{2+}]', 'fontsize', 16, 'fontweight', 'bold')

% now fitting

pguess=[logK1 logK2 log10(LT1) log10(LT2) log10(lessefficient1)
log10(lessefficient2)];
lbfactor=0.8; ubfactor=1.2;
LBfactor=[lbfactor lbfactor   1/lbfactor 1/lbfactor 1/lbfactor 1/lbfactor];
UBfactor=[ubfactor ubfactor  1/ubfactor 1/ubfactor 1/ubfactor 1/ubfactor];
lb=LBfactor.*pguess;
ub=UBfactor.*pguess;
%lb=[6 6]; %lb=[];
%ub=[10 10]; %ub=[];
%options = optimset(@fmincon);
options = optimset(@fminunc);
%options = optimset(@fminsearch);
%options = optimset(options,'Display','iter','TolFun',1e-6,'TolX',1e-
6,'MaxFunEvals',1000,'TolCon',0.3,'ScaleProblem','obj-and-constr');
options = optimset(options,'Display','iter','TolFun',1e-4,'TolX',1e-
4,'MaxFunEvals',1000,'ScaleProblem','obj-and-constr');

%x = fmincon(@myfun,x0,A,b,Aeq,beq,lb,ub,@mycon)
%[p2] = fmincon(@returnFerr,pguess,[],[],[],[],lb,ub,[],options,CuT',F1,F2,pH,flag)

f = @(p)returnFerr(p,CuT,F1meas,F2meas,pH,flag);
c = @(p)mycon(p,662e-9,pH,flag);
t=f(pguess)
[tc,tcc]=myconreal(pguess,662e-9,pH,flag)

pause
```

```
 [p2] = fminunc(f,pguess,options)
%[p2]=fminsearch(f,pguess,options)
%p2 = fmincon(f,pguess,[],[],[],[],lb,ub,c,options)

t=f(p2)
[tc,tcc]=myconreal(p2,662e-9,pH,flag)

logK1=p2(1); logK2=p2(2); LT1=10^p2(3); LT2=10^p2(4); lessefficient1=10^p2(5);
lessefficient2=10^p2(6);

[L1,CuL1,L2,CuL2,Cu]=Cu_seawater_calculate_fluorescence_two_ligand(CuTplot,pH,l
ogK1,logK2,LT1,LT2,flag);

n=size(F1meas,1); constantF=0; %constantF=1.4;
k11=mean(F1meas(1:3)-constantF)/LT1; %k12=mean(F1meas(n-2:n)-constantF)/LT1;
%k12=0;
k12=lessefficient1*k11;
F1calc=k11*L1+k12*CuL1+constantF;

n=size(F2meas,1); constantF=0; %constantF=0.64;
k21=mean(F2meas(1:3)-constantF)/LT2; %k22=mean(F2meas(n-2:n)-constantF)/LT2;
%k22=0;
k22=lessefficient2*k21;
F2calc=k21*L2+k22*CuL2+constantF;

figure(1); subplot(221); hold on
plot(CuTplot,F1calc,'linewidth',2)

figure(1); subplot(222); hold on
plot(CuTplot,F2calc,'r','linewidth',2)

figure(1); subplot(223); hold on
plot(CuTplot,log10(Cu),'k','linewidth',2)

end

function II=returnFerr(p,CuT,F1meas,F2meas,pH,flag)

logK1=p(1); logK2=p(2); LT1=10^p(3); LT2=10^p(4); lessefficient1=10^p(5);
lessefficient2=10^p(6);
%LT1=5e-6; LT2=2e-6;

[L1,CuL1,L2,CuL2,Cu]=Cu_seawater_calculate_fluorescence_two_ligand(CuT,pH,logK
1,logK2,LT1,LT2,flag);
```

```
n=size(F1meas,1); constantF=0; %constantF=1.4;
k11=mean(F1meas(1:3)-constantF)/LT1; %k12=mean(F1meas(n-2:n)-constantF)/LT1;
%k12=0;
k12=lessefficient1*k11;
F1calc=k11*L1+k12*CuL1+constantF;

n=size(F2meas,1); constantF=0; %constantF=0.64;
k21=mean(F2meas(1:3)-constantF)/LT2; %k22=mean(F2meas(n-2:n)-constantF)/LT2;
%k22=0;
k22=lessefficient2*k21;
F2calc=k21*L2+k22*CuL2+constantF;

residuals=[F1meas-F1calc' F2meas-F2calc'];

II=log10(det(residuals'*residuals));
%II=(det(residuals'*residuals));

end

function
[II,GG,HH,QQ,RR]=Cu_seawater_calculate_fluorescence_two_ligand(CuT,pH,logK1,lo
gK2,LT1,LT2,flag)

%CuT=1e-7:5e-7:10e-6; pH=8.2; logK1=8; LT1=1e-6; flag=3; % flag for solid species
% flag=2 malachite only
% flag=1 tenorite only
% flag=3 no ppte

[species,
names]=Cu_seawater_species_two_ligand(CuT,pH,logK1,logK2,LT1,LT2,flag);

for i=1:size(CuT,2)
for j=1:size(species,2)
      txt=[names(j,:),'(i)=species(i,j);'];
      eval(txt)
end
end

%plot(CuT,L1,'ko')

II=L1; GG=CuL1; HH=L2; QQ=CuL2; RR=Cu;

end

function [II,GG]=Cu_seawater_species_two_ligand(CuT,pH,logK1,logK2,LT1,LT2,flag)
```

```
warning('off')

% seawater concentrations

ClT=0.6;
NaHCO3=200; %mg/L from recipe
NaHCO3AW=100; %g/mol
CT=(NaHCO3*1e-3)/NaHCO3AW;

[KSOLUTION,KSOLID,ASOLUTION,ASOLID,SOLUTIONNAMES,SOLIDNAMES]
=get_equilib_defn(logK1,logK2,flag);
% flag determines what solids can form.

numpts=size(CuT,2);
Ncp=size(ASOLID,1);
solid_summary=zeros(numpts,Ncp);

for i=1:size(SOLIDNAMES,1)
   txt=[SOLIDNAMES(i,:),'=zeros(numpts,1);']; eval(txt)
end

for i=1:size(CuT,2)

   % adjust for fixed pH


[Ksolution,Ksolid,Asolution,Asolid]=get_equilib_fixed_pH(KSOLUTION,KSOLID,AS
OLUTION,ASOLID,pH);

   Asolid_SI_check=Asolid; Ksolid_SI_check=Ksolid;

   % number of different species
   Nx=size(Asolution,2); Ncp=size(Asolid,1); Nc=size(Asolution,1);

   % initial guess
   Cu_guess=[-10.5]; CuOH2s_guess=0.1*CuT(i);  CuCO3s_guess=0.1*CT;
   guess=[10.^Cu_guess CT./10 CuOH2s_guess CuCO3s_guess]; iterations=1000;
criteria=1e-16;
   T=[CuT(i) CT ClT LT1 LT2]; guess=T./10;

   % calculate species using NR

   solids=zeros(1,Ncp);
```

```
   if i==1;
[species,err,SI]=NR_method_solution(Asolution,Asolid,Ksolid,Ksolution,T',[guess(1:Nx
)]',iterations,criteria); end
   if i>1;

[species,err,SI]=NR_method_solution(Asolution,Asolid,Ksolid,Ksolution,T',[species(2:N
x+1)],iterations,criteria);
   end

   for qq=1:Ncp

      [Y,I]=max(SI);

      if Y>1.000000001
         Iindex(qq)=I;
         Asolidtemp(qq,:)=Asolid_SI_check(I,:);
         Ksolidtemp(qq,:)=Ksolid_SI_check(I,:);
         solidguess(qq)=T(I)*0.5;
        % solidguess(qq)=min(T)*0.015;
         if i>1;
            %if max(solids)>0
            txt=['solidguess(qq)=',SOLIDNAMES(I,:),'(i-1);']; eval(txt);
            %end
         end
         guess=[species(2:Nx+1)' solidguess];

[species,err,SItst,solids]=NR_method(Asolution,Asolidtemp',Ksolidtemp,Ksolution,T',gu
ess',iterations,criteria);
          for q=1:size(solids,1);
            txt=[SOLIDNAMES(Iindex(q),:),'(i)=solids(q);']; eval(txt)
          end
      end

      Q=Asolid*log10(species(2:Nx+1)); SI=10.^(Q+Ksolid); Ifirst=I;

   end

   Q=Asolid*log10(species(2:Nx+1)); SI=10.^(Q+Ksolid);
   SI_summary(i,:)=SI;

   species_summary(i,:)=species;
   mass_err_summary(i,:)=(err(1));

   Asolidtemp=[]; Ksolidtemp=[];

end
```

```
for i=1:size(species_summary,2)
   txt=[SOLUTIONNAMES(i,:),'=species_summary(:,i);']; eval(txt)
end

II=[species_summary tenorite malachite CuCO3s CuOH2s];
GG=strvcat(SOLUTIONNAMES,'tenorite','malachite','CuCO3s','CuOH2s');


end

% -------------------- NR method solids present

function
[species,err,SI,solids]=NR_method(Asolution,Asolid,Ksolid,Ksolution,T,guess,iterations,
criteria)

Nx=size(Asolution,2); Ncp=size(Asolid,2); Nc=size(Asolution,1); X=guess;

for II=1:iterations

   Xsolution=X(1:Nx); Xsolid=[]; if Ncp>0; Xsolid=X(Nx+1:Nx+Ncp); end

        logC=(Ksolution)+Asolution*log10(Xsolution); C=10.^(logC); % calc species

   if Ncp>0;
      Rmass=Asolution'*C+Asolid*Xsolid-T;
   end


   if Ncp==0; Rmass=Asolution'*C-T; end % calc residuals in mass balance

   Q=Asolid'*log10(Xsolution); SI=10.^(Q+Ksolid);
   RSI=ones(size(SI))-SI;

        % calc the jacobian

        z=zeros(Nx+Ncp,Nx+Ncp);

        for j=1:Nx;
                for k=1:Nx;
                                for i=1:Nc;
z(j,k)=z(j,k)+Asolution(i,j)*Asolution(i,k)*C(i)/Xsolution(k); end
        end
   end
```

```
    if Ncp>0;
    for j=1:Nx;
                    for k=Nx+1:Nx+Ncp;
              t=Asolid';
                                        z(j,k)=t(k-Nx,j);
          end
    end
    end

    if Ncp>0
    for j=Nx+1:Nx+Ncp;
                    for k=1:Nx
                                        z(j,k)=-1*Asolid(k,j-Nx)*(SI(j-Nx)/Xsolution(k));
          end
    end
    end

    if Ncp>0
    for j=Nx+1:Nx+Ncp
       for k=Nx+1:Nx+Ncp
          z(j,k)=0;
       end
    end
    end

    R=[Rmass; RSI]; X=[Xsolution; Xsolid];

    deltaX=z\(-1*R);
    %deltaX=-1*inv(z)*(R);
          one_over_del=max([1, -1*deltaX'./(0.5*X')]);
          del=1/one_over_del;
          X=X+del*deltaX;

    %X=X+deltaX;

          tst=sum(abs(R));
          if tst<=criteria; break; end

end

logC=(Ksolution)+Asolution*log10(Xsolution); C=10.^(logC); % calc species
RSI=ones(size(SI))-SI;

if Ncp>0; Rmass=Asolution'*C+Asolid*Xsolid-T; end % calc residuals in mass balance
if Ncp==0; Rmass=Asolution'*C-T; end % calc residuals in mass balance
```

```
err=[Rmass];

species=[C];
solids=Xsolid;

end

% ----------- NR method just solution species

function
[species,err,SI]=NR_method_solution(Asolution,Asolid,Ksolid,Ksolution,T,guess,iteratio
ns,criteria)

Nx=size(Asolution,2); Ncp=size(Asolid,1); Nc=size(Asolution,1); X=guess;

for II=1:iterations

   Xsolution=X(1:Nx);

        logC=(Ksolution)+Asolution*log10(Xsolution); C=10.^(logC); % calc species

   Rmass=Asolution'*C-T;

   Q=Asolid*log10(Xsolution); SI=10.^(Q+Ksolid);
   RSI=ones(size(SI))-SI;

        % calc the jacobian

        z=zeros(Nx,Nx);

        for j=1:Nx;
                for k=1:Nx;
                                for i=1:Nc;
z(j,k)=z(j,k)+Asolution(i,j)*Asolution(i,k)*C(i)/Xsolution(k); end
        end
   end

   R=[Rmass]; X=[Xsolution];

   deltaX=z\(-1*R);
   %deltaX=-1*inv(z)*(R);
        one_over_del=max([1, -1*deltaX'./(0.5*X')]);
        del=1/one_over_del;
        X=X+del*deltaX;

   %X=X+deltaX;
```

```
        tst=sum(abs(R));
        if tst<=criteria; break; end

end

logC=(Ksolution)+Asolution*log10(Xsolution); C=10.^(logC); % calc species
RSI=ones(size(SI))-SI;

Q=Asolid*log10(Xsolution); SI=10.^(Q+Ksolid);
RSI=ones(size(SI))-SI;

Rmass=Asolution'*C-T;

err=[Rmass];

species=[C];

end



% ----- equilib definition ----------

function
[KSOLUTION,KSOLID,ASOLUTION,ASOLID,SOLUTIONNAMES,SOLIDNAMES]
=get_equilib_defn(logK1,logK2,flag);

logKw=-14.082;
logKh1=-7.982;
logKh1=-7.182;
logBh2=-15.2;
logBh2=-14.8;
logBh3=-27.2;
logBh4=-40.4;
logBh22=-10.98;
pKa1=6.3;
pKa2=10.3;
logKCuCO3=6.77;
%logKCuCO3=6.47;
logKCuCO32=10.2;
logKCuHCO3=1.03;
logKCuCl=0.3;
logKCuL1=logK1;
logKCuL2=logK2;
```

```
KSOLUTION=[...
    0
    0
    0
    0
    0
    0
    logKw
    logKh1
    logBh2
    logBh3
    logBh4
    logBh22
    pKa2
    pKa2+pKa1
    logKCuCO3
    logKCuCO32
    logKCuHCO3
    logKCuCl
    logKCuL1
    logKCuL2];

ASOLUTION=[...
   %H     M     CO3   Cl  L1  L2
    1     0     0     0   0   0
    0     1     0     0   0   0
    0     0     1     0   0   0
    0     0     0     1   0   0
    0     0     0     0   1   0
    0     0     0     0   0   1
    -1    0     0     0   0   0
    -1    1     0     0   0   0
    -2    1     0     0   0   0
    -3    1     0     0   0   0
    -4    1     0     0   0   0
    -2    2     0     0   0   0
    1     0     1     0   0   0
    2     0     1     0   0   0
    0     1     1     0   0   0
    0     1     2     0   0   0
    1     1     1     0   0   0
    0     1     0     1   0   0
    0     1     0     0   1   0
    0     1     0     0   0   1];
```

```
SOLUTIONNAMES=strvcat('H','Cu','CO3','Cl','L1','L2','OH','CuOH','CuOH2','CuOH3','
CuOH4','Cu2OH2','HCO3','H2CO3','CuCO3aq','CuCO32aq','CuHCO3','CuCl','CuL1','Cu
L2');


   % ---------- solid values

   logKsp=-18.7;
   logKcuoh2s=-logKsp+2*logKw;
   logKCuCO3s=11.5;
   logKmalachite=33.18+2*logKw;
   logKmalachite=32.0+2*logKw;
   logKtenorite=20.48+2*logKw;
   if flag==1; logKmalachite=1; end
   if flag==2; logKtenorite=-100; end
   if flag==3; logKtenorite=-100; logKmalachite=1; end

   logKcuoh2s=-10;
   logKCuCO3s=1;
   %logKtenorite=-100;
   %logKmalachite=1;

   KSOLID=[...
   logKtenorite
   logKmalachite
   logKcuoh2s
   logKCuCO3s];

   ASOLID=[...
    -2     1   0      0  0 0
    -2     2   1      0  0 0
    -2     1   0      0   0 0
    0      1   1      0   0 0];

 SOLIDNAMES=strvcat('tenorite','malachite','CuOH2s','CuCO3s');


end

% ----------- for fixed pH ----------------

function
[Ksolution,Ksolid,Asolution,Asolid]=get_equilib_fixed_pH(KSOLUTION,KSOLID,AS
OLUTION,ASOLID,pH)

   [N,M]=size(ASOLUTION);
```

```
    Ksolution=KSOLUTION-ASOLUTION(:,1)*pH;
    Asolution=[ASOLUTION(:,2:M)];
    [N,M]=size(ASOLID);
    Ksolid=KSOLID-ASOLID(:,1)*pH;
    Asolid=[ASOLID(:,2:M)];

end

function [MT,F1,F2]=returndata

% BT data

data=[...
%       Humic Fulvic  Tyr      Trp
0.01    3.6139 0.7321 0.6127 0.2414
9.99    3.3868 0.7062 0.6823 0.2871
29.9    3.1425 0.6647 0.6311 0.2053
59.6    2.8862 0.6281 0.6017 0.1281
99      2.6422 0.6102 0.582   0.1037
% 138.1        2.4727 0.5915 0.5852 0.0889
% 186.5        2.3094 0.5687 0.5678 0.0702
% 234.4        2.1965 0.545   0.5622 0.073
% 291.3        2.0608 0.5264 0.5755 0.1107
% 347.5        1.9673 0.5665 0.6333 0.1481
0.01    3.672   0.7538 0.6637 0.5073
9.99    3.4398 0.7104 0.7338 0.724
29.9    3.1916 0.6757 0.7053 0.6178
59.6    2.9207 0.6512 0.6726 0.5436
99      2.7041 0.6235 0.6685 0.5763
% 138.1        2.513   0.6234 0.6425 0.4652
% 186.5        2.3577 0.5857 0.6249 0.4913
% 234.4        2.218   0.5671 0.6345 0.4695
% 291.3        2.1269 0.5578 0.653   0.4415
% 347.5        2.0218 0.5509 0.6711 0.436
% 403.1        1.9008 0.5699 0.6676 0.3396
0.01    3.434   0.7024 0.6416 0.4035
9.99    3.2329 0.6677 0.6449 0.4041
29.9    3.0366 0.6138 0.62     0.4474
59.6    2.8426 0.6006 0.6198 0.4395
99      2.6294 0.5797 0.5999 0.3948
% 138.1        2.472   0.5642 0.5879 0.3711
% 186.5        2.3653 0.5617 0.6198 0.3898
% 234.4        2.21     0.5394 0.5979 0.3308
% 291.3        2.0911 0.5268 0.6049 0.3103
% 347.5        1.978   0.5192 0.6207 0.2818
% 403.1        1.8896 0.5057 0.6285 0.2659
```

```
];

MT=data(:,1); % ppb conc of Cu
MT=(MT*1e-6)./63.5463;
humic=data(:,2);
% fulvic=data(:,4);
fulvic=data(:,3);
% tyr=data(:,3);
tyr=data(:,4);
trp=data(:,5);

subdata=[MT humic fulvic trp];
sortdata=sortrows(subdata,1);

MT=sortdata(:,1);
F1=sortdata(:,2);
F2=sortdata(:,3);
F3=sortdata(:,4);

end

function [c,ceq] = mycon(p,CuT,pH,flag)

logK1=p(1); logK2=p(2); LT1=10^p(3); LT2=10^p(4);

[species,
names]=Cu_seawater_species_two_ligand(CuT,pH,logK1,logK2,LT1,LT2,flag);

for i=1:size(CuT,2)
for j=1:size(species,2)
      txt=[names(j,:),'(i)=species(i,j);'];
      eval(txt)
end
end

c = [];     % Compute nonlinear inequalities at x.
testceq = [(-9.98-log10(Cu))];   % Compute nonlinear equalities at x.
if abs(testceq)<=0.3; testceq=0; end
ceq=testceq;
%ceq = [(-9.98-log10(Cu))];
end

function [c,ceq] = myconreal(p,CuT,pH,flag)

logK1=p(1); logK2=p(2); LT1=10^p(3); LT2=10^p(4);
```

```
[species,
names]=Cu_seawater_species_two_ligand(CuT,pH,logK1,logK2,LT1,LT2,flag);

for i=1:size(CuT,2)
for j=1:size(species,2)
      txt=[names(j,:),'(i)=species(i,j);'];
      eval(txt)
end
end

c = [];     % Compute nonlinear inequalities at x.
ceq = [(-9.98-log10(Cu))];
end
```

C3. Plots of contribution of fluorophores to total fluorescence

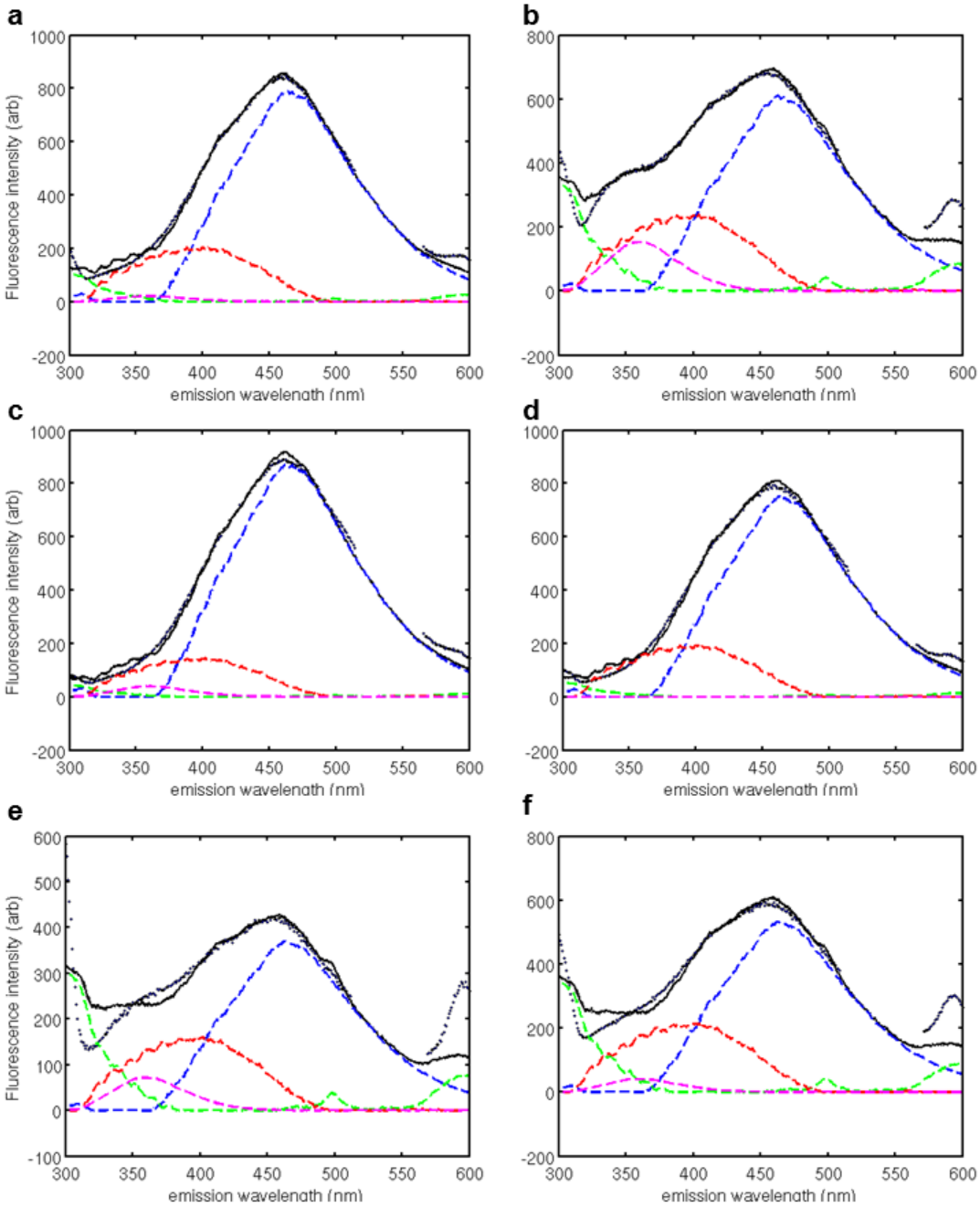

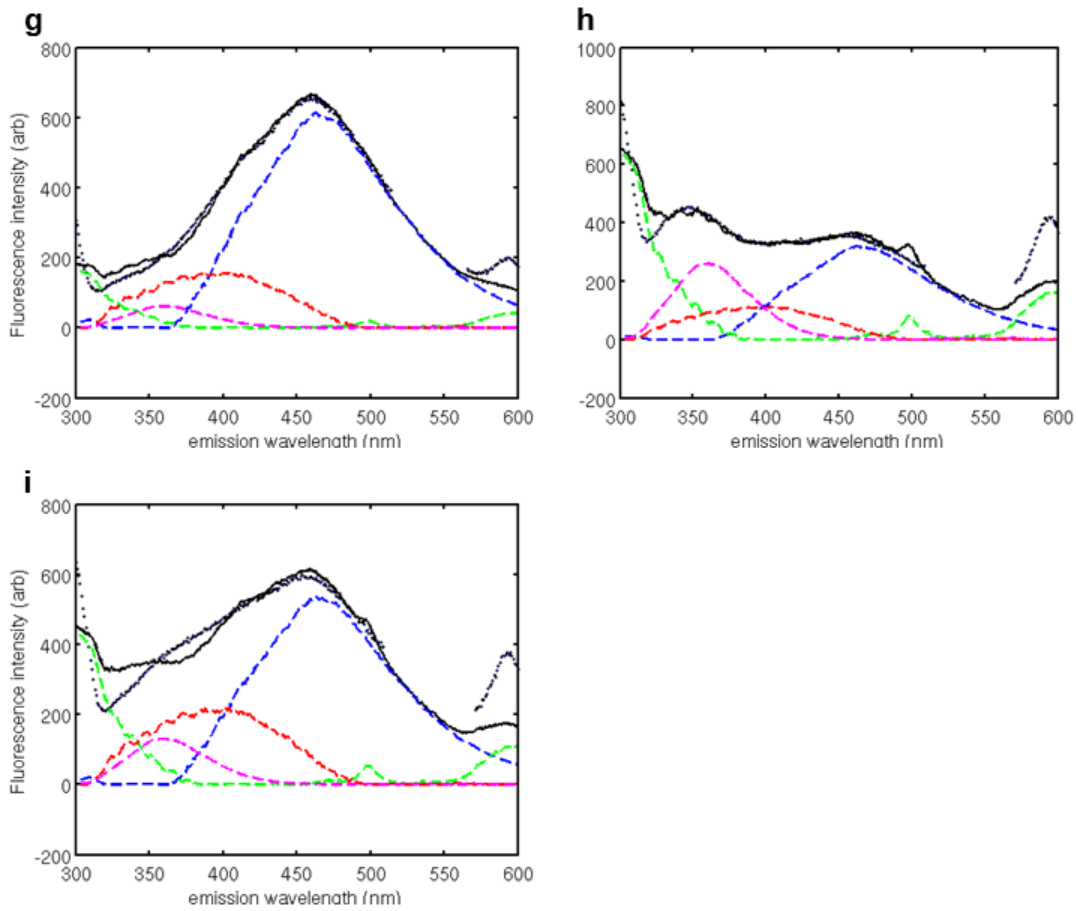

Figure C1. Contribution of humic- (blue), fulvic (red), tryptophan (pink), and tyrosine (green) fractions to total fluorescence in a. Bouctouche, b. Petit Rocher, c. Major Kollock Creek, d. Naufrage Harbour, e. Rathtrevor Beach, f. Hawke's Bay, g. Blackberry Bay, h. Chesterman Beach, and i. Jimbo. Dotted black line is the measured fluorescence while the solid black line is the modeled curve to determine fluorophore contributions.

C4. Resolved fluorescence quenching curves with Ryan-Weber fitting

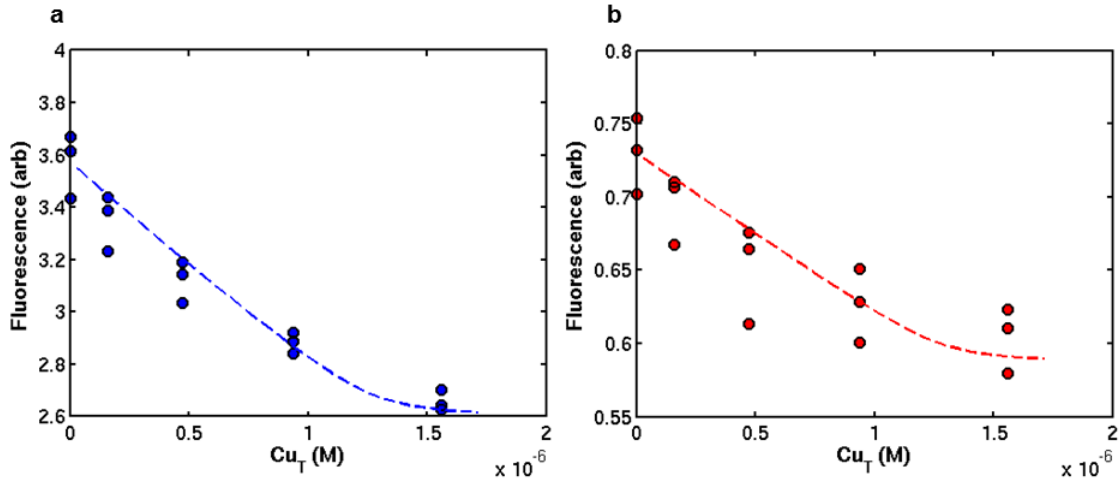

Figure C2. Resolved quenching curves with Ryan-Weber fitting for a. humic- and b. fulvic-like fractions of Bouctouche.

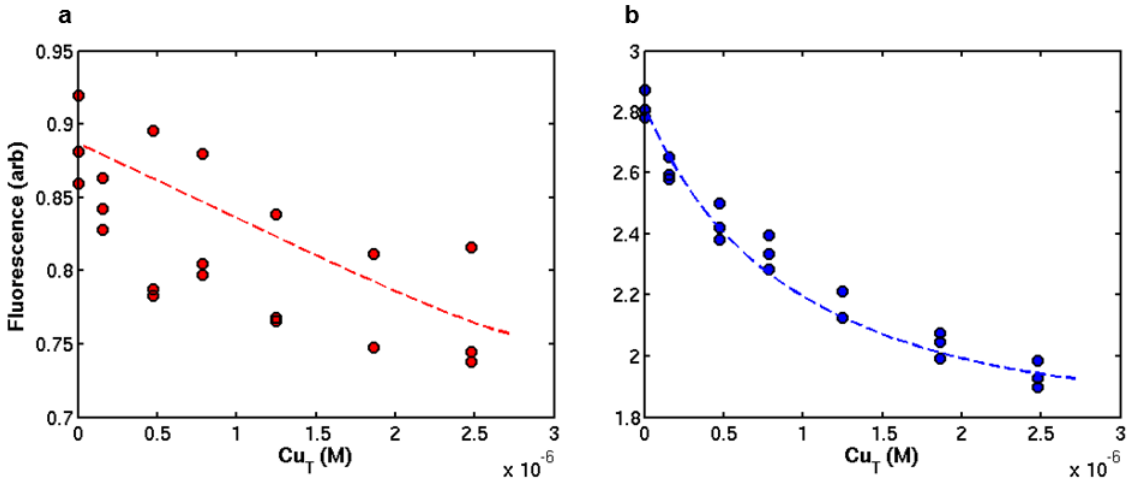

Figure C3. Resolved quenching curves with Ryan-Weber fitting for a. humic- and b. fulvic-like fractions of Petit Rocher.

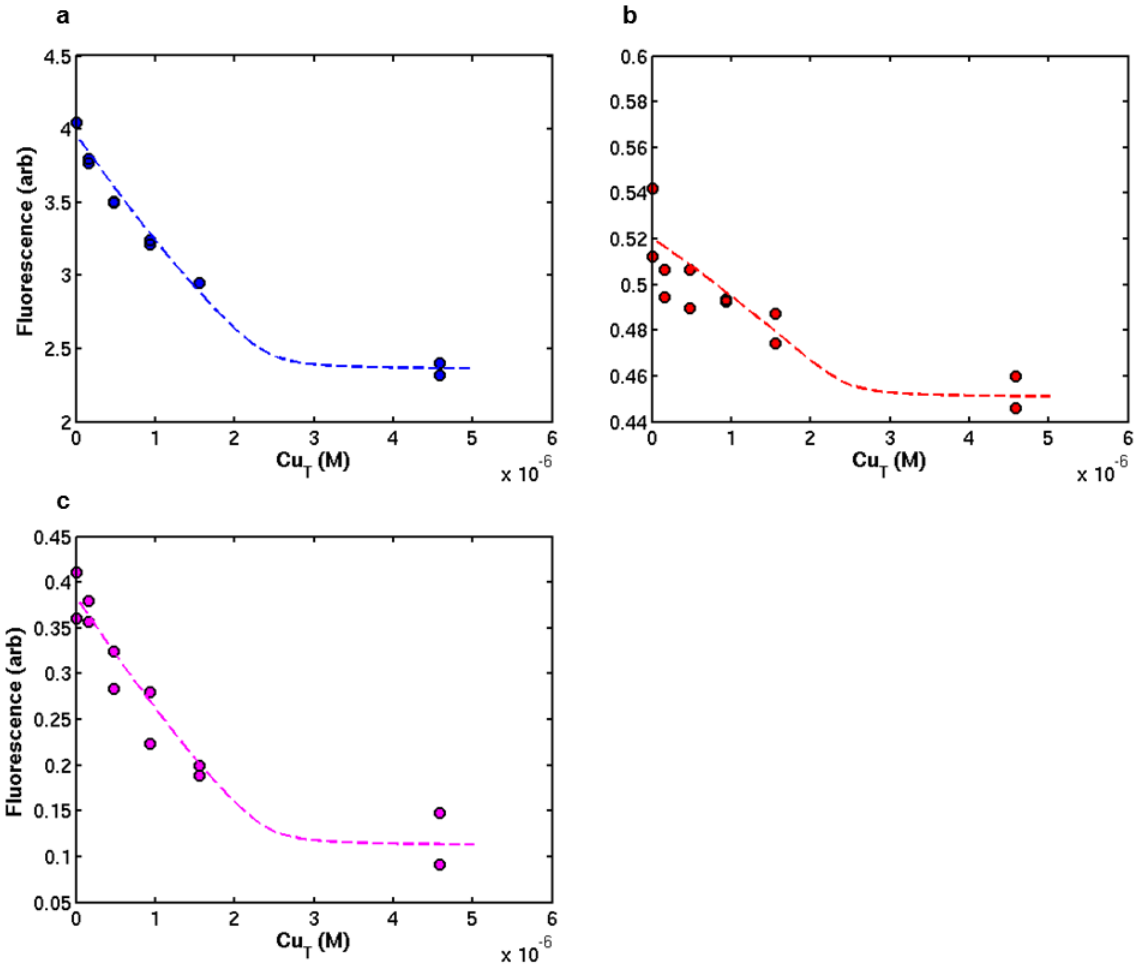

Figure C4. Resolved quenching curves with Ryan-Weber fitting for a. humic-, b. fulvic-, and c. tryptophan-like fractions of Major Kollock Creek.

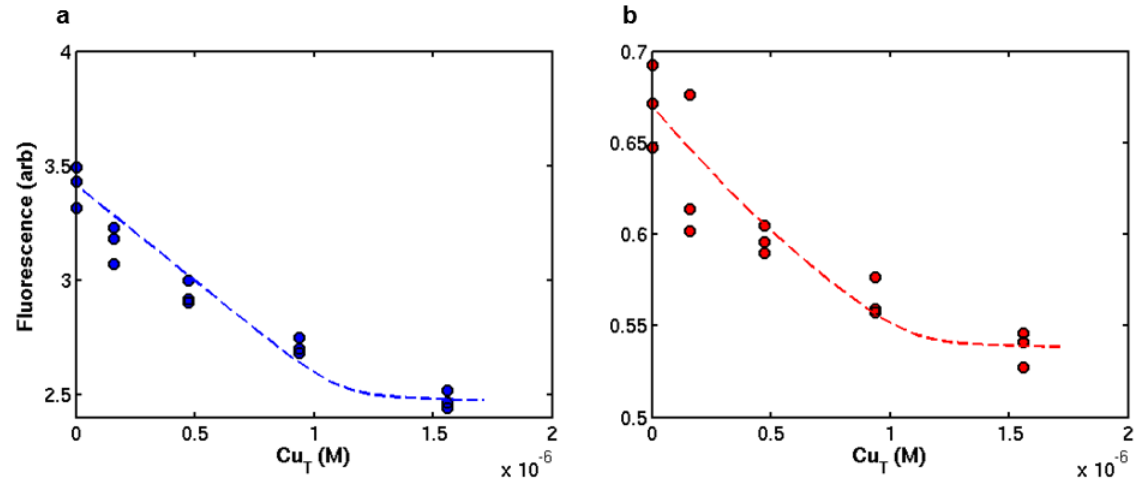

Figure C5. Resolved quenching curves with Ryan-Weber fitting for a. humic- and b. fulvic-like fractions of Naufrage Harbour.

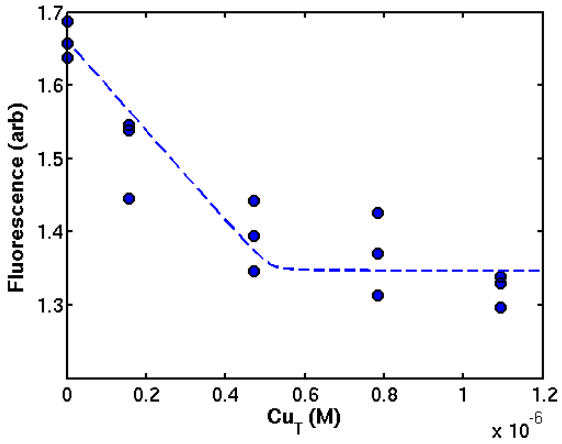

Figure C6. Resolved quenching curves with Ryan-Weber fitting for the humic-like fraction of Rathtrevor Beach.

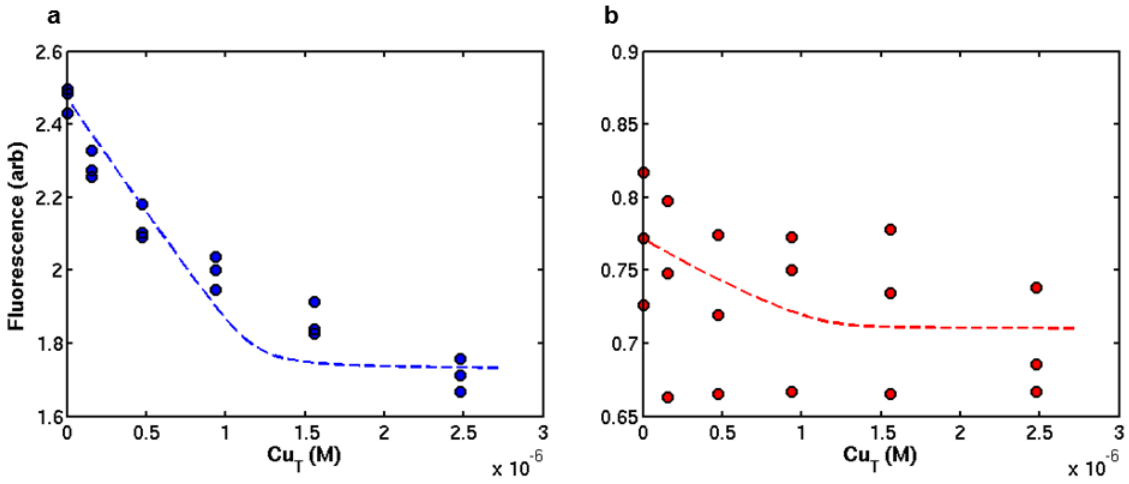

Figure C7. Resolved quenching curves with Ryan-Weber fitting for a. humic- and b. fulvic-like fractions of Hawke's Bay.

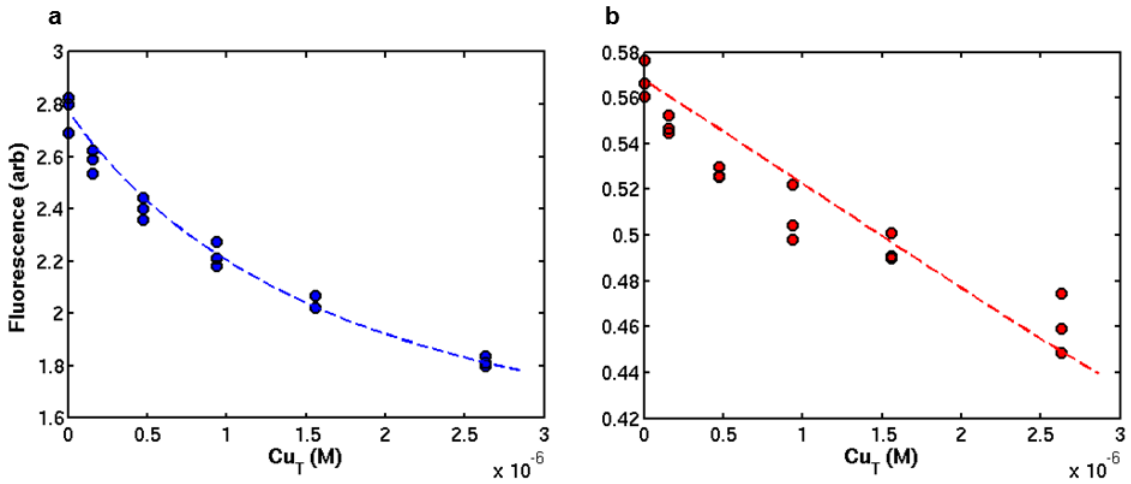

Figure C8. Resolved quenching curves with Ryan-Weber fitting for a. humic- and b. fulvic-like fractions of Blackberry Bay.

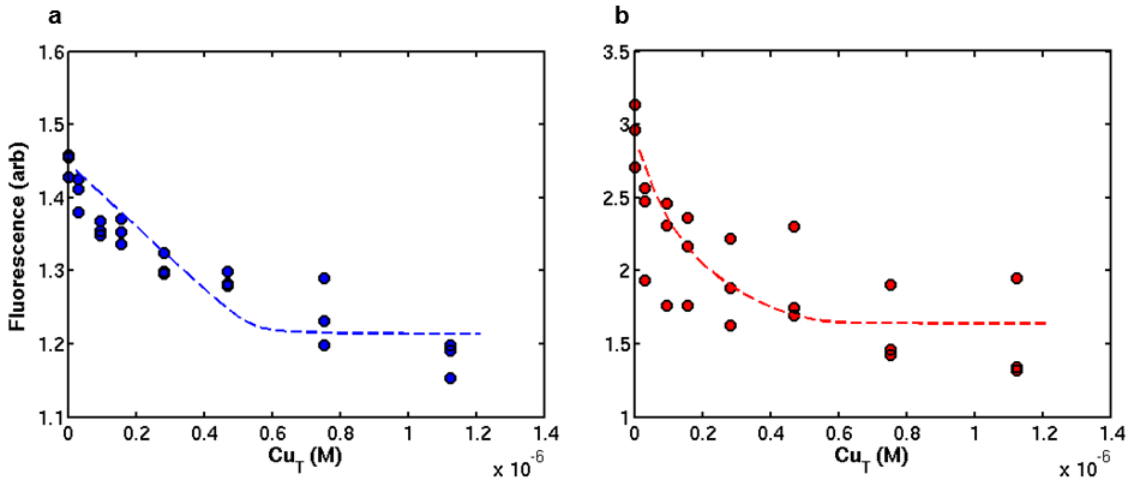

Figure C9. Resolved quenching curves with Ryan-Weber fitting for a. humic- and b. tryptophan-like fractions of Chesterman Beach.

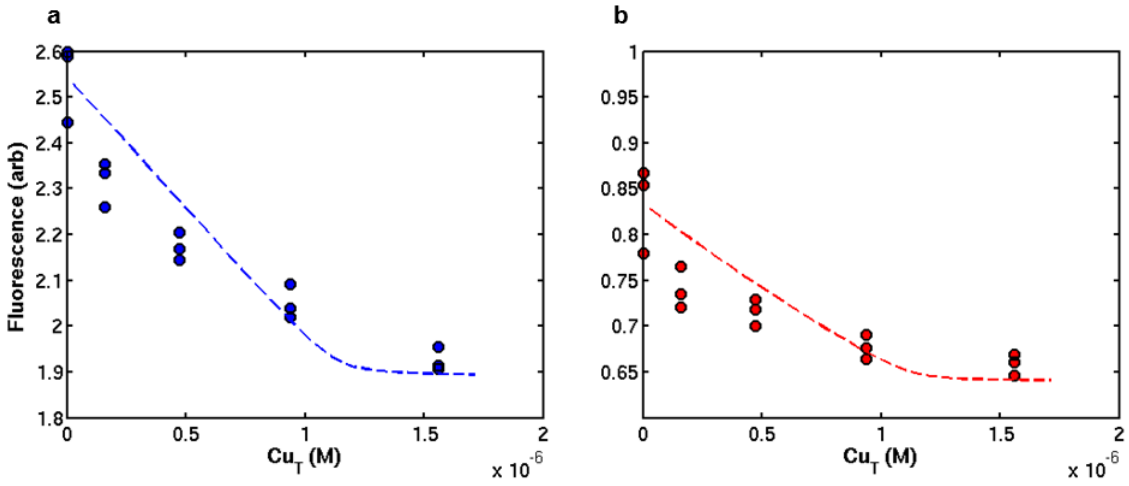

Figure C10. Resolved quenching curves with Ryan-Weber fitting for a. humic- and b. fulvic-like fractions of Jimbo.

C5. Comparison of modeled free copper using fluorescence quenching data and measured free copper using the Cu ISE

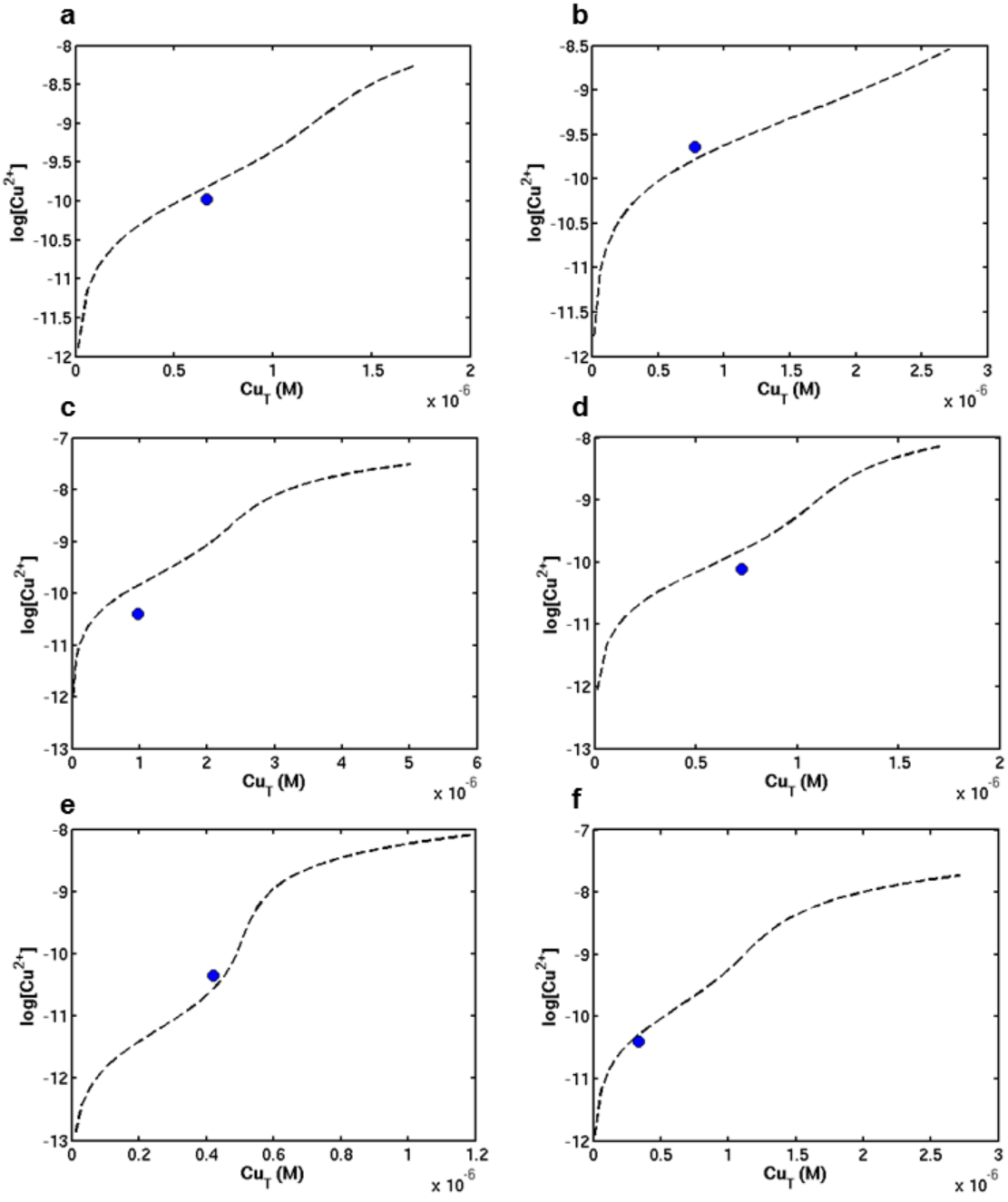

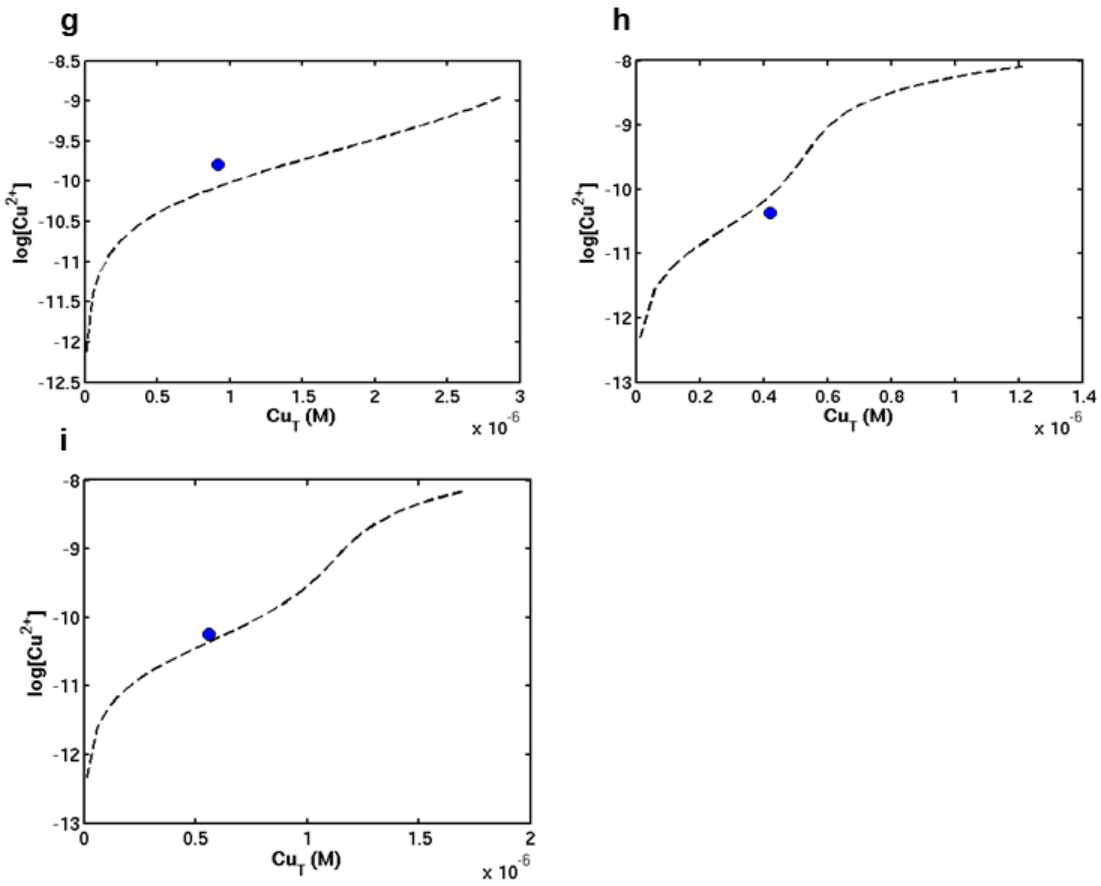

Figure C11. Comparison of modeled free copper (dashed) using fluorescence data and measured free copper (circle) using a copper ion-selective electrode for a. Bouctouche, b. Petit Rocher, c. Major Kollock Creek, d. Naufrage Harbour, e. Rathtrevor Beach, f. Hawke's Bay, g. Blackberry Bay, h. Chesterman Beach, and i. Jimbo.